This is to certify that the

dissertation entitled

KINETICS STUDIES AND ANALYTICAL APPLICATIONS OF THE REACTION BETWEEN AROMATIC ALDEHYDES AND o-DIANISIDINE

presented by

Mayda I. Lopez Nieves

has been accepted towards fulfillment
of the requirements for

Ph. D. degree in Chemistry

Major professor

Date July 31, 1989.

KINETICS STUDIES AND ANALYTICAL APPLICATIONS OF THE REACTION BETWEEN AROMATIC ALDEHYDES AND o-DIANISIDINE

By

Mayda I. Lopez Nieves

A DISSERTATION

Submitted to
Michigan State University
in partial fulfillment of the requirements
for the degree of

DOCTOR OF PHILOSOPHY

Department of Chemistry

1989

ABSTRACT

KINETICS STUDIES AND ANALYTICAL APPLICATIONS OF THE REACTION BETWEEN AROMATIC ALDEHYDES AND o-DIANISIDINE

By

Mayda I. Lopez Nieves

Initial-rate kinetics studies were performed to investigate the mechanism of Schiff base formation between aromatic aldehydes and o-dianisidine in ethanol as solvent. The studies were conducted at 40° C using acetic acid and stannic chloride as catalysts. The evidence supports a three-path mechanism in going from reactants to products. Two paths are catalyzed by acetic acid and the other by stannic chloride. In the acetic acid catalyzed paths, it is propose that the first step involves the reaction of the aldehyde with a solvated proton (i.e., specific acid catalysis). Depending on the acidity of the medium, free or monoprotonated o-dianisidine attacks the carbonyl carbon to form a carbinolamine intermediate which then dehydrates to form the product. In the stannic chloride catalyzed path, it is propose that the aldehyde is first complexed to stannic chloride. The complexed aldehyde is then attacked by a 2:1 o-dianisidine stannic chloride complex to form a carbinolamine which continues to react to form the product. The rate law derived from the proposed mechanism is in agreement with the

experimental data and observations. The analytical implications of the kinetics studies are discussed.

The reaction between o-dianisidine and aromatic aldehydes using stannic chloride as catalyst was automated by adapting it to an air-segmented continuous-flow analysis system. Figures of merit of the method (e.g., sensitivity, limits of detection, and accuracy) for 13 aromatic aldehydes are reported. Selectivity studies performed indicated that aromatic aldehydes exhibit about 400 times more response than ketones towards the o-dianisidine reagent and about 180 times more response than aliphatic aldehydes. Water was found to be a major interferent, causing as much as a 78% decrease in the signal at concentrations of water as low as 8%. The analytical method was applied to the determination of furfural in a real sample.

ACKNOWLEDGEMENTS

Many people have had a direct or indirect input in this work. Among them, first are my parents, for they taught me perseverance and always placed a great value on the pursuit of education. Second are my two mentors, Dr. Nestor Rodriguez and Dr. George M. Rubottom, both at the University of Puerto Rico when they helped me through my first encounters with chemistry. Through his command of the art of teaching chemistry, Don Nestor inspired me to follow a career in the subject I most hated in my high school years. Dr. Rubottom "spoon-fed me" with all the nitty-gritties of the research endeavor and showed me that research is a challenge that can be lots of fun even against all odds.

My encounter of the third kind with chemistry has been linked to a computer. Fortunately, the gallant Dr. Peter D. Wentzell came to my rescue. Peter taught me about computers, starting from how to turn on the computer, up to how to write computer interfacing programs. Thanks Peter, I owe you a lot!

I am very grateful to Dr. Stanley R. Crouch, my research advisor at Michigan State University. He was always there with the right advice to prevent me from drowning in the vast research sea. As I safely approach the seashore, I look back to realize that one of your greatest virtues as an advisor is to have equally high expectancies for all of your apprentices regardless of sex, race, national origin, or grades.

As the saying more or less goes, the ugliest stone in a deck can become the most valuable one upon polishing.

I would like at this point to acknowledge some other professors who also were instrumental in the completion of this work. From the organic faculty, Dr. Chi K. Chang, Dr. Donald G. Farnum and Dr. Harold H. Hart provided most of the aldehyde and ketone samples needed in this research. From the physical chemistry faculty, I am grateful to Dr. James L. Dye for the use of the KINFIT program and for providing helpful suggestions on experiments to perform.

Last, but not least, I would like to express my deepest love and appreciation to my friend Gladys. She was always there when I needed a shoulder to cry on, an ear to listen, a word of encouragement, a joke to laugh or just some juicy gossiping.

As usually heard on TV, this research presentation would not have been possible without support from the National Science Foundation, the Administration of Regional Colleges of the University of Puerto Rico, the National Hispanic Scholarship Fund, the Committee on Institutional Cooperation of the Big Ten Universities, and, at Michigan State University, the Chemistry Department and the Competitive Minority Doctoral Fellowship Program.

TABLE OF CONTENTS

LIST OF TABLES

LIST OF FIGURES

CHAPTER I

INTRODUCTION

A. Project Overview

The main goal of this research was to study the reaction of aldehydes with o-dianisidine in order to develop a new analytical method for the determination of aromatic aldehydes.

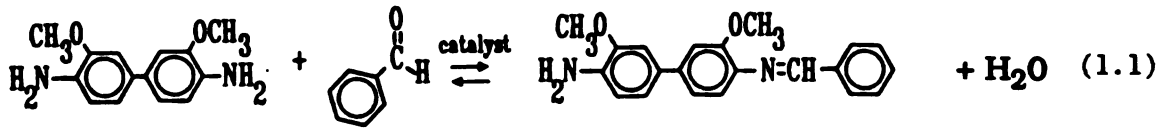

o-dianisidine aldehyde 1:1 adduct

The possibility of forming either the 1:1 adduct shown above or a 2:1 aldehyde to o-dianisidine adduct was investigated by NMR, mass spectrometry and UV-visible absorption spectrophotometry. These experiments are described in Chapter II.

An understanding of the equilibria and kinetics of a reaction to be used in quantitative determinations allows the chemist to choose the most appropiate conditions. In Chapter III, the kinetics of the reaction of o-dianisidine with a representative aldehyde were studied prior to the development of the analytical method.

For many wet chemical analyses, automated methods are preferable to manual methods. In Chapter IV, the analytical reaction between aromatic aldehydes and o-dianisidine was automated by adapting it to an air-segmented continuous-flow analysis system. The method developed was then applied to the determination of aromatic aldehydes in practical samples.

Finally, possible applications of the o-dianisidine-aldehyde reaction in HPLC post-column derivatization is explored in Chapter V.

B. History of o-Dianisidine in Aldehyde Detection

Aromatic aldehydes are present in trace amounts in the air, in waste waters and in foods[1]. Some aldehydes are carcinogens, while others are used to enrich the flavor or aroma of commercially processed foods. In other cases, the decomposition of certain foods can be monitored by determining the amount of a particular aldehyde being produced or consumed. Therefore, trace analysis of aromatic aldehyde is required to protect our health and our environment.

In 1937, Wasicky and Frehden[2] reported that the Feigl spot test for aldehydes[3] was very sensitive (0.05-200 μg). The test was based on the formation of colored Schiff bases upon reaction of mainly aromatic aldehydes with o-dianisidine in the presence of concentrated acetic acid. The colors obtained and the detection limits (non photometric) were tabulated for 34 aldehydes[2]. Ketones were reported not to interfere generally. Nevertheless, o-dianisidine has not been used to any great extent for the quantitative colorimetric determination of

aldehydes. The reasons quoted for its neglect and for the preference for other methods are:

i) The color was reported to be unstable and the reaction unsuitable for quantitative use[4].

ii) Positive results were obtained with some ketones but the sensitivity was 10 to 100 times less than for aldehydes[5].

In the above two cases, details of the o-dianisidine reagent preparation and the conditions for the analysis were not given.

Attaway et al.[6] used o-dianisidine for the determination of unsaturated aldehydes in aqueous citrus essences. However, selectivity tests of the o-dianisidine reagent were not reported nor were the reasons given for using another reagent to determine saturated aldehydes. The conditions used for the determination were 4% acetic acid and at least 40% water (exact amount not specified).

Other reported applications of o-dianisidine in connection with aldehyde determinations are its use in GC reactors. In an aldehyde reactor, o-dianisidine reacts with (or absorbs) the aldehydes present in a sample causing all aldehyde peaks to be eliminated from the chromatogram. These o-dianisidine reactors have been placed at the injection port of a GC column[7,8], at the end of a GC column[9,10], and as a dual channel GC post-column microreactor[11].

C. Other Methods for Aromatic Aldehyde Determination

The majority of the work in the determination of aromatic aldehydes has been done in the fields of UV-visible absorption spectrophotometry[1]. The colorimetric methods used for aromatic aldehyde

determinations are listed in Table 1-1. Comparison between the methods is difficult because, for most of them, the detection limits, dynamic ranges and reproducibilities were not reported. By looking at Table 1-1, it can be inferred that the only colorimetric method specific for aromatic aldehyde determination is the diphenylamine method. The two most common interferents with most of the other methods are aliphatic aldehydes and ketones. The use of the diphenylamine method in automated aromatic aldehyde determination is precluded by the long reaction time required (30-60 minutes) and the high temperatures (65-75°C) used in this method.

Very few fluorimetric methods have been developed for the determination of aromatic aldehydes (Table 1-2). All of the reported fluorimetric methods have very low detection limits $\approx 10^{-7}$ M; however, none of them is suitable for developing an automated method due to the long reaction times and high temperatures required, and/or the use of concentrated acids or bases.

Despite the fact that a large number of aromatic aldehydes exhibit fairly intense phosphorescence, phosphorimetry has been used less often than direct spectrophotometric analysis, colorimetry or fluorimetry.

The most important arguments for using o-dianisidine for aromatic aldehyde determination are the simplicity and selectivity of the method. These become important considerations in the analysis of a complex material such as polluted water, foods, or pharmaceuticals where the presence of substances like ketones could interfere with direct spectrophotometric analysis or with indirect colorimetric methods.

TABLE 1-1. Colorimetric Methods for Aromatic Aldehyde Determinations.

Reagent	Acid Concentration	Interferences	Ref.
p-Aminophenol	100% Acetic Acid	unsaturated aliphatic aldehydes	12
Azulene	38% Acetic Acid + 38% H_2SO_4	aliphatic aldehydes, alcohols	13
3,5-Dihydroxy-4-phenylisoxazole		aliphatic aldehydes, ketones	14
N,N-Dimethyl-p-phenylenediamine	100% Acetic Acid	aliphatic aldehydes	15
2,4-Dinitrophenylhydrazine		aliphatic aldehydes, ketones	16
Diphenylamine	50% conc. HCl		17, 18
Fluoranthene	70% Trifluoroacetic Acid		19
4-Nitrophenylhydrazine		aliphatic aldehydes, ketones	20, 21
4-Phenylazophenylhydrazine-ß-sulphonate		ketones	22
Borohydrides		aromatic ketones, amines and nitro compounds	23
Sulphuric Acid	95% H_2SO_4	ketones, carboxylic acids, and phenols	24
Thiobarbituric Acid	16% Trichloroacetic Acid	α,ß-unsaturated aldehydes	25, 26
Thiosemicarbazide	0.1N HCL	aliphatic aldehydes, ketones	27
$KMnO_4$ + Crown Ethers		aliphatic aldehyde	28

TABLE 1-2. Fluorimetric Methods for Aromatic Aldehyde Determinations.

Reagent	Reaction Time (min.)	Temperature (°C)	Acid Conc.	Detection Limit (M)	Comments	Ref.
4,5-Dimethoxy-1,2-diamino-benzene	50	37	very dil. HCl	10^{-7}	0.05 M NaOH required to occur fluorescence	29
1,2-Diaminobenzene	60	75			not all aromatic aldehydes react	30
Mansylhydrazine					amines, aminoacids and phenolic steroids react	31
2,2′-Dithiobis-(1-amino-naphthalene)	30	37			cumbersome procedure	32
o-Aminothiophenol	60	60	90% H_2SO_4			33, 34
1,2-Diaminonaphthalene	20	100		10^{-7}-10^{-6}	0.4 M NaOH required to occur fluorescence, aliphatic aldehydes react	35
Dansylhydrazine	75				interference of amines, phenols, aminoacids and ketones	36
2-Diphenyl-1,3-indanedione-1-hydrazone	> 60				ketone interference, reagent fluoresces too	37
1,4-Dimethyl-3-carbamoyl-pyridinium chloride	50	37		10^{-7}		38

CHAPTER II

CHARACTERIZATION OF THE PRODUCT FORMED

A. Statement of the Problem

The first problem encountered in this research was that o-dianisidine has two reactive sites. In principle, two products can be formed as shown in Figure 2-1.

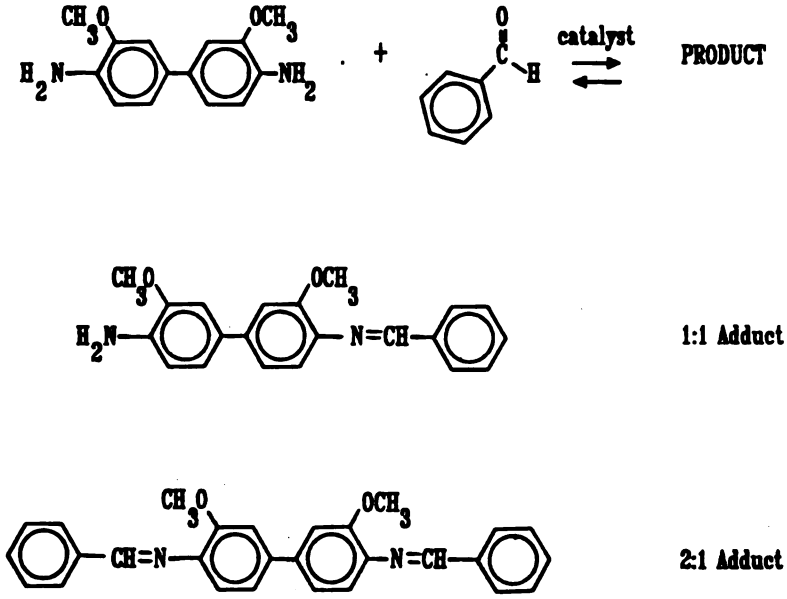

Figure 2-1. Possible products from the reaction of o-dianisidine and aldehydes

These two products will hereafter be referred to as the 1:1 and 2:1 adducts accordingly. Attempts to isolate the product formed using silica gel column chromatography were unsuccessful due to decomposition

and rearrangement of the product on the column. For the same reasons, thin layer chromatography (TLC) was not useful.

The synthesis of the 2:1 adduct as well as its purification was easily accomplished. To form the 2:1 adduct, o-dianisidine was mixed with an excess of the aldehyde in the presence of 4% acetic acid using ethanol as solvent. Purification of the 2:1 adduct consisted of several washes with warm ethanol to eliminate the acetic acid and the excess aldehyde. Synthesis of the 1:1 adduct was also easy. However, its purification from the excess o-dianisidine, which was necessary in order to form the 1:1 adduct preferentially over the 2:1 adduct, was not possible.

The elucidation of which product was formed in the reaction of an aromatic aldehyde with a 30-fold molar excess of o-dianisidine was attempted in three different ways: mass spectral, NMR, and molar ratio studies.

B. Mass Spectral Studies

The instrument used for the mass spectral studies was an EI-CI-Finnigan Mass Spectrometer. First, an electron-impact (EI) mass spectrum (70 eV) of the reaction mixture of salicylaldehyde and o-dianisidine at a 2% acetic acid concentration was taken after removing the solvent in vacuo. This mass spectrum (Figure 2-2) showed a peak at m/e 340, which corresponds to the 1:1 adduct. No peak was found at m/e 452, which corresponds to the 2:1 adduct. The 2:1 adduct between salicylaldehyde and o-dianisidine was easily synthesized by mixing excess aldehyde with o-dianisidine. The identity and purity were

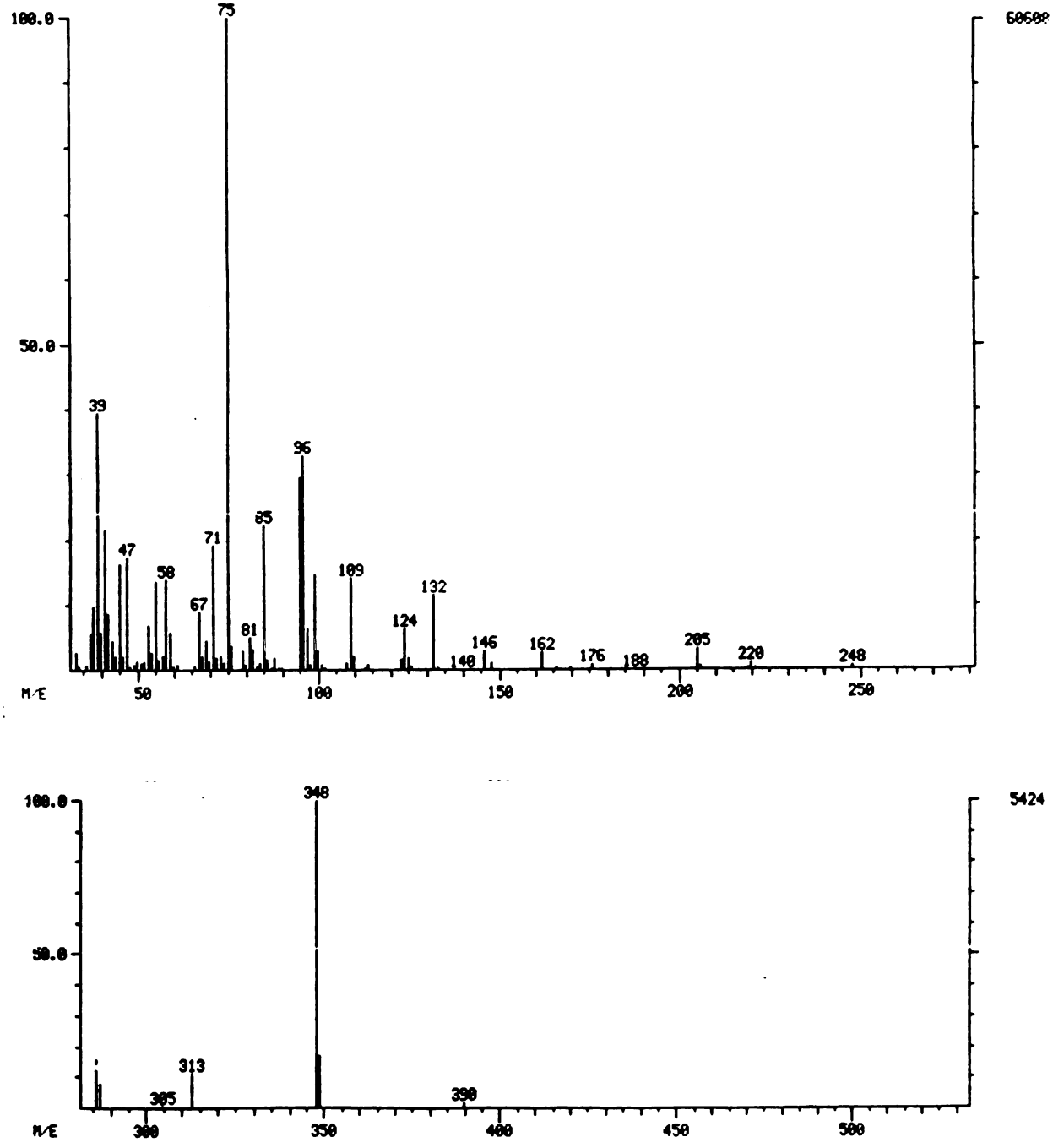

Figure 2-2. Electron-impact mass spectrum of the reaction between salicylaldehyde and o-dianisidine in 2% acetic acid after removal of solvent.

established by NMR, melting point, and thin layer chromatography. An EI mass spectrum of this pure compound (Figure 2-3) showed both the 348 and 452 m/e peaks. The 452 m/e parent ion was very prominent.

Questions regarding the stability of the molecular ion of the 2:1 adduct in EI mass spectrometry prompted the use of chemical ionization (CI) mass spectrometry. Here, the reaction mixture made from 2,4-dichlorobenzaldehyde and o-dianisidine was divided in two equal parts. To one of the aliquots, enough 2:1 adduct of the 2,4-dichlorobenzaldehyde was added as to make its concentration equal to that of the expected product, the 1:1 adduct. After removing the solvent from both samples, CI mass spectra were taken. The mass spectrum of the reaction mixture containing the 2:1 adduct showed the molecular ions for both adducts. The peaks corresponding to the 1:1 adduct were about two times more intense than those corresponding to the 2:1 adduct. The mass spectrum of the reaction mixture without the 2:1 adduct showed only the molecular ion for the 1:1 adduct. This evidence strongly supports the exclusive formation of the 1:1 adduct when an excess of o-dianisidine is reacted with an aromatic aldehyde.

C. NMR Studies

Another approach to the problem of elucidating the structure of the product formed when an aldehyde is reacted with an excess of the o-dianisidine, was taking nuclear magnetic resonance spectra of the reaction mixture. The spectrometer used was a 250 MHz Bruker WM-250 instrument. The aldehyde chosen for these studies was 2,4-dichlorobenzaldehyde. The o-dianisidine was used in at least a 30-fold molar

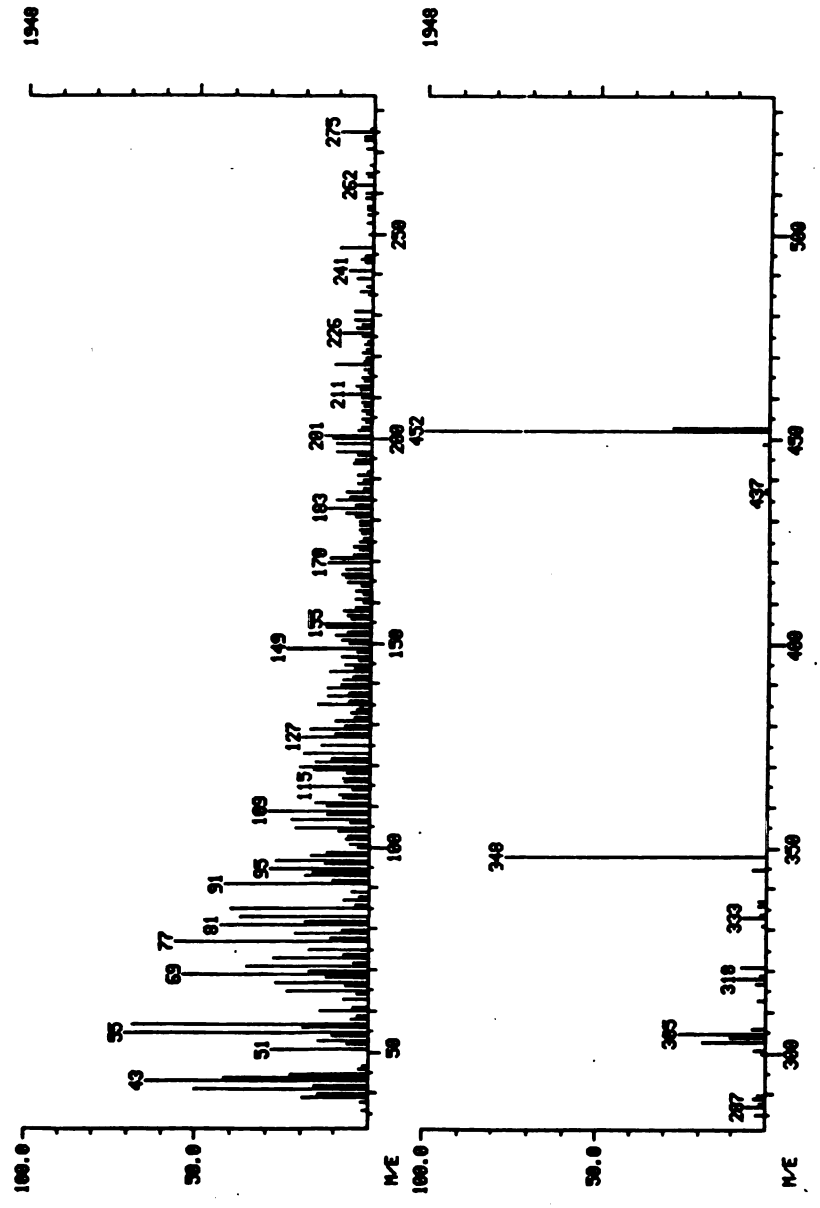

Figure 2-3. Electron-impact mass spectrum of the 2:1 adduct between salicylaldehyde and o-dianisidine.

excess. The solvent used was dried absolute ethanol and the catalysts were acetic acid and stannic chloride. The reaction was run in a large-scale vessel and thermostatted for 3 hours at 40°C. After the reaction period, the solvent was evaporated on a rotary evaporator and the residue was dried further in vacuo. Then the NMR spectrum of the product formed was taken using chloroform-d as solvent.

In Figure 2-4, the spectrum on the right is an expansion of the 7.5 to 9.5 ppm region of the above dry reaction mixture. The spectrum on the left corresponds to a mixture that contains o-dianisidine, the 1:1 and 2:1 adducts. The NMR proton signal for the azomethine group, H_a, appears as a singlet peak at 8.939 δ units. The normal range for the azomethine proton as reported in the literature[39] is from 8.37 to 9.37 δ units for imines formed from aromatic amines and aromatic aldehydes. In these compounds the hydrogen labeled b, which is located in the ortho position of the aldehyde benzene, gives a doublet in the NMR spectrum. The chemical shifts corresponding to the doublet of the 2:1 adduct are at a lower magnetic field than those of the 1:1 adduct. The equivalent peaks in the NMR spectrum of the reaction mixture appear at a lower magnetic field than those of either adduct. Figure 2-5 shows much better the position of these peaks in the spectrum.

The left column in Figure 2-5 indicates the number of spectra used in the determination of the chemical shift range and in the calculation of the confidence interval for the chemical shift of each peak. For each compound listed, the upper chemical shift range corresponds to the experimental range while the lower range corresponds to the 95% confidence range for the chemical shift.

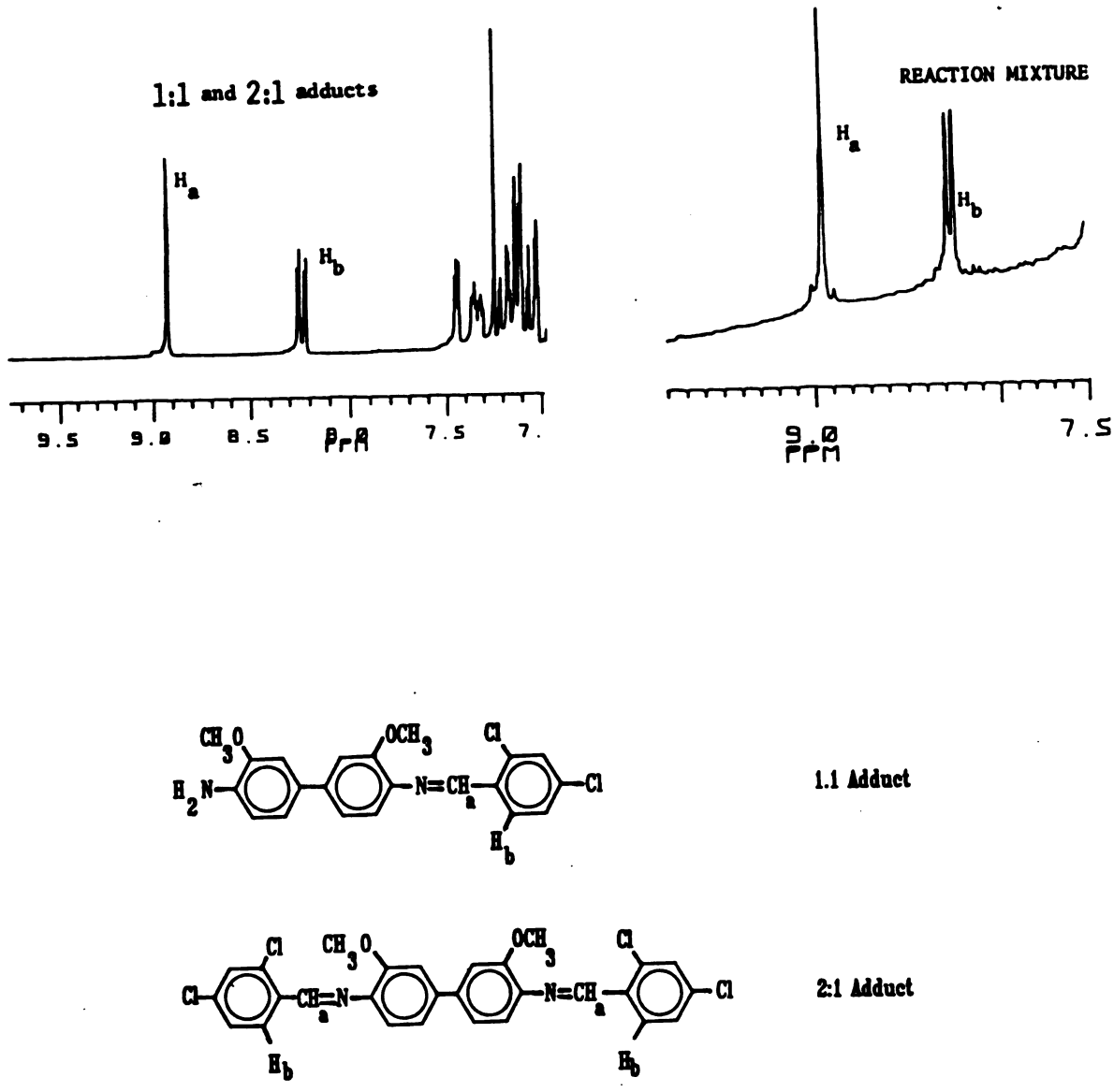

Figure 2-4. Top right: expansion of the 7.5 to 9.5 ppm region of the NMR spectrum of the reaction mixture between 2,4-dichlorobenzaldehyde and o-dianisidine. Top left: expansion of the 7.0 to 9.5 ppm region of the NMR spectrum of a mixture containing the 1:1 and 2:1 adducts of 2,4-dichlorobenzaldehyde and o-dianisidine. Bottom: structures of the two adducts.

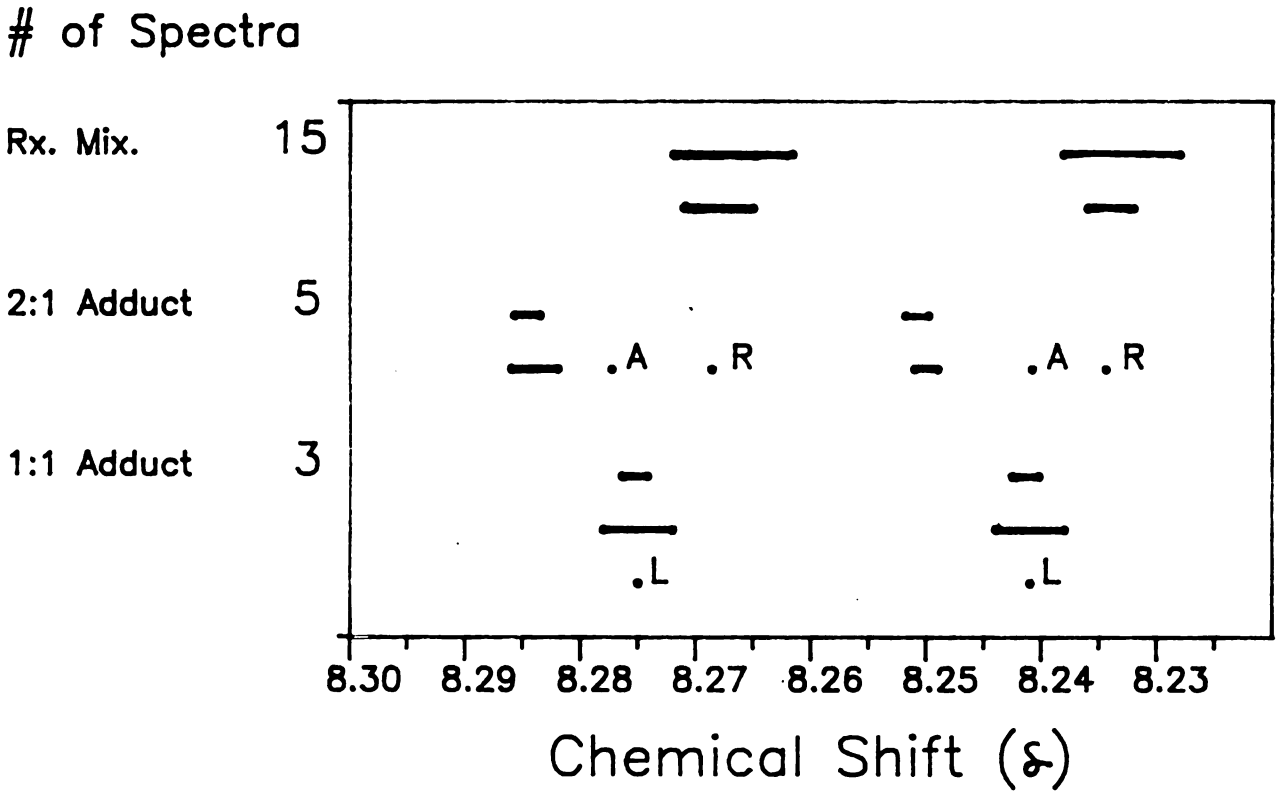

Figure 2-5. Chemical shift for the aldehydic ortho proton of the 1:1 and 2:1 adducts of 2,4-dichlorobenzaldehyde with o-dianisidine. Points marked as A represent the position for the chemical shift for the aldehydic ortho proton in a pure sample of the 2:1 adduct in acetic acid. Points marked as R represent the chemical shift for the aldehydic ortho proton in a reaction mixture to which the 2:1 adduct was added on purpose. Points marked as L represent the chemical shift obtained for the aldehydic ortho proton in a low temperature NMR spectrum of the reaction mixture.

Although the chemical shifts of the reaction mixture are closer to those of the 1:1 than to those of the 2:1 adduct, we cannot conclude based on these NMR results that the adduct being formed is the 1:1 adduct, especially in light of the next experiment performed.

In another experiment, after mixing all the reactants, the reaction mixture was divided into two equal parts. After adding to one half the pure 2:1 adduct, both solutions were thermostatted for 3 hours at 40°C. After the reaction period, the solvent was evaporated on a rotary evaporator and the samples dried further in vacuo. The NMR spectrum of the reaction mixture containing the added 2:1 adduct was expected to show two sets of double peaks corresponding to the 1:1 and 2:1 adducts if only the 1:1 adduct is formed under the reaction conditions. The NMR spectra of the reaction mixture alone was expected to show only one set of double peaks as in Figure 2-4. The NMR spectrum of the reaction mixture containing the 2:1 adduct showed only one set of double peaks at the same chemical shift as the reaction mixture without the 2:1 adduct, point marked as R in Figure 2-5. Therefore, we are probably seeing in the NMR of the reaction mixture an equilibrium between free (1:1 or 2:1) adduct and complexed adduct. The complexing agent is probably stannic chloride, since the 2:1 adduct in acetic acid has a chemical shift at a higher magnetic field (marked as A in Figure 2-5) than that of the reaction mixture alone. Tin (IV) complexes with Schiff bases are not new in the literature[40-42]. A low temperature NMR spectrum of the reaction mixture was taken at -13°C to study the possible formation of a stannic chloride complexed adduct. The low temperature NMR showed the peak appearing at the exact position as the free 1:1 adduct (marked as L in Figure 2-5). In the same spectrum two

much smaller sets of double peaks appeared at higher magnetic field, probably accounting for the resolved signal of the complexed adduct.

The NMR experiments performed are not conclusive in deciding which of the two adducts is formed. The NMR experiments only suggest the formation of the 1:1 adduct, some of it complexed to stannic chloride.

D. Molar Ratio Studies

The molar ratio method of Yoe and Jones[43] was also employed to determine whether the 1:1 or 2:1 adduct is formed during the reaction. This involves plotting the absorbance versus increasing molar ratio of o-dianisidine to aldehyde as shown in Figure 2-6.

In this method, if the product is very little dissociated, the graph is a straight line from the origin to the point of the actual molar ratio of the species in the product and then the absorbance shows a sudden plateau parallel to the abscissa (curve A). With less stable products or products of low formation constant, the plot is a smooth curve, but the linear portions may be extrapolated to the point of intersection to give the molar ratio of the species in the product (curve B). This method resembles a spectrophotometric titration[44] except that a different sample is analyzed for every absorbance reading and that the total volume is always the same.

Figure 2-7 is a composite of the results of the molar ratio experiment when 2,4-dichlorobenzaldehyde was reacted with o-dianisidine. If the 1:1 adduct is the product formed, a plateau should be seen starting at a molar ratio of 1, but if the 2:1 adduct is the preferred product the plateau should start at a molar ratio of 0.5. At first glance it

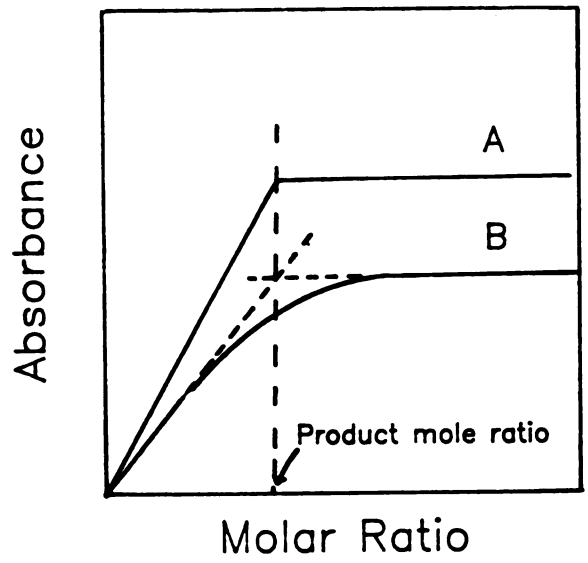

Figure 2-6. Yoe and Jones' Molar Ratio Plot.

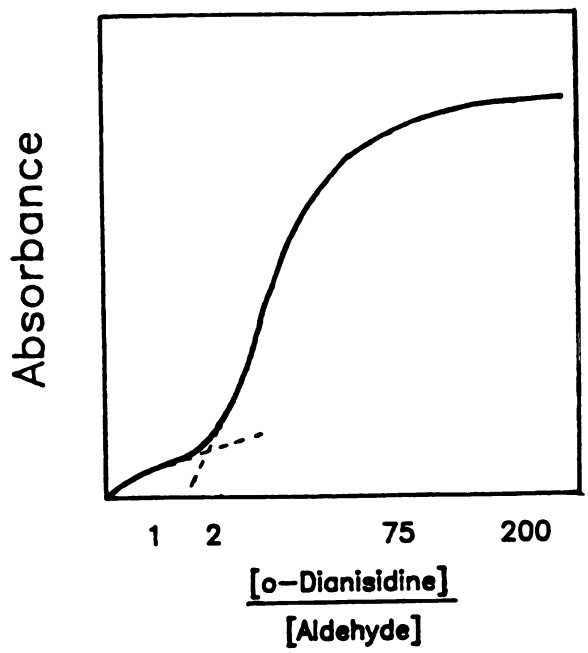

Figure 2-7. Composite molar ratio plot for the reaction between 2,4-dichlorobenzaldehyde and o-dianisidine.

can be seen that the curve does not look like that predicted by theory. There is an inflection point at a molar ratio of o-dianisidine to aldehyde of 2, indicating that either of the two products can be formed. The products depends on the ratio of reactants.

From chemical intuition it is expected that at high aldehyde concentration the 2:1 adduct is the preferred product. At high o-dianisidine concentration the 1:1 adduct should be preferred. The molar ratio study itself is not conclusive in deciding which of the two products is formed in the analytical reaction where the molar ratio is usually 30 to 1 o-dianisidine to aldehyde.

The molar absorptivity determined for the 2:1 adduct of 2,4-dichlorobenzaldehyde at 380 nm is 2.68×10^4 $M^{-1}cm^{-1}$. The molar absorptivity of the 1:1 adduct has not yet been determined because a pure sample of this compound is not available. An alternative route used to calculate the molar absorptivity of the 1:1 adduct is to assume that under very high o-dianisidine concentration the only product formed quantitatively is the 1:1 adduct. In a preliminary experiment, a molar ratio of at least 200:1 o-dianisidine to aldehyde was required for the absorbance of a fixed amount of the aldehyde to plateau. Therefore, the molar absorptivity of the 1:1 adduct was taken to be equal to the slope of a graph of absorbance versus concentration of 2,4-dichlorobenzaldehyde where the amount of o-dianisidine at each concentration of the aldehyde was always in a 400:1 molar ratio. In this manner, a molar absorptivity of 1.34×10^4 $M^{-1}cm^{-1}$ was assigned to the 1:1 adduct between o-dianisidine and 2,4-dichlorobenzaldehyde (at a wavelength of 380 nm). The absorbance of the 2:1 adduct exactly doubles that of the 1:1 adduct. This is an interesting fact because both adducts also seem

to have the same absorption spectrum in the visible region. This implies that the chromophore in both compounds is probably the same, as shown in Figure 2-8.

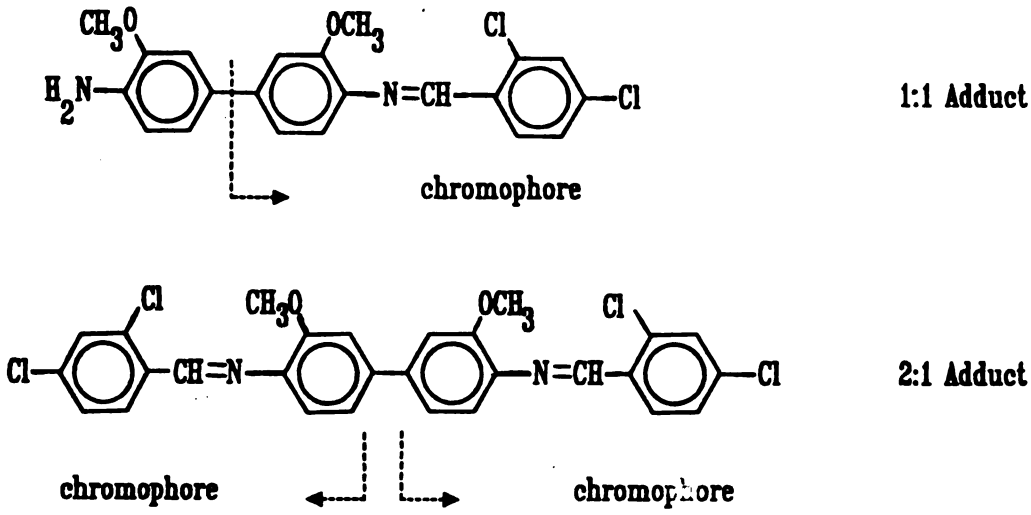

Figure 2-8. Chromophore in the 1:1 and 2:1 adducts of 2,4-dichlorobenzaldehyde and o-dianisidine

If this is the case, then regardless of which adduct is formed in the reaction mixture the quantitative determination of aldehydes with this reagent should not be affected as long as the aldehyde reacts to the same extent in sample and standards. In other words, no matter which adduct is formed, the absorbance per aldehyde that reacted will be the same. It is highly probable that the actual structure of the chromophore does not involve any of the o-dianisidine benzene rings since NMR and IR spectra studies of aromatic azomethines[45] suggest that the molecular structure of this type of compounds is not planar (i.e., the benzene ring of the amine part is distorted from the plane of the trans-benzalamino skeleton). Consequently, conjugation will only be

possible between the azomethine group and the benzene ring of the aldehyde.

E. Conclusions

Molar ratio studies suggest the formation of the 1:1 adduct in preference over the 2:1 adduct as the concentration of o-dianisidine is increased relative to that of the aldehyde. A low temperature NMR spectrum suggests the formation of the 1:1 adduct, some of it complexed to stannic chloride. The most significant evidence in favor of the 1:1 adduct comes from the mass spectral studies in which detection of the molecular ion due to 1:1 adduct is possible while detection of the molecular ion for the 2:1 adduct is only possible when it is added on purpose to the reaction mixture.

CHAPTER III

KINETICS STUDIES

A. Chapter Overview

In this chapter, studies on the kinetics of the reaction of an aromatic aldehyde with o-dianisidine are presented. First, the accepted mechanism of Schiff base formation in water as solvent is presented to serve as a basis for later comparison. Next, a few comments are given on the choice of conditions for the kinetics experiments (i.e. solvent, aldehyde, catalyst and temperature). After the experimental section and the results, the rate law obtained is presented followed by a discussion of the proposed mechanism. Finally, the analytical implications of the kinetics studies are discussed.

B. Mechanism of Schiff Base Formation in Water

Addition of primary amines to carbonyl groups (in water as solvent) has been studied extensively[46-50], particularly by Jencks and Sayer. Aldehydes react with primary amines to form a Schiff base as shown in the simplified equilibrium reaction below.

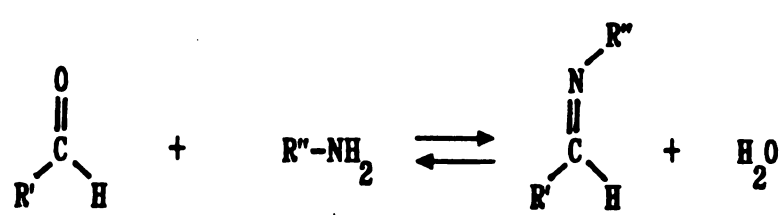

(3.1)

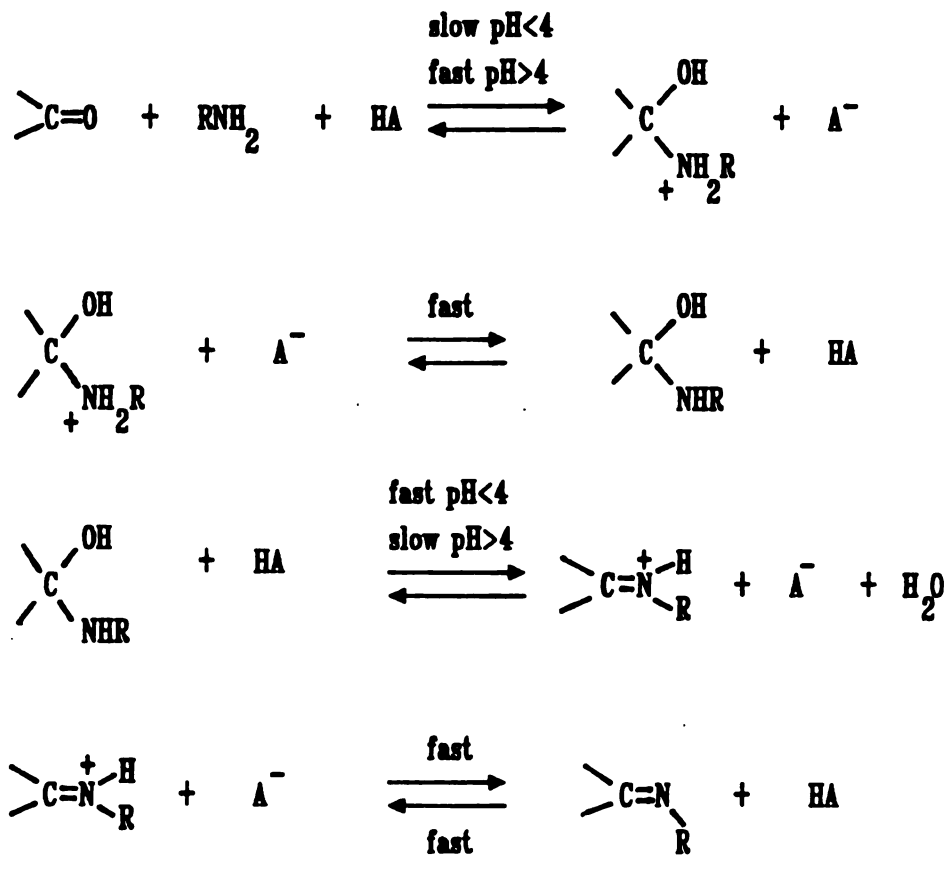

Figure 3-1. Mechanism for Schiff base formation in water.

In water as solvent, the proposed mechanism is as shown in Figure 3-1. The initial attack of the amine at the carbonyl carbon to form the carbinolamine[48-49] can occur via specific or general acid catalysis depending on the basicity of the amine and the strength of the acidic catalyst. To apply the steady-state approximation a simplified mechanism is often employed. In the simplified mechanism, the addition of amines to aldehydes is proposed to occur in two generalized steps: (1) formation of the carbinolamine intermediate; (2) subsequent dehydration of the carbinolamine intermediate to form the imine.

STEP 1 $\quad >C=O + NH_2R \underset{k_{-1}}{\overset{k_1}{\rightleftharpoons}} RNH-\underset{|}{\overset{|}{C}}-OH$ fast equlibrium

STEP 2 $\quad RNH-\underset{|}{\overset{|}{C}}-OH + HA \xrightarrow{k_2} >C=N-R + H_2O + A^-$ slow

When examining the rate of the forward reaction the reverse of Step 2 is neglected because it is assumed that the reverse of Step2 is not occurring to any great extent initially. This mechanism involves an intermediate species that does not appear in the overall stoichiometric equation, $RNH-\underset{|}{\overset{|}{C}}-OH$. The steady-state approximation assumes that the rate of formation of this reaction intermediate essentially equals its rate of destruction so as to keep it at a steady-state concentration.

The overall rate is given by Step 2 as:

$$\text{rate} = k_2 \left[RNH-\underset{|}{\overset{|}{C}}-OH\right] [HA] \tag{3.2}$$

To find $[RNH-\underset{|}{\overset{|}{C}}-OH]$, the concentration time derivative for this intermediate is set equal to zero. Since $RNH-\underset{|}{\overset{|}{C}}-OH$ is formed by Step 1 and consumed by Steps -1 and 2, one gets:

$$\frac{d\left[RNH-\underset{|}{\overset{|}{C}}-OH\right]}{dt} = k_1[>C=O]\,[NH_2R] - k_{-1}\left[RNH-\underset{|}{\overset{|}{C}}-OH\right] - k_2\left[RNH-\underset{|}{\overset{|}{C}}-OH\right][HA] = 0 \tag{3.3}$$

$$\left[RNH-\underset{|}{\overset{|}{C}}-OH\right] = \frac{k_1[>C=O]\,[NH_2R]}{k_{-1} + k_2[HA]} \tag{3.4}$$

Substituting in the rate expression:

$$\text{rate} = \frac{k_2 k_1 [\rangle C{=}O] [NH_2R] [HA]}{k_{-1} + k_2 [HA]} \qquad (3.5)$$

At high acid concentration, $k_2[HA] >> k_{-1}$, and the rate equation reduces to:

$$\text{rate} = k_1 [\rangle C{=}O] [NH_2R] \qquad (3.6)$$

Therefore, Step 1, the amine attack, is rate determining at low pH. At low acid concentration, $k_{-1} >> k_2[HA]$, and the rate expression reduces to:

$$\text{rate} = \frac{k_2 k_1 [\rangle C{=}O] [NH_2R] [HA]}{k_{-1}} \qquad (3.7)$$

In this latter case, the dehydration of the carbinolamine addition product is rate determining at low acid concentrations.

In conclusion, in Schiff base formation using water as solvent, either the addition step or the elimination step may be rate determining depending on the pH.

The objective of this research was to study the reaction of o-dianisidine with a representative aldehyde prior to the development of an analytical method for the determination of aromatic aldehydes. Experimental conditions were chosen close to those that on preliminary experiments were found to be optimum for this reaction. Therefore, the kinetics studies that follow are not exhaustive.

C. Preliminary Considerations

In this section a few comments are given on the choice of reagents and experimental conditions.

1. Solvent Choice

As was stated before, aldehydes react with primary amines to form a Schiff base liberating water in the process. Therefore, to enhance product formation, water in the system must be absent. Also, most aldehydes are insoluble or only slightly soluble in water.

Initially, the performance of the reaction was tested in several solvents: dimethyl sulfoxide, dimethyl formamide, hexane, and ethanol. Absolute ethanol was the solvent chosen not only because of the higher product formation obtained when using it, but also because its low cost and non toxicity. Another advantage is that most aldehydes are readily soluble in ethanol.

It was found that the presence of even small amounts of water will decrease the amount of product formed for most aldehydes. Exceptions to the above were salicylaldehyde, p-chlorosalicylaldehyde, and p-dimethylaminobenzaldehyde in which a slight increase in product formation was observed when small amounts of water were added to the system.

2. Aldehyde Choice

Preliminary studies were performed to select an aromatic aldehyde which could be considered representative. Absorbance versus time measurements were made at different temperatures and catalyst concentrations. The instrument used for these preliminary studies was a modular single-beam spectrophotometer equipped with a temperature-

controlled cell compartment, a tungsten lamp, and 1 cm glass cell (CGA McPherson, Acton, MA). Of the 14 aromatic and α,β-unsaturated aldehydes studied, 2,4-dichlorobenzaldehyde was chosen as the model compound. This aldehyde was found to exhibit an intermediate reactivity with o-dianisidine and also showed the same response pattern toward changes in the concentration of the acids employed as catalyst as did most of the other aldehydes.

3. Temperature Choice

Graphs similar to the one shown in Figure 3-2 for 2,4-dichlorobenzaldehyde were constructed for the other aldehydes. From these preliminary studies it was found that the rate of the reaction increased as the temperature was increased. Nevertheless, an upper limit to the increase in temperature was set at 40°C to prevent problems with fast solvent vaporization. Also, fluctuations in the room temperature should affect less the reproducibility of volume measurements if the experiments are conducted at temperatures close to room temperature than at much higher temperatures.

4. Catalyst Choice

The catalysts studied were zinc chloride, stannic chloride, and stannous chloride. These Lewis acids were tested in the presence and in the absence of acetic acid. Of the three Lewis acids tested, stannic and stannous chloride gave the faster rates. Stannic chloride was the catalyst chosen due to the slightly higher rate and to the expected better stability of the stannic chloride solutions[51].

When stannic chloride and acetic acid were used simultaneously as catalysts, there was an interaction which seemed to be useful in

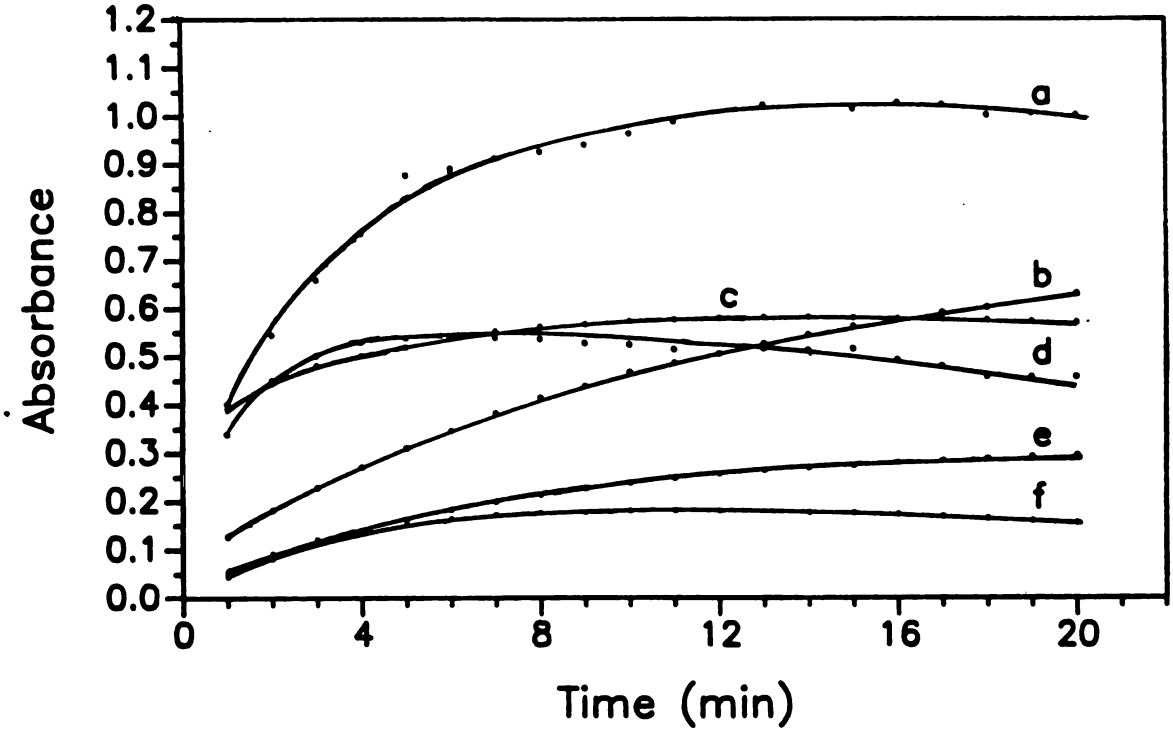

Figure 3-2. Acid and temperature effects in the reaction between 2,4-dichlorobenzaldehyde and o-dianisidine. Experimental conditions: a) 40°C, 0.1% acetic acid, and 3.00 X 10^{-4} M stannic chloride; b) 25°C, 0.1% acetic acid, and 3.00 X 10^{-4} M stannic chloride; c) 30°C, 6% acetic acid; d) 40°C, 8% acetic acid; e) 20°C, 6% acetic acid; f) 20°C, 10% acetic acid.

obtaining higher product formation at shorter reaction times and in reaching equilibrium much faster (Figure 3-3).

The stannic chloride and acetic acid concentrations chosen were based on previous absorbance versus time experiments. For example, the concentration of stannic chloride was varied over a wide range at a constant concentration of acetic acid to establish working limits for the concentration of this reagent. The desirable upper limit was the one that gave maximum initial rate with little or no decomposition of the reaction products. The lower limit was that concentration of stannic chloride which still had some effect on the rate of the reaction.

The effect of increasing concentrations of acetic acid upon the stability of the product formed was also studied. The concentration of the acetic acid was changed by two orders of magnitude (between 5 X 10^{-3} to 0.5 M). Over this concentration range no decomposition of product was seen. The main effect of the acetic acid was to shift the equilibrium position towards reactants (Figure 3-3). At higher concentrations of acetic acid, the product decomposes slowly. The shift of the equilibrium towards reactants with increasing acid concentration is also observed in Schiff base formation in water[52]. It can be attributed to the reversibility of all the steps of the reaction causing hydrolysis of product as the concentration of acid increases.

The catalytic behavior of acetic acid in Schiff base formation was known from the literature[2,3,6,52]. To test whether stannic chloride is also a true catalyst or a reagent, long reaction time experiments were performed encompassing a wide range of stannic chloride concentrations.

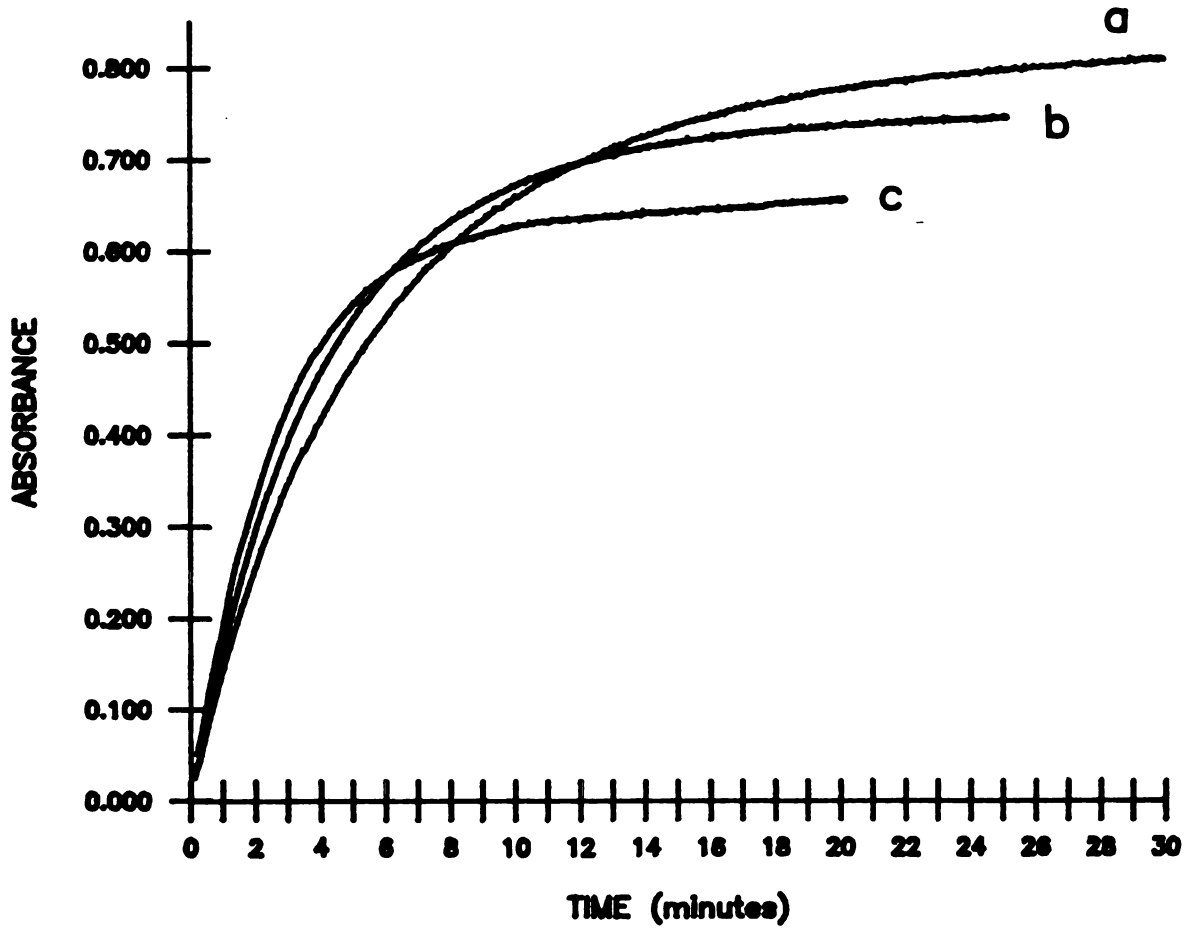

Figure 3-3. Effect of acetic acid concentration on the reaction between 2,4-dichlorobenzaldehyde and o-dianisidine. The o-dianisidine concentration was 4.00 X 10^{-3} M, while the stannic chloride concentration was 2.25 X 10^{-4} M and that of the aldehyde was 6.00 X 10^{-5} M. The concentrations of acetic acid were: a) 7.0 X 10^{-3} M, b) 9.0 X 10^{-2} M, and c) 4.0 X 10^{-1} M.

If stannic chloride were a reagent and not a catalyst, the expected behavior would be a dramatic increase in the equilibrium absorbance due to the formation of more products as the concentration of stannic chloride is increased. This was not the case (Figure 3-4). At all three concentrations the amount of product formed at equilibrium was essentially the same, except for a slight decrease in product formation as the concentration of stannic chloride was increased. Therefore, it can be concluded that stannic chloride is a catalyst, not a reagent. The slight decrease in product formation at high stannic chloride concentrations is believed to arise from some decomposition side reaction. As is shown later, stannic chloride is not recovered in its original form; hence, it is probably better to apply the term activator than catalyst.

5. Determination of pH in Ethanol

Ethanol has a smaller autoprotolysis constant than water (pK_{ETOH} = 19.1, pK_W = 14.0). Consequently, substances dissolved in ethanol are stronger acids and bases than in water. The apparent pH obtained with glass electrodes in nonaqueous solvents can not be directly related to the concentration of solvated hydrogen ions in the medium[53,54]. In other words, two solutions in mixed solvent media of different composition may have the same nominal "pH", but behave in a totally different manner in acid-base reactions. Consequently, it is not a trivial task to perform kinetics experiments in which the actual activity of solvated H^+ in the system is measured. Instead, an approximation is made by assuming that the dissociation of acetic acid is very small relative to its analytical concentration, $[HAc]_o$. The

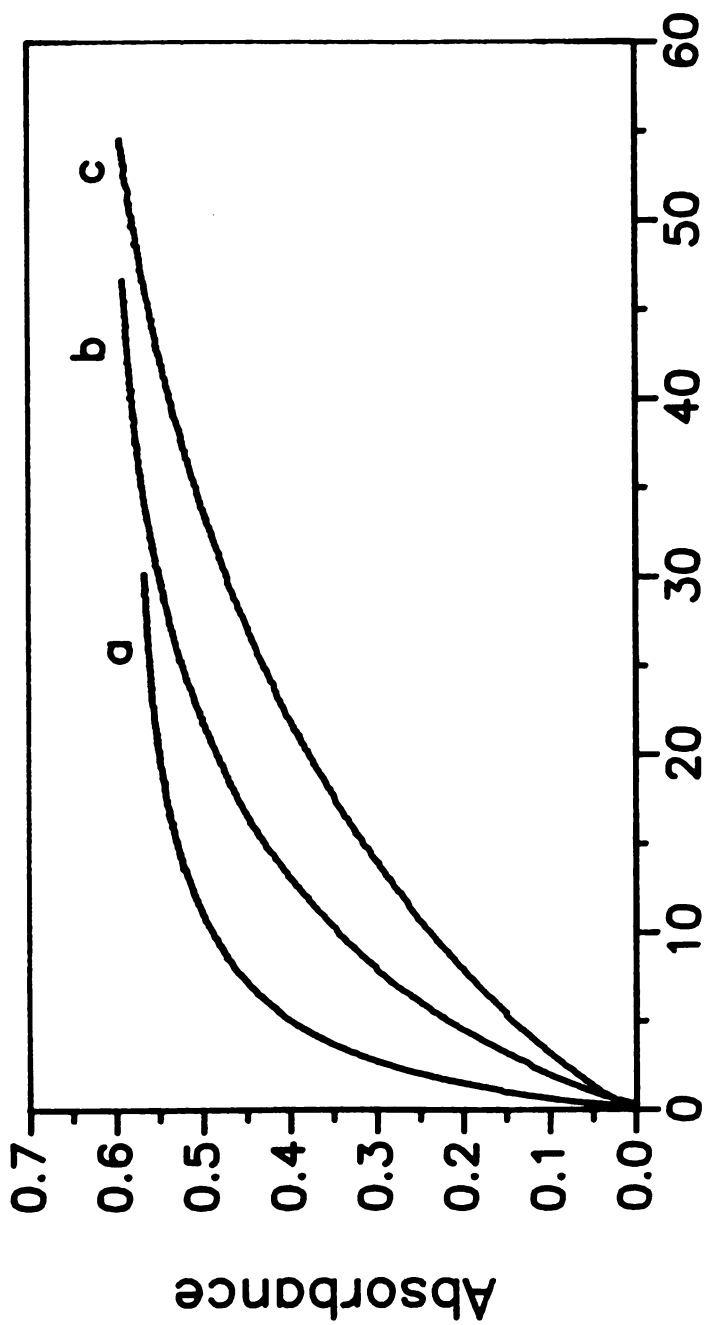

Figure 3-4. Catalytic behavior of stannic chloride. The o-dianisidine concentration was 6.00 X 10^{-3} M, while the acetic acid concentration was 6.00 X 10^{-2} M and that of 2,4-dichlorobenzaldehyde was 5.00 X 10^{-5} M. The concentrations of stannic chloride were: a) 2.54 X 10^{-4} M, b) 6.33 X 10^{-5} M, and c) 1.66 X 10^{-5} M.

value of K_a for acetic acid[55] in ethanol is 5.92×10^{-11} at 25°C and in the absence of electrolytes. This approach also assumes that $[H^+]$ from solvent is negligible, so that $[H^+] = [Ac^-]$. The autoprotolysis constant for ethanol, pK_{ETOH}, is 19.1.

For $HAc \rightleftharpoons H^+ + Ac^-$

$$K_a = \frac{[H^+][Ac^-]}{([HAc]_0 - [H^+])} \qquad \text{if } [H^+] \text{ is small, then}$$

$$K_a = \frac{[H^+]^2}{[HAc]_0}$$

$$[H^+] = \sqrt{K_a}\sqrt{[HAc]_0} \qquad (3.8)$$

In these kinetics studies, the concentration of the solvated H^+ in ethanol was approximated to be proportional to the square root of the acetic acid concentration.

D. Experimental

1. Reagents

a. Ethyl Alcohol

Commercial absolute ethanol was dried using 3A molecular sieves (Davison Chemical, Baltimore, MD). After at least one week, the ethanol was decanted from the molecular sieves and filtered through a 0.40 μm pore filter (Millipore, Bedford, MA).

b. o-Dianisidine

This reagent was obtained commercially under the name 3,3'-dimethoxybenzidine (Eastman Kodak Co., Rochester, NY). The tan-colored o-dianisidine was recrystallized four to five times from ethanol using 50- to 200- mesh activated coconut charcoal as decolorizing agent (Fisher, Livonia, MI). The final product was vacuum dried and stored in a desiccator away from light exposure. The net yield was around 38% of white to off-white crystals. The pure crystals are stable for more than six months if all the solvent is removed before storage. On the other hand, solutions of o-dianisidine needed to be made fresh daily.

c. Stannic Chloride

Anhydrous stannic chloride was obtained commercially in self-sealing bottles (Aldrich, Milwaukee, WI). Syringe techniques were used to prepare stock solutions of stannic chloride from the commercial sealed bottle. A 100 ml volumetric flask with a serum stopper was weighed on the analytical balance after being flushed with dry nitrogen. Then, 7.00 ml of stannic chloride was taken from the commercial sealed

bottle using a syringe and injected into the volumetric flask. After weighing again the volumetric flask, ethanol was injected until the volume of liquid reached the mark. Molarity calculations were based on the weight of stannic chloride obtained not on the volume used. Nitrogen gas was used to replace the volume of stannic chloride taken from the original bottle. Subsequent dilutions of this stock stannic chloride solution ($\approx$ 0.600 M) were made in the open air.

d. Acetic Acid

Glacial acetic acid (EM Science, Gibbstown, NJ) was purified by fractional distillation. Only the fraction boiling at 118°C was used when preparing stock solutions.

2. Procedure

No previous knowledge of the rate law for this particular reaction was available. The method of initial rates was employed to determine an experimental rate law. By using initial rate measurements we hoped to avoid complications with product decomposition observed when high concentrations of stannic chloride are used. The order with respect to a particular reagent was determined in the presence of both catalysts (acetic acid and stannic chloride) and in the presence of each catalyst separately.

The molar ratio of o-dianisidine to aldehyde was never lower than 10:1. This is a necessary precaution to ensure formation of the 1:1 adduct in preference to the 2:1 aldehyde:o-dianisidine adduct, and also to enhance product formation. As the reader may recall from the molar ratio study, there exists an apparent equilibrium which favors product formation as the amount of o-dianisidine is increased.

The general procedure for the kinetics experiments was as follows. The required volume of each solution was added into the 1.0 cm quartz cell using micropipettes. The o-dianisidine solution was added first, followed by the aldehyde solution and mixing. After thermostatting the cell for 5.0 minutes, a 0.50 ml sample of the catalysts mixture was added with a 1.0 ml syringe.

Kinetic data (absorbance at 380 nm versus time) were acquired every second with an IBM compatible personal computer (Bentley T, Round Rock, TX) interfaced to the thermostatted, modular, single-beam Heath spectrophotometer. The interfacing program (named ABS-SEC), initially developed by Dr. Peter D. Wentzell was modified to use an IBM data acquisition board (Mendelson Electronics Co. Inc., Dayton, OH). After data acquisition, the initial rate was calculated for each run by dividing the initial slope of the absorbance versus time plot by the molar absorptivity of the colored product, in our case, the 1:1 o-dianisidine adduct of 2,4-dichlorobenzaldehyde. The initial slope for each run was determined using a graphical slope-calculating program (named ROCALC) written in Quick BASIC by Dr. P. D. Wentzell. For each set of conditions, the initial rate measurements were always made in triplicate.

Temperature was maintained at 40.0 ± 0.2°C by circulating water from a constant temperature bath around the cell in the sample compartment. All solutions were kept at 40°C for at least fifteen minutes prior to use.

3. Determination of Reaction Orders

Reaction orders were evaluated by carrying out experiments in which the concentrations of all but one of the reagents were kept constant. The reaction order was determined from the slope of the plot of the logarithm of the initial rate against the logarithm of the concentration of the reagent varied. In some cases, linear plots were not obtained throughout the concentration ranges used. This is sometimes due to changes in reaction orders, as for acetic acid and o-dianisidine. In other cases, decomposition of an intermediate or the product as the concentration of a particular reagent is increased could also be the cause, as was the case for stannic chloride. Any proposed rate law should account for the observed effect of orders for every reagent besides giving a good fit to all the experimental data over wide ranges of concentration.

In the case of stannic chloride, it was not possible to use a wide concentration range. As the concentration of this reagent was increased a side reaction which caused decomposition of the product or of an intermediate became more evident.

4. Curve Fitting

A general-purpose curve-fitting program was used to test the agreement of the experimental data with the predictions of a variety of possible rate laws. This program, known as KINFIT, was developed by Dye and Nicely[56]. KINFIT is a FORTRAN program to fit equations to data using the least-squares approach[57]. If the relative variances are specified for the dependent and independent variables, the program will give the best fit by weighting each data point according to its relative

error. KINFIT also provides the user with a listing of the standard error in the parameters and the extent of coupling between them.

A single rate law was found which gave a reasonable fit for all the conditions studied in the kinetic experiments. In all the log-log plots that follow, the error bars represent the experimental points plus or minus one standard deviation (calculated from three determinations). The solid line represents the fit of the best rate law obtained to the particular set of experimental points as calculated in the KINFIT global fit of all the data points to that particular rate law.

E. Results

In this section, the dependence of the initial rate on the concentrations of the reagents is described followed by the presentation of the best empirical rate law.

1. Dependence on Aldehyde Concentration

The dependence of the initial rate of the reaction on the concentration of 2,4-dichlorobenzaldehyde using stannic chloride as catalyst, acetic acid as catalyst, or a mixture of stannic chloride and acetic acid as catalyst is shown in Figures 3-5, 3-6, and 3-7, respectively. The concentration of the aldehyde was varied from 6.31×10^{-6} M to 3.98×10^{-4} M. The concentration of the o-dianisidine was 6.31×10^{-3} M in all three cases. The calculated order from the log-log plots of rate versus the aldehyde concentration was found to be 0.93 ± 0.06 for stannic chloride catalysis, 0.87 ± 0.03 for acetic acid catalysis, and 0.86 ± 0.05 for a mixture of both catalysts. The order with respect to the aldehyde was taken to be 1.0 in the KINFIT curve fitting.

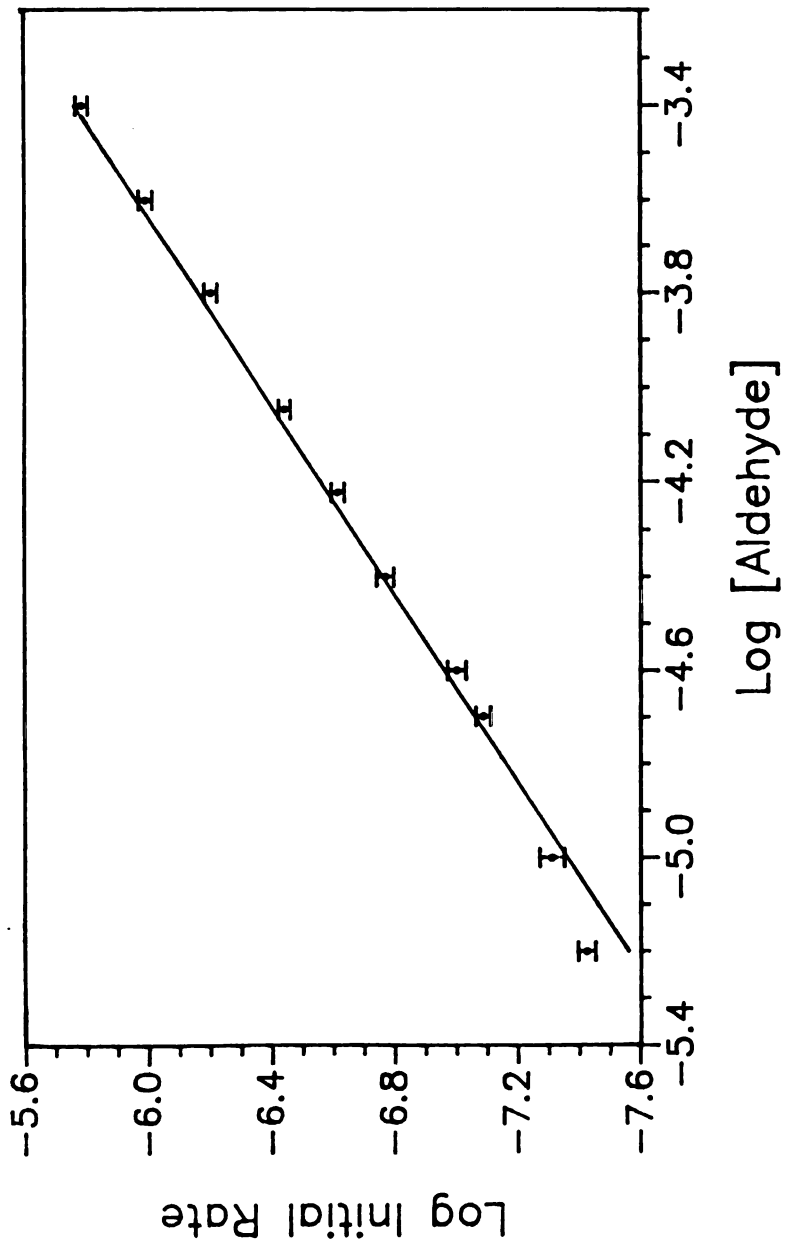

Figure 3-5. Initial rate vs. aldehyde concentration for stannic chloride catalysis. The o-dianisidine concentration was 6.31 X 10^{-3} M, while the stannic chloride concentration was 3.98 X 10^{-4} M. The error bars represent the experimental points ± one standard deviation. The solid line represents the fit of the best rate law obtained.

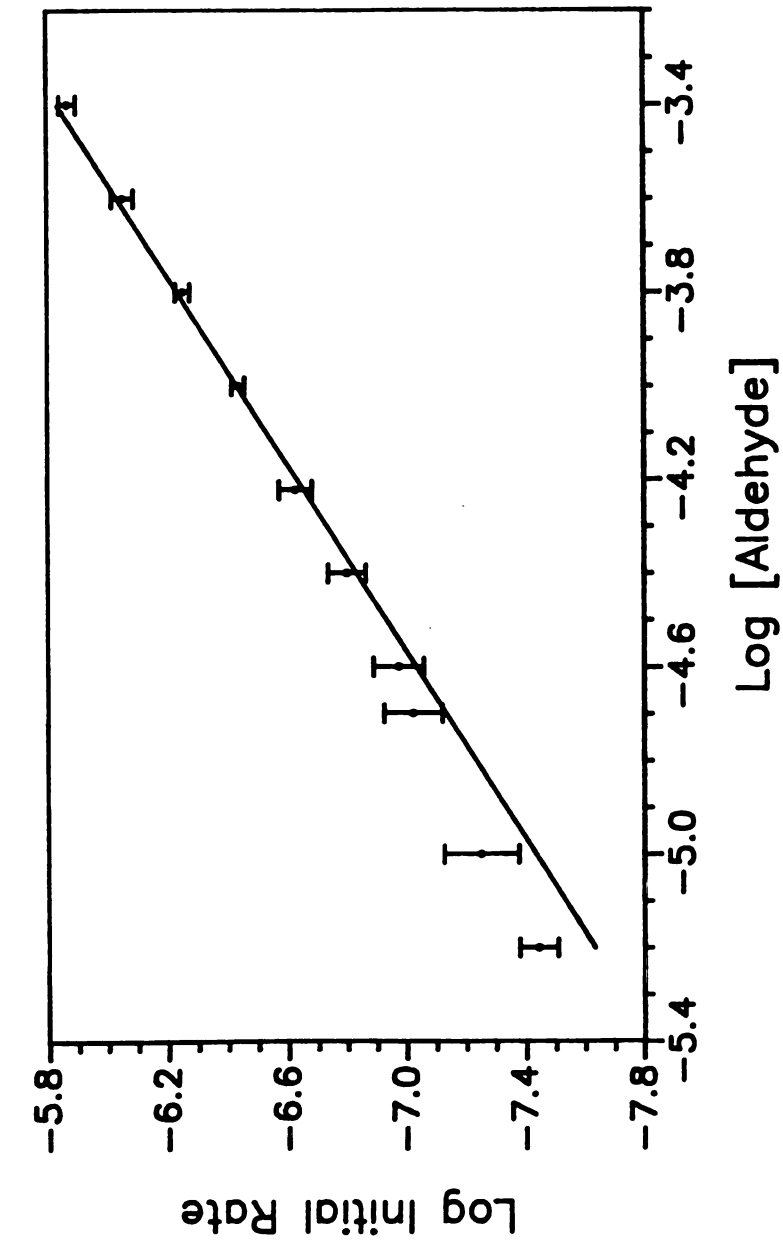

Figure 3-6. Initial rate vs. aldehyde concentration for acetic acid catalysis. The o-dianisidine concentration was 6.31 X 10^{-3} M, while the acetic acid concentration was 1.00 M. The error bars represent the experimental points ± one standard deviation. The solid line represents the fit of the best rate law obtained.

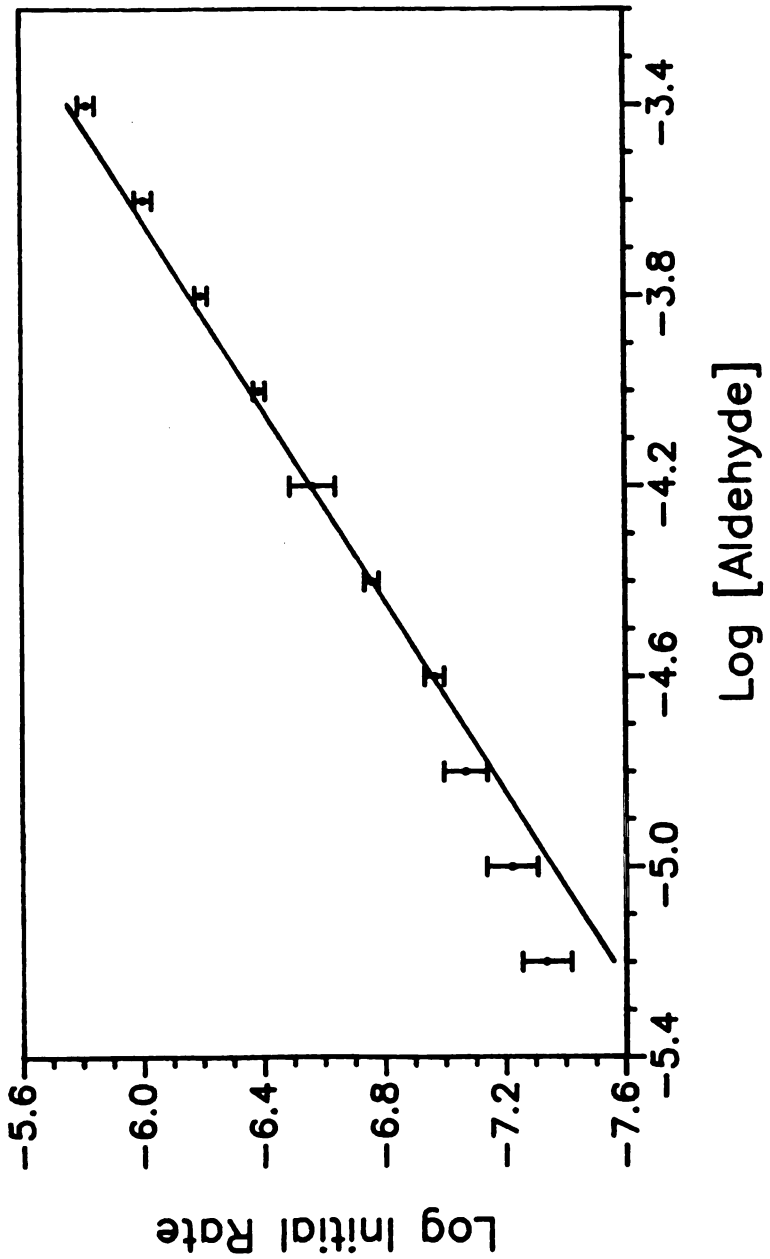

Figure 3-7. Initial rate vs. aldehyde concentration for a mixture of stannic chloride and acetic acid as catalysts. The o-dianisidine concentration was 6.31×10^{-3} M, while the stannic chloride concentration was 2.51×10^{-4} M, and the acetic acid concentration was 0.562 M. The error bars represent the experimental points ± one standard deviation. The solid line represents the fit of the best rate law obtained.

2. Dependence on Stannic Chloride Concentration

Figures 3-8 and 3-9 show the dependence of the initial rate of the reaction on the concentration of stannic chloride in the absence and in the presence of 1.00×10^{-2} M acetic acid respectively. The concentration of stannic chloride was varied from 1.00×10^{-6} M to 2.51×10^{-3} M in both cases. At concentrations below 1.59×10^{-5} M in stannic chloride, the reaction rate becomes immeasurably slow (Figure 3-9). At these low concentrations of stannic chloride, when acetic acid is present, the reaction that occurs is due to the acetic acid only (Figure 3-9). The effect of the stannic chloride at these very low concentrations of acetic acid is to cause decomposition of product or an intermediate formed by the acetic acid catalyzed reaction. The order with respect to stannic chloride at low concentrations was found to be 1.8 ± 0.6 in both cases. At higher concentrations the log-log plot begins to curve, and the reaction order goes even to negative values at concentrations of stannic chloride higher than 2.50×10^{-3} M. This suggests the occurrence of a decomposition side reaction as the concentration of stannic chloride is increased. When the KINFIT program was used to fit the data, four stannic chloride dependent terms were found in the rate law (page 56). One term appeared in the acetic acid catalyzed pathway, accounting for the decomposition observed at low stannic chloride concentration, in the presence of acetic acid. Two terms in the stannic chloride catalyzed pathway, one in the numerator, and the other in the denominator, both account for a forward reaction. The fourth term appeared also in the denominator of the stannic chloride

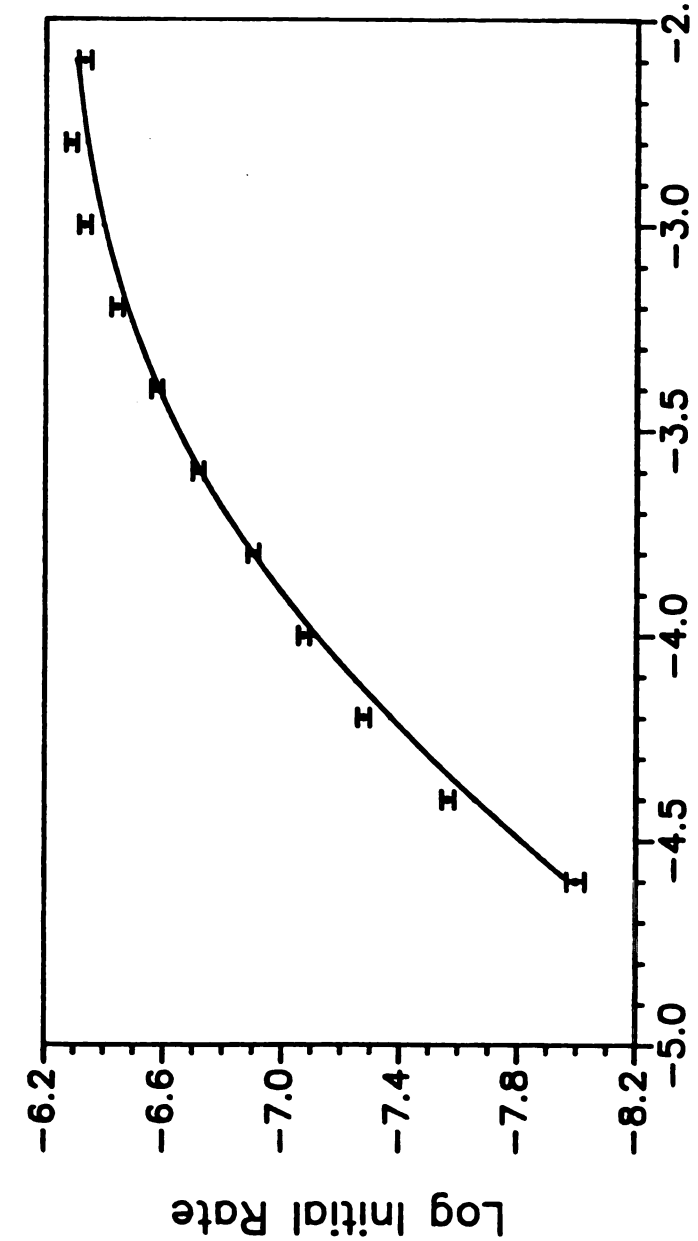

Figure 3-8. Initial rate vs. stannic chloride concentration in the absence of acetic acid. The o-dianisidine concentration was 6.31×10^{-3} M, while the aldehyde concentration was 6.00×10^{-5} M. The error bars represent the experimental points ± one standard deviation. The solid line represents the fit of the best rate law obtained.

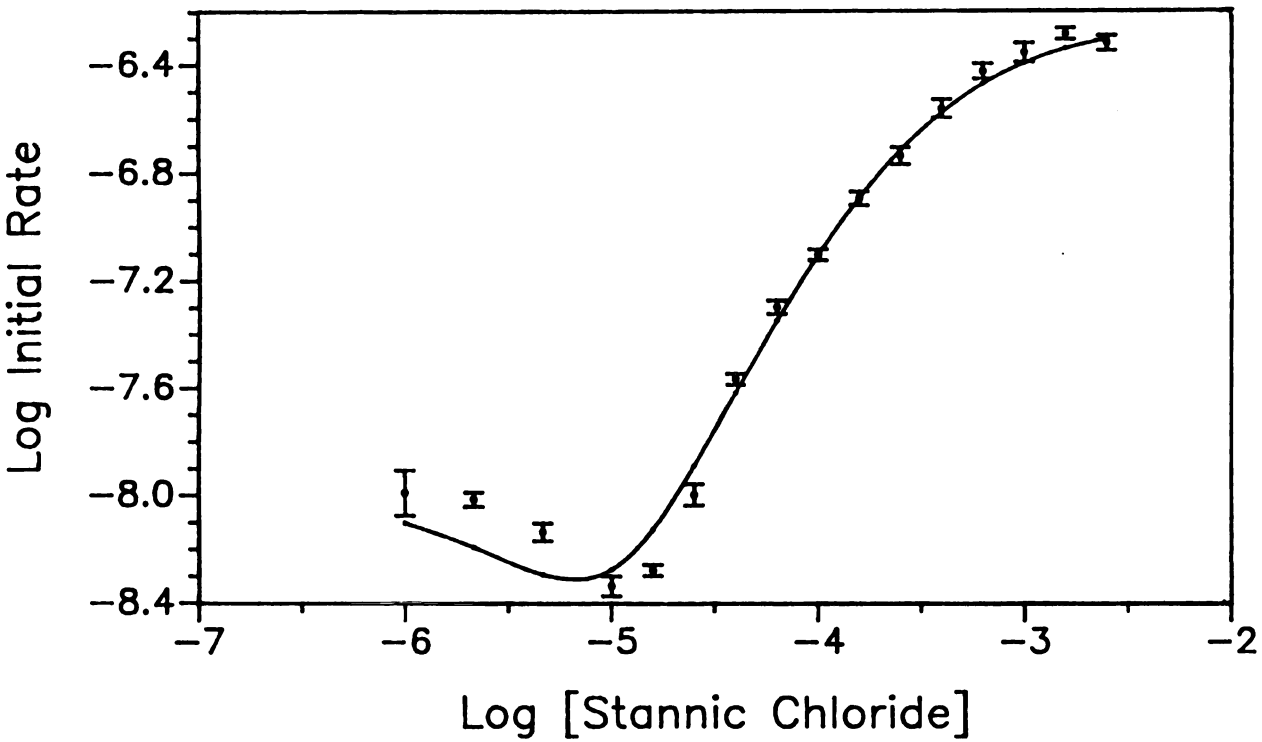

Figure 3-9. Initial rate vs. stannic chloride concentration in the presence of 0.0100 M acetic acid. The o-dianisidine concentration was 6.31 X 10^{-3} M, while the aldehyde concentration was 6.00 X 10^{-5} M. The error bars represent the experimental points ± one standard deviation. The solid line represents the fit of the best rate law obtained.

pathway; it accounts for the decomposition observed at high stannic chloride concentrations.

3. Dependence on o-Dianisidine Concentration

The dependence of the initial rate of the reaction on the concentration of o-dianisidine in the presence of acetic acid and/or stannic chloride is shown in Figures 3-10 to 3-13. The concentration of o-dianisidine was varied from 6.31 X 10^{-4} M to 0.0126 M. The lower limit of the concentration range was set by the requirement that the o-dianisidine to aldehyde ratios were greater than 10:1. The upper limit was set by the solubility of o-dianisidine in ethanol. The o-dianisidine in the stock solution began to precipitate at concentrations higher than 0.03 M.

Figures 3-10 and 3-11 show log-log plots of initial rate versus the o-dianisidine concentration at acetic acid concentrations of 0.01768 M and 0.562 M, respectively. At concentrations of o-dianisidine lower then 3.16 X 10^{-3} M, the slope of the log-log plot was found to be 0.73 ± 0.1 for Figure 3-10, and 0.86 ± 0.06 for Figure 3-11. Both orders decreased to lower values as the o-dianisidine concentration increased.

The rate law obtained using the KINFIT program contains two terms in the acetic acid catalyzed pathway. Both of the terms involve o-dianisidine with an order of 1.0 in the numerator, but one of them has an o-dianisidine term in the denominator. As the concentration of acetic acid increases the term involving o-dianisidine only in the numerator becomes increasingly important. Hence, the order with respect to o-dianisidine increases as the acetic acid concentration increases.

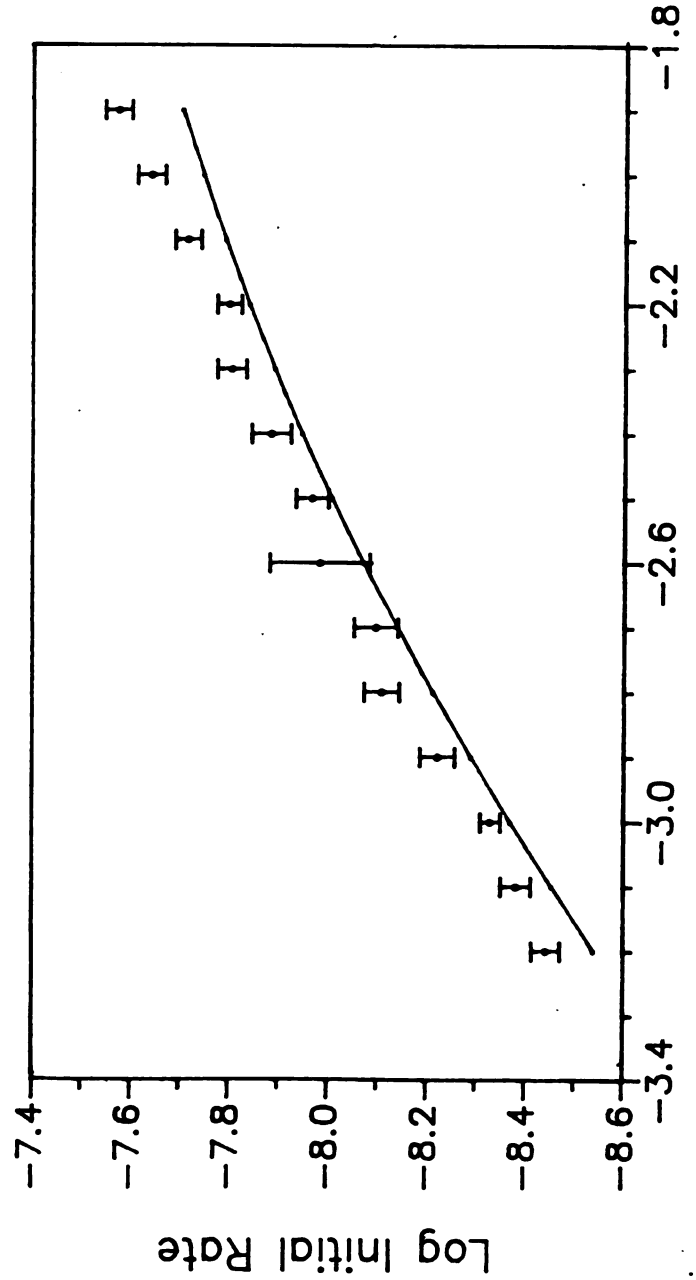

Figure 3-10. Initial rate vs. o-dianisidine concentration for acetic acid catalysis. The aldehyde concentration was 6.00 X 10^{-5} M, while the acetic acid concentration was 0.0178 M. The error bars represent the experimental points ± one standard deviation. The solid line represents the fit of the best rate law obtained.

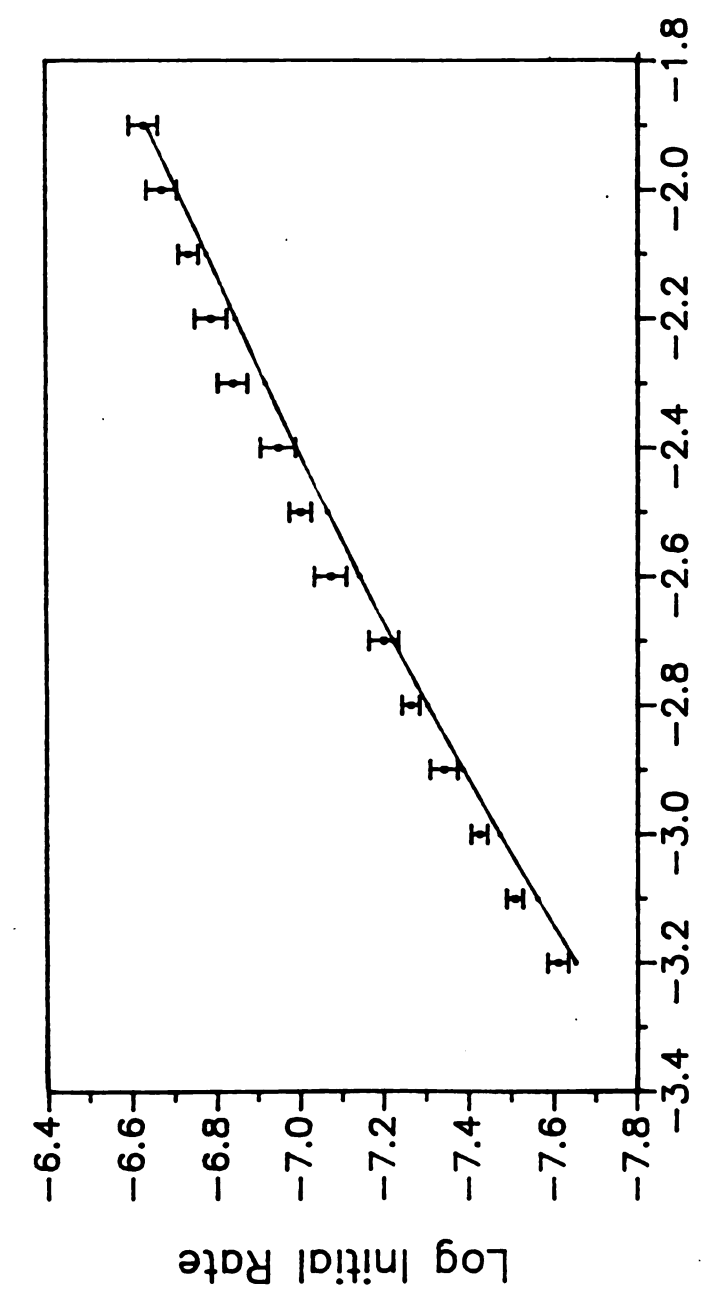

Figure 3-11. Initial rate vs. o-dianisidine concentration for acetic acid catalysis. The aldehyde concentration was 6.00 X 10^{-5} M, while the acetic acid concentration was 0.562 M. The error bars represent the experimental points ± one standard deviation. The solid line represents the fit of the best rate law obtained.

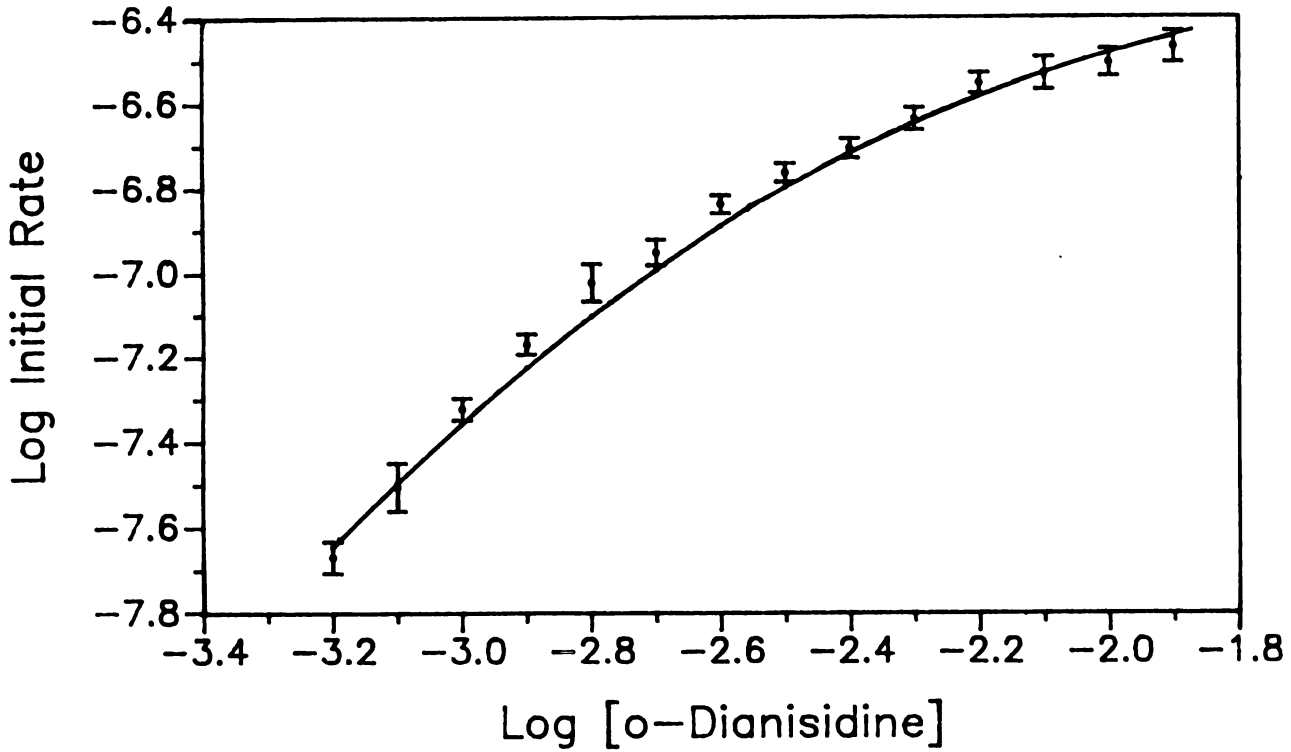

Figure 3-12. Initial rate vs. o-dianisidine concentration in the presence of 3.98 X 10^{-4} M stannic chloride as catalyst. The aldehyde concentration was 6.00 X 10^{-5} M. The error bars represent the experimental points ± one standard deviation. The solid line represents the fit of the best rate law obtained.

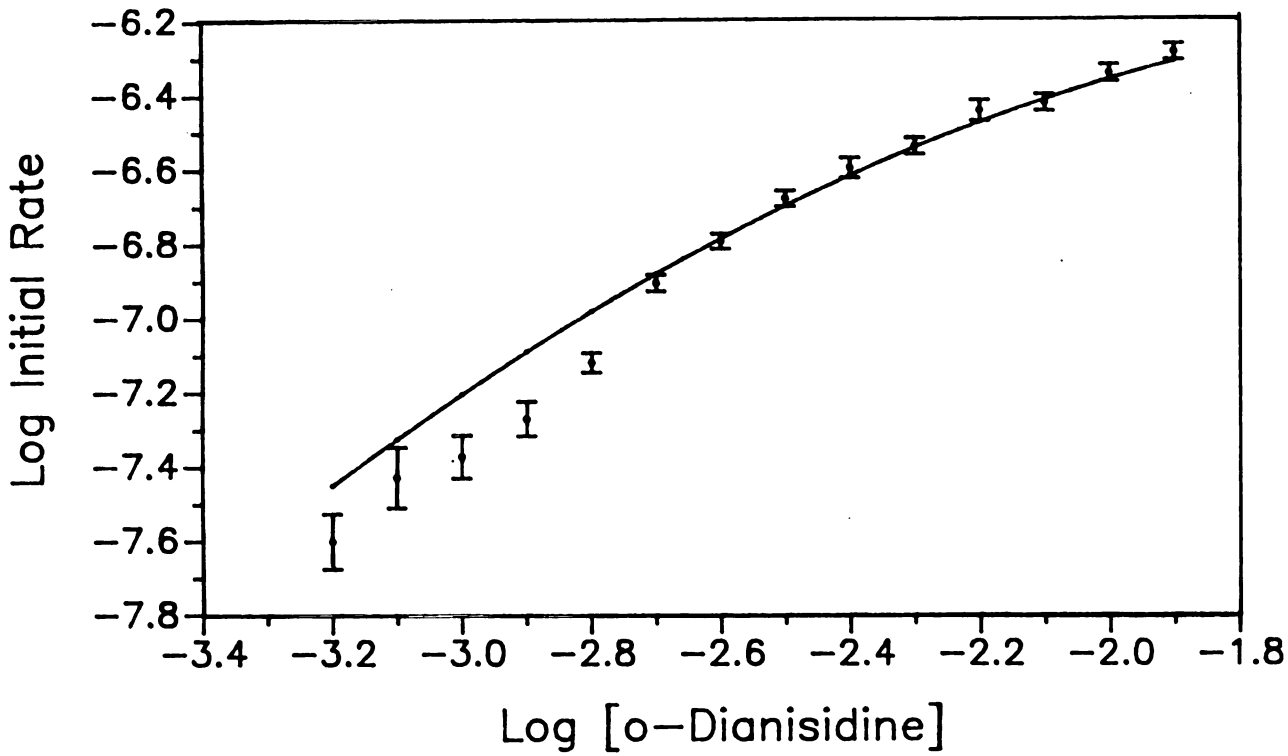

Figure 3-13. Initial rate vs. o-dianisidine concentration in the presence of 6.31 X 10^{-4} M stannic chloride and 0.0100 M acetic acid as catalysts. The aldehyde concentration was 6.00 X 10^{-5} M. The error bars represent the experimental points ± one standard deviation. The solid line represents the fit of the best rate law obtained.

Plots of log initial rate versus log o-dianisidine concentration are shown for stannic chloride catalysis (Figure 3-12), and for stannic chloride and acetic acid catalysis (Figure 3-13). The order with respect to o-dianisidine was found to be 1.7 ± 0.2 in the absence of acetic acid and 1.3 ± 0.3 in its presence. Again, both orders decrease to lower values as the o-dianisidine concentration increases.

The order of 1.3 for o-dianisidine when the mixture of the catalysts was employed suggests a simultaneous formation of product via two paths. The acetic acid catalyzed path is first order with respect to o-dianisidine, while the stannic chloride catalyzed path is second order.

The data used for the o-dianisidine log-log plots (Figures 3-10 through 3-13) are less precise than the data obtained for varying other reagent's concentration. These larger standard deviations account for the poorer fit of these data to the rate law. Because of the poorer precision, KINFIT weights the o-dianisidine data less heavily than data from the variation of other reagents.

4. Dependence on Acid Concentration

The concentration of the solvated H^+ in ethanol was approximated to be proportional to the square root of the acetic acid concentration (Equation 3.8). The dependence of the initial rate on the solvated H^+ concentration is affected by the concentration of o-dianisidine. At low o-dianisidine concentration (6.39×10^{-4} M) as in Figure 3-14, the reaction order with respect to H^+ was found to be 1.46 ± 0.05 (dashed line). As the concentration of o-dianisidine is increased to

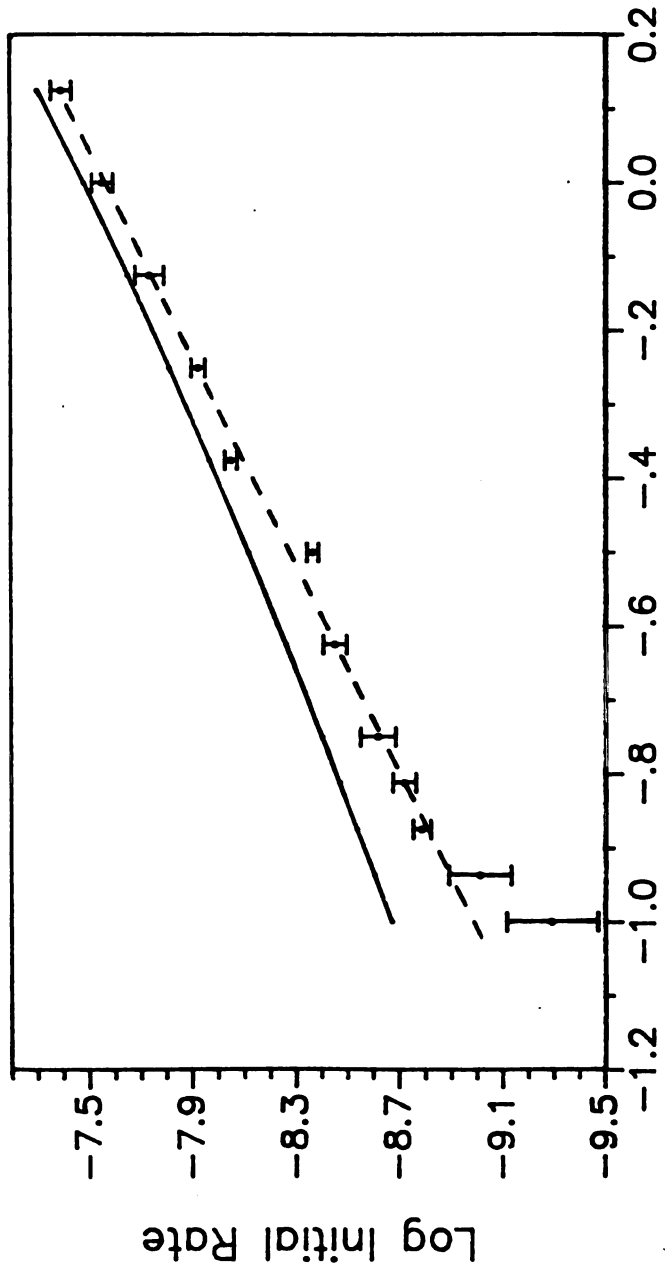

Figure 3-14. Initial rate vs. hydrogen ion concentration at 6.31×10^{-4} M o-dianisidine. The aldehyde concentration was 6.00×10^{-5} M. The error bars represent the experimental points ± one standard deviation. The solid line represents the fit of the best rate law obtained. An order of 1.46 was calculated from the slope of the dashed line.

6.31×10^{-3} M, 1.50×10^{-2} M, and 0.0240 M (Figures 3-15 to 3-17 respectively), a gradual break in the initial rate profile of the log-log plots begins to appear as shown by the dashed line in Figure 3-17. This suggests a change in order with respect to H^+ as the concentration of o-dianisidine increases. In Figure 3-17, the orders were 1.14 at concentrations of acetic acid between 1.00×10^{-2} M and 5.62×10^{-2} M, and 2.00 at concentrations between 1.78×10^{-1} M and 1.78 M. At low concentrations of o-dianisidine (Figure 3-14), a mixed order is observed.

The rate law obtained using the KINFIT program contains two terms in the acetic acid catalyzed portion which account for the experimentally determined orders for the H^+ rate dependence.

Figure 3-18 shows the dependence of the initial rate of the reaction on the concentration of H^+, but with stannic chloride also present. At low concentrations of acetic acid, the order with respect to H^+ is essentially zero. This indicates that the reaction is catalyzed primarily by stannic chloride in preference over acetic acid. Once the concentration of acetic acid is larger than 0.178 M, the effect of acetic acid as a catalyst begins to be observed. Stannic chloride is a better catalyst than acetic acid because much smaller concentrations of stannic chloride are needed to effect the same response as with acetic acid.

5. Experimental Rate Law

A global fit of all the experimental points to a variety of possible rate laws was undertaken using the KINFIT[56] curve fitting program. To guide the search for the best experimental rate law, the

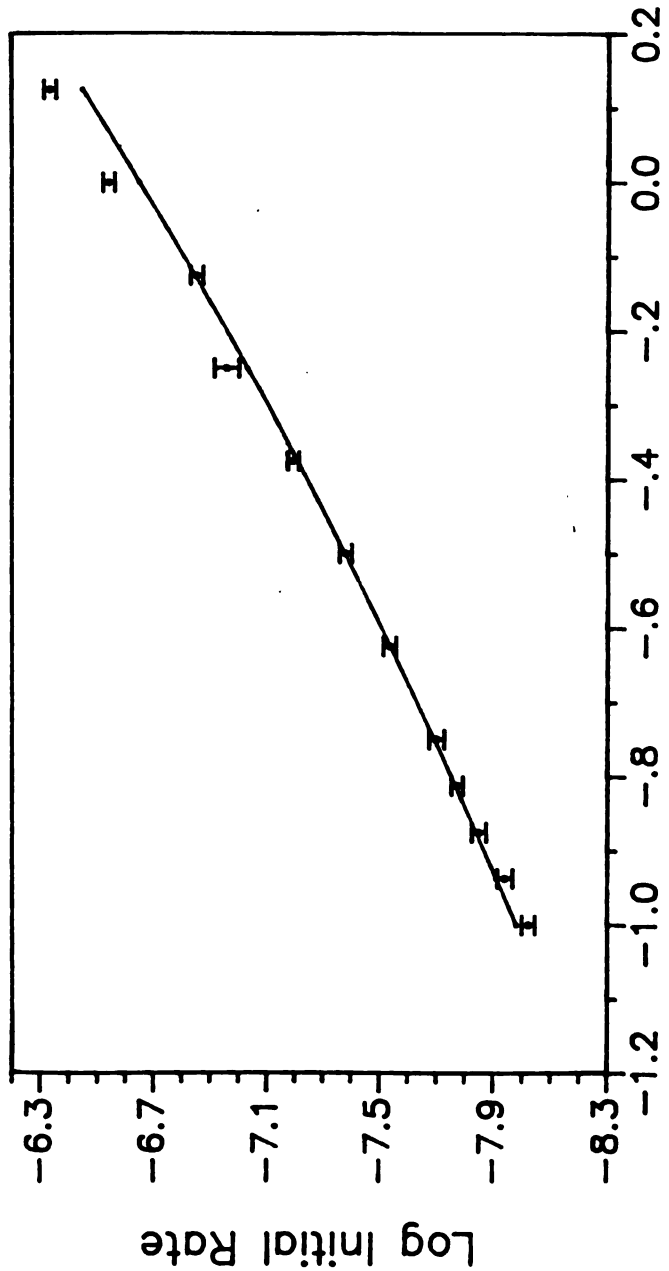

Figure 3-15. Initial rate vs. hydrogen ion concentration at 6.31×10^{-4} M o-dianisidine. The aldehyde concentration was 6.00×10^{-5} M. The error bars represent the experimental points ± one standard deviation. The solid line represents the fit of the best rate law obtained.

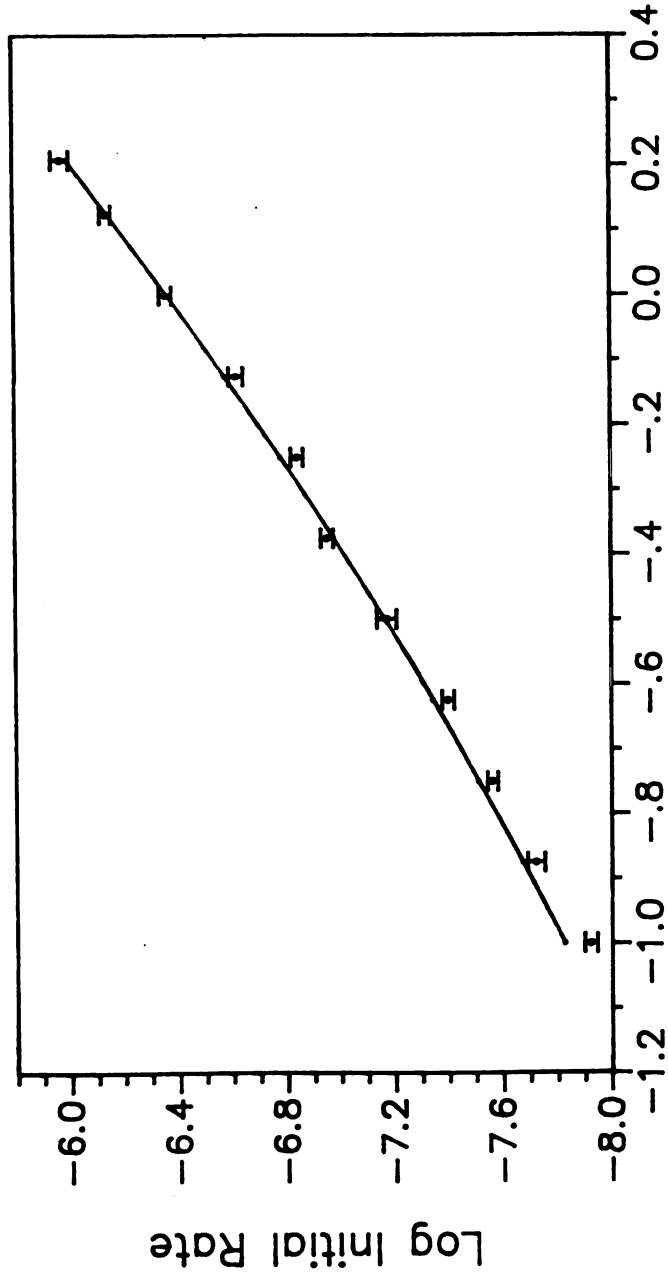

Figure 3-16. Initial rate vs. hydrogen ion concentration at 0.0150 M o-dianisidine. The aldehyde concentration was 6.00 X 10^{-5} M. The error bars represent the experimental points ± one standard deviation. The solid line represents the fit of the best rate law obtained.

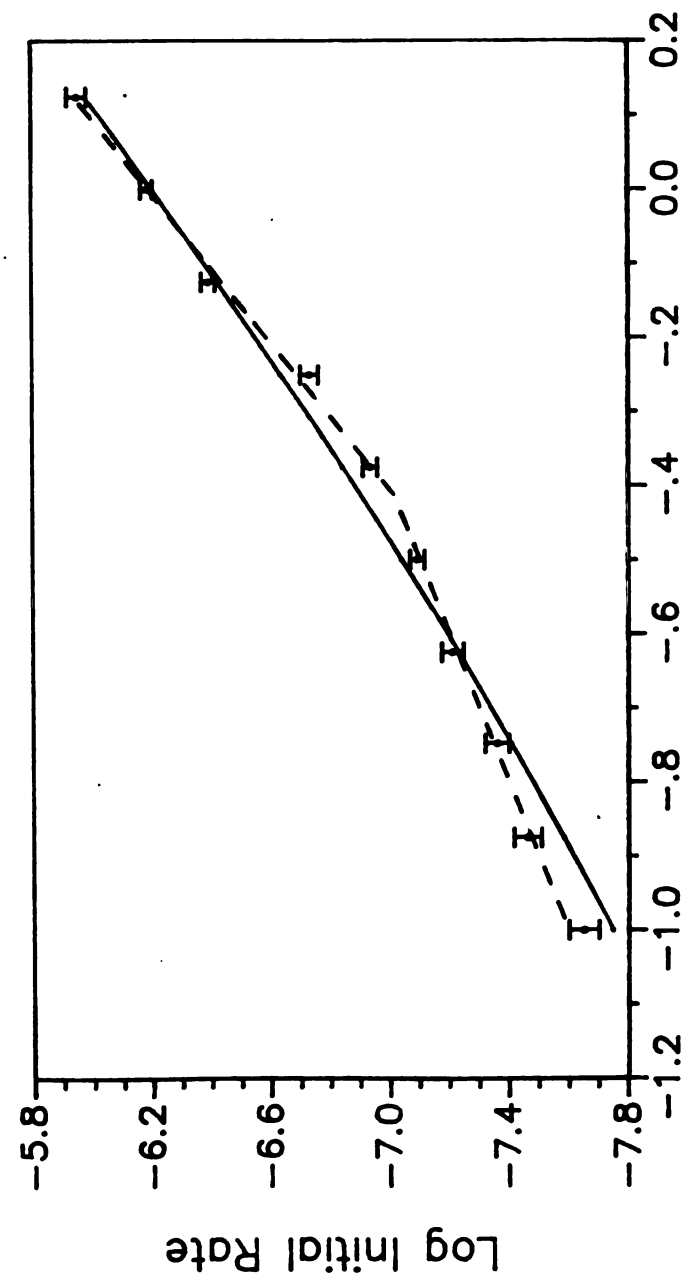

Figure 3-17. Initial rate vs. hydrogen ion concentration at 0.0240 M o-dianisidine. The aldehyde concentration was 6.00 X 10^{-5} M. The error bars represent the experimental points ± one standard deviation. The solid line represents the fit of the best rate law obtained. The dashed line illustrates the break in the initial rate profile as the concentration of acetic acid increases.

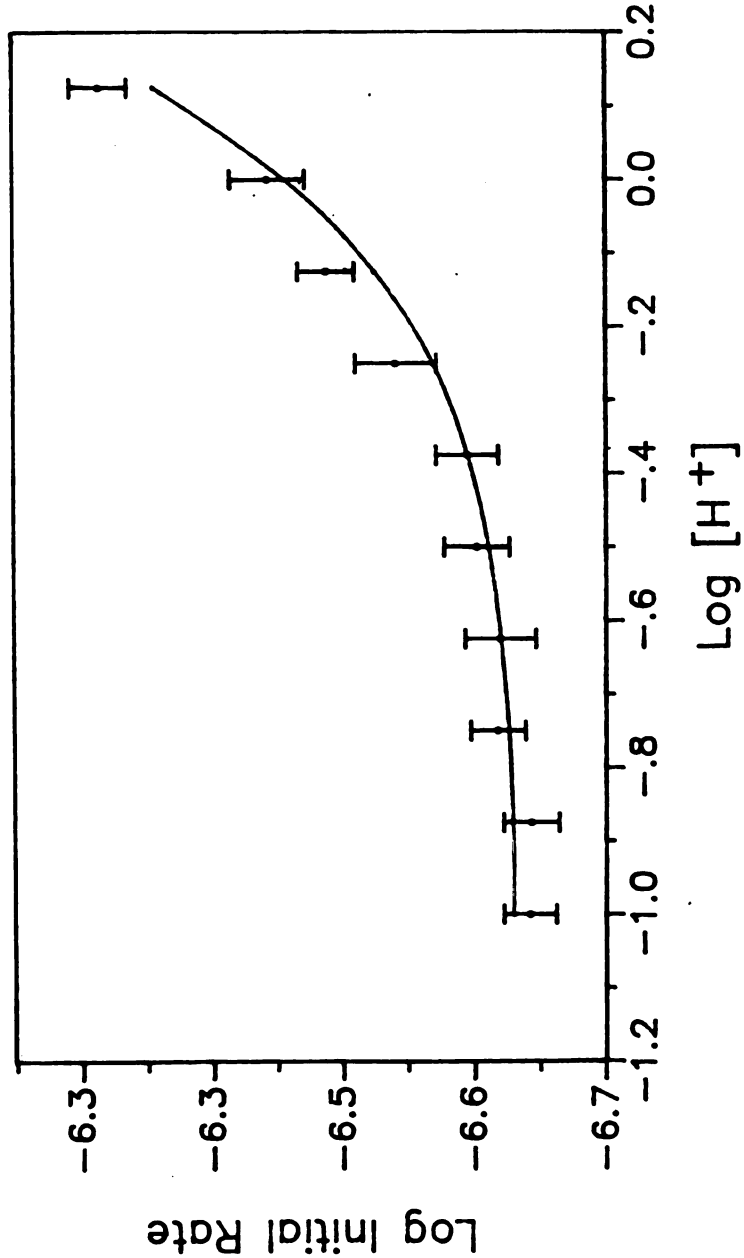

Figure 3-18. Initial rate vs. hydrogen ion concentration for mixtures of stannic chloride and acetic acid as catalysts. The o-dianisidine concentration was 6.31 X 10^{-3} M, while the stannic chloride concentration was 3.98 X 10^{-4} M. The error bars represent the experimental points ± one standard deviation. The solid line represents the fit of the best rate law obtained.

known mechanisms for Schiff base formation in water were used along with the experimental orders found. To derive rate expressions from the mechanisms, letters were used to represent the species involved as follows: A = 2,4-dichlorobenzaldehyde, B = o-dianisidine, H^+ = solvated hydrogen ion, and S = stannic chloride. About 450 rate laws were tested, of which the one below gave the best fit.

$$\text{Rate} = [A]\left[\text{Par}(1)\,[B]\,[H^+]^2 + \frac{\text{Par}(2)\,[B]\,[H^+]}{1 + \text{Par}(3)\,[B] + \text{Par}(7)\,[S]} + \frac{\text{Par}(4)\,[S]^2\,[B]^2}{\text{Par}(6) + \text{Par}(5)\,[S]^2\,[B] + [S]\,[B]^2}\right] \quad (3.9)$$

Par(1) to Par(7) are parameters that represent products of rate constants or ratios of rate constants. The statistical figures of merit for the experimental rate law as calculated by the KINFIT program are listed in Table 3-1. A proper estimate of the reliability of the proposed rate law should use the standard deviation of the parameters rather than the correlation coefficient. Regardless of the possible correlations among the parameters for the equation that was used, the particular parameter is reliable to an extent given by the estimate of the standard deviation. By inspection of Table 3.1, we can see that the standard deviations for parameters one through six are small in comparison to the actual value for the parameters. The parameter with the largest standard deviation is parameter seven. Parameter seven accounts for the decomposition in the acetic acid pathway caused by stannic chloride as observed in Figure 3-9. Only five data points were used to characterize this portion of the curve and one of them has a very high standard deviation. Consequently, the reliability of

parameter seven as calculated by KINFIT was less than for the other parameters for which more precise data were used.

The fit of the experimental rate law to the actual experimental data points is acceptable considering that a simultaneous global fit of all the experimental data points to a single equation was performed. The experimental values plus or minus one standard deviation is roughly equal to a 68% confidence interval.

Once the proposed mechanism is presented, the parameters in the rate law will be replaced by the corresponding rate and/or equilibrium constants.

Table 3-1. Figures of merit of the experimental rate law.

Parameter	Value	Std. Dev.	Mul. Corr. Coef.
1	0.344	0.018	0.72
2	0.604	0.074	0.95
3	24.1	4.8	0.95
4	22.5	1.3	0.97
5	14.7	1.4	0.95
6	2.14×10^{-9}	2.5×10^{-10}	0.83
7	9.76×10^{5}	3.1×10^{5}	0.55

F. Discussion

In this section a mechanism is proposed for the reaction between o-dianisidine and aromatic aldehydes based on the experimental rate law obtained and the mechanism for Schiff base formation in water.

1. Proposed Mechanism

Useful working rules for deriving a mechanism from the stoichiometric equation and the empirical rate law can be found in the paper by Edwards, Greene, and Ross[58]; and in chapter five of Espenson's book[59]. Of the very few mechanisms that can be written to agree with the empirical rate law, only one was chemically plausible. In this proposed mechanism, there are three distinct paths. Two paths are catalyzed by acetic acid, the other by stannic chloride. For the sake of clarity, the mechanism for each path will be presented separately. In each mechanism, letters are used to represent the species involved: A = 2,4-dichlorobenzaldehyde, B = o-dianisidine, S = stannic chloride, and H^+ = solvated hydrogen ion.

a. Acetic acid path at low acetic acid concentrations

The mechanism described next will be the preferred path at low acetic acid concentrations or when the concentration of o-dianisidine is large relative to that of the acid. At small concentrations of acetic acid, Step 1 is relatively slow . Therefore, the steady-state approach can be used to find an expression for the concentration of intermediate A^+H. Since initial rates were determined, the reverse of Step 2 was neglected.

STEP 1 $$A + H^+ \underset{k_{-1}}{\overset{k_1}{\rightleftharpoons}} A^+H$$

STEP 2 $$A^+H + B \underset{k_{-2}}{\overset{k_2}{\rightleftharpoons}} AHB^+$$

Post-Equilibria:

$$AHB^+ \rightleftharpoons \text{Product} + H_2O + H^+ \text{ fast}$$

Side Reaction: $$A^+H + S \xrightarrow{k_d} \text{decomposition}$$

$$\frac{d[A^+H]}{dt} = k_1[A][H^+] - k_{-1}[A^+H] - k_2[A^+H][B] - k_d[A^+H][S] = 0 \qquad (3.10)$$

$$[A^+H] = \frac{k_1[A][H^+]}{k_{-1} + k_2[B] + k_d[S]} \qquad (3.11)$$

Since all of the steps following Step 2 are rapid, the rate of product formation is given by the rate of Step 2 (with the back reaction negligible).

$$\text{rate} = \frac{d[\text{product}]}{dt} = k_2[A^+H][B] \qquad (3.12)$$

After substitution of the concentration of intermediate A^+H in Equation 3.12, the same rate expression as the midle term in the experimental rate law is obtained;

$$\text{rate} = \frac{k_1 k_2 [A] [H^+] [B]}{k_{-1} + k_2 [B] + k_d [S]} \qquad (3.13)$$

where:

$$\text{Par (2)} = \frac{k_1 k_2}{k_{-1}}$$

$$\text{Par (3)} = \frac{k_2}{k_{-1}}$$

$$\text{Par (7)} = \frac{k_d}{k_{-1}}$$

Another possible mechanism that satisfies the rate expression for the reaction path at low acetic acid concentration predicts that the [B] term in the denominator accounts for product decomposition as shown below:

Pre-Equilibria: $A + H^+ \rightleftharpoons \overset{+}{A}H$

STEP 1 $\overset{+}{A}H + B \underset{k_{-1}}{\overset{k_1}{\rightleftharpoons}} AHB^+$

STEP 2 $AHB^+ \overset{\sim H}{\rightleftharpoons} \overset{+}{H}AB$

Post-Equilibria: $\overset{+}{H}AB \rightleftharpoons$ Product + H_2O fast

Side Reactions: $AHB^+ + B \longrightarrow BH + A + B$

$AHB^+ + S \longrightarrow$ decomposition

This mechanism was disregarded because of the following reasons:

i) Decomposition by base should involve the stronger base present, acetate not o-dianisidine.

ii) In this mechanism AHB^+ is the steady-state intermediate. Therefore, the rate expression should reflect the effect of proton removal from AHB^+ aided also by o-dianisidine. This would involve the appearance of a $[B]^2$ term in the numerator, which is not observed.

iii) If proton loss from intermediate AHB^+ is so fast as to not to require base catalysis, then proton addition to form the H_2O^+ leaving group should be observed. Rate-determining addition of a proton requires the appearance of an $[H^+]$ term in the denominator of the rate expression. In water as the solvent, the rate-determining addition of a proton is observed (page 22). In ethanol as the solvent, rate-determining addition of a proton was not observed.

iv) If proton removal and addition are very fast, then carbon-oxygen bond cleavage during the dehydration of the carbinolamine intermediate must be rate determining. Anhydrous ethanol is depleted of water molecules and is less viscous than water. Contrary to this mechanism's predictions, carbon-oxygen bond cleavage should be easier than in water.

b. Acetic acid path at high acetic acid concentrations

At high acetic acid concentrations, Step 1 in the previous mechanism is rapid. Consequently, there is a fast and large production of intermediate A^+H in a pre-equilibrium step. At this high concen-

tration of acetic acid most of the o-dianisidine should also be protonated. Therefore, a plausible mechanism is that the A^+H intermediate is attacked by protonated o-dianisidine rather than by neutral o-dianisidine giving rise to a different path for product formation. The mechanism for this new path is presented next.

Pre-Equilibria:

$$A + H^+ \rightleftharpoons A^+H \qquad K_{AH} = \frac{[A^+H]}{[A][H^+]}$$

$$B + H^+ \rightleftharpoons B^+H \qquad K_{BH} = \frac{[B^+H]}{[B][H^+]}$$

Rate Determining Step:

$$A^+H + B^+H \underset{k''_{-1}}{\overset{k''_1}{\rightleftharpoons}} AHB^+ + H^+$$

Post-Equilibria:

$$AHB^+ \rightleftharpoons \text{Product} + H_2O + H^+ \quad \text{fast}$$

The protonated species A^+H and B^+H originate in equilibria prior to the rate-determining step. After substituting for the concentration of A^+H and B^+H in the rate expression in terms of the concentration of the initial reactants, Equation 3.15 is obtained. Equation 3.15 agrees with the first term in the experimental rate law. In the experimental rate law Par(1) stands for $k''_2 K_{AH} K_{BH}$.

$$\text{rate} = \frac{d[\text{product}]}{dt} = k''_1 [A^+H][B^+H] \tag{3.14}$$

$$\text{rate} = k''_1 K_{AH} K_{BH} [A][B][H^+]^2 \tag{3.15}$$

In a separate set of experiments, the existence of o-dianisidine as a free, a mono, and/or a diprotonated species was investigated. These experiments consisted of pH titrations of o-dianisidine versus standardized glacial acetic acid in anhydrous ethanol and versus standardized HCl, also in anhydrous ethanol. In the region for the expected addition of the first proton, a buffer region was observed at a "pH" of about 3.05. A sudden decrease in the pH reading during the HCl titration corresponding to the addition of the second proton to o-dianisidine was observed at a "pH" of 1.00. The titration of the same amount of o-dianisidine against acetic acid ony showed a gradual decrease in pH. At a concentration of acetic acid equal to 1.77 M, the highest used in the kinetics experiments, a "pH" of 4.36 was observed. These results support the existence of only free and monoprotonated o-dianisidine during the kinetic experiments when acetic acid is the catalyst.

Two parallel paths have been proposed when acetic acid is the catalyst. The total rate in the presence of acetic acid is given by the summation of the two rate expressions derived before.

$$\text{rate} = k_1'' K_{AH} K_{BH} [A][B][H^+]^2 + \frac{k_1 k_2 [A][H^+][B]}{k_{-1} + k_2[B] + k_d[S]} \qquad (3.16)$$

At low acetic acid concentrations, the order with respect to o-dianisidine is expected to decrease from first to zero as the concentration of o-dianisidine is increased. At high acetic acid concentrations, a first order with respect to o-dianisidine should be

observed, but decreasing less readily to lower values as the concentration of o-dianisidine is increased. This kind of behavior was indeed observed in Figures 3.10 and 3.11. The order with respect to o-dianisidine increased from 0.73 to 0.86 as the concentration of acetic acid was increased from 0.0178 M to 0.562 M. In both cases, a decrease in the order with respect to o-dianisidine was observed as its concentration was increased. This decrease was much less at the higher concentration of acetic acid due to the gradual shift from one reaction path to the other as the concentration of the free o-dianisidine increased.

At low o-dianisidine concentrations, a mixed order was found with respect to H^+ (Figure 3.14). At high concentrations of o-dianisidine, the order with respect to hydrogen ions was found to increase from first to second. At low concentrations of o-dianisidine, a larger proportion of the o-dianisidine will be protonated since the various concentrations of acetic acid used were kept the same for all the H^+ order determinations. At these low concentrations of o-dianisidine, the competition for the protonated aldehyde by the free and protonated o-dianisidine is expected to be greater, giving rise to a mixed order for H^+ (i.e., the reaction will proceed by both paths simultaneously). As the concentration of o-dianisidine is increased, more free o-dianisidine is available to react via the preferred path (i.e., attack of the neutral o-dianisidine on the protonated aldehyde) giving rise to a first order effect with respect to H^+ at low acetic acid concentrations. As the concentration of acetic acid is increased, less of the neutral o-dianisidine will be available. The only path possible for the reaction to occur is by attack of the protonated amine on the protonated aldehyde, giving rise to second order effect with respect to H^+.

c. Stannic chloride catalyzed path

The exact formula for the active stannic chloride species was not investigated. From the literature, it is known that stannic chloride rapidly forms stable coordination complexes upon mixing with ethanol, acetic acid, amines, and carbonyl compounds[60-63]. The most usual stoichiometry of these compounds is L_2SnCl_4, but the presence of 1:1 ligand to stannic chloride complexes has also been demonstrated in solution[63]. The Sn (IV) in stannic chloride is coordinatively unsaturated, but is enabled to attain its stable coordination of six by formation of two coordination bonds using vacant 5d atomic orbitals. In L_2SnCl_4, the bonding is assumed to be sp^3d^2, which leads to an octahedral arrangement of hybrid orbitals around the central atom.

The kinetics experiments using stannic chloride as catalyst suggest the presence of both 1:2 and 2:1 stannic chloride/o-dianisidine complexes. Expressions for the concentration of these species in terms of the starting reagents were derived assuming equilibrium reactions leading to their formation. In the S_2B complex, coordination stability can still be achieved via a possible bidentate complex formation due to the proximity of a methoxy group to the amino group in each of the o-dianisidine benzene rings[64].

Aminostannanes of the form $-\overset{|}{\underset{|}{Sn}}-\overset{|}{N}-$ cannot generally be prepared by direct aminolysis of stannic chloride[65]. Therefore, the following possible structures for the active species are proposed:

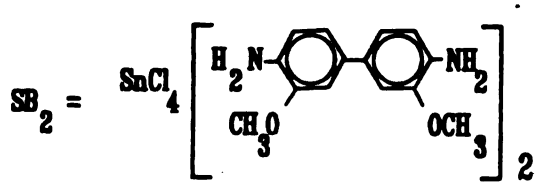

S_2B =

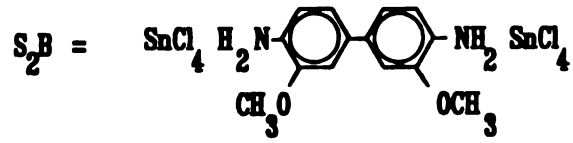

Next, the proposed mechanism is presented. Letters will be used to represent the starting reagents and intermediates.

Pre-Equilibria:

$$S + B \rightleftharpoons SB \qquad K_{1SB} = \frac{[SB]}{[S][B]}$$

$$SB + B \rightleftharpoons SB_2 \qquad K_{2SB} = \frac{[SB_2]}{[SB][B]}$$

STEP 1

$$A + S \underset{k'_{-1}}{\overset{k'_1}{\rightleftharpoons}} AS$$

STEP 2

$$AS + SB_2 \underset{k'_{-2}}{\overset{k'_2}{\rightleftharpoons}} ASB + SB$$

Post-Equilibria:

STEP 3

$$ASB \rightleftharpoons AB + S \qquad \text{fast}$$

$$AB + H^+ \rightleftharpoons \text{Product} + H_2O + H^+ \qquad \text{fast}$$

Side Reactions:

$$SB + S \rightleftharpoons S_2B \qquad K_{3SB} = \frac{[S_2B]}{[SB][S]}$$

$$AS + S_2B \xrightarrow{k'_d} \text{decomposition}$$

Application of the steady-state approximation to the AS intermediate results in the expressions for the AS concentration and the rate law shown below (the back reaction in Step 2 is neglected here).

$$[AS] = \frac{k'_1 [A] [S]}{k'_{-1} + k'_d [S_2B] + k'_2 [SB_2]} \tag{3.17}$$

$$\text{rate} = \frac{d[\text{product}]}{dt} = \frac{k'_2 k'_1 [A] [S] [SB_2]}{k'_{-1} + k'_d [S_2B] + k'_2 [SB_2]} \tag{3.18}$$

Upon substitution of the stannic chloride/o-dianisidine species in terms of the starting reagents, the rate expression becomes:

$$\text{rate} = \frac{k'_2 k'_1 K_{1SB} K_{2SB} [A] [S]^2 [B]^2}{k'_{-1} + k'_d K_{1SB} K_{3SB} [S]^2 [B] + k'_2 K_{1SB} K_{2SB} [S] [B]^2} \tag{3.19}$$

This rate expression is identical to the stannic chloride catalyzed term in the experimental rate law, where:

$$\text{Par (4)} = k'_1$$

$$\text{Par (5)} = \frac{k'_d K_{3SB}}{k'_2 K_{2SB}}$$

$$\text{Par (6)} = \frac{k'_{-1}}{k'_2 K_{1SB} K_{2SB}}$$

This mechanism is consistent with the observation that an increase in the stannic chloride concentration increases the decomposition side reaction, by presumably increasing the production of S_2B. On the other hand, it was observed that an increase in the o-dianisidine concentration decreased the decomposition side reaction as shown in Figure 3-19. Larger concentrations of o-dianisidine should favor the equilibrium reaction leading to the formation of SB_2 at the expense of the formation of S_2B. The formation of S_2B may occur initially, upon mixing of the reagents, and during the course of the reaction as SB and S are released in Steps 2 and 3, respectively.

For S_2B to be able to decompose product which has already been formed, all steps in this reaction path must be reversible. If any of the steps is not reversible, the decomposition of the product can still occur via the reverse of the mechanism proposed for the formation of the 1:1 adduct at low acetic acid concentrations[66,67]. In either case, some time will elapse before the effect of the newly formed S_2B species in the rate and equilibrium is observed.

A more descriptive chemical mechanism for the stannic chloride catalyzed path is presented in Figure 3-20. The rapid steps following the rate-determining step are speculative. They are based on the known mechanism for Schiff base formation in water, and are added merely for the purpose of completeness.

The net stoichiometric equation derived from this mechanism is:

$$A + 2S + 2B \rightleftharpoons \text{product} + H_2O + S + SB \qquad (3.20)$$

The stoichiometric equation points to the necessity of using a large excess of o-dianisidine to enhance the formation of the SB_2

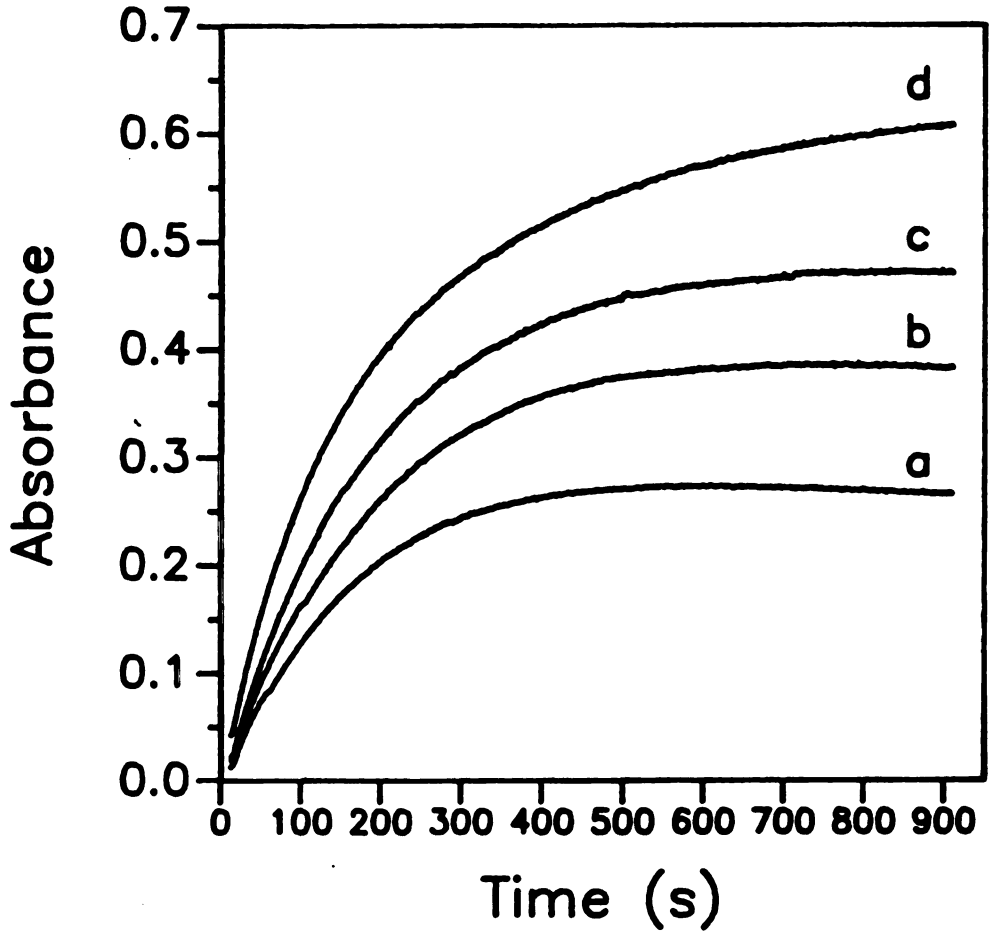

Figure 3-19. Effect of o-dianisidine in decreasing the decomposition side reaction. The acetic acid concentration was 6.00 X 10^{-2} M, while the stannic chloride concentration was 2.74 X 10^{-4} M, and that of the 2,4-dichlorobenzaldehyde was 5.00 X 10^{-5} M. The o-dianisidine concentrations were: a) 1.00 X 10^{-3} M, b) 1.41 X 10^{-3} M, c) 2.24 X 10^{-3} M, and d) 6.31 X 10^{-3} M.

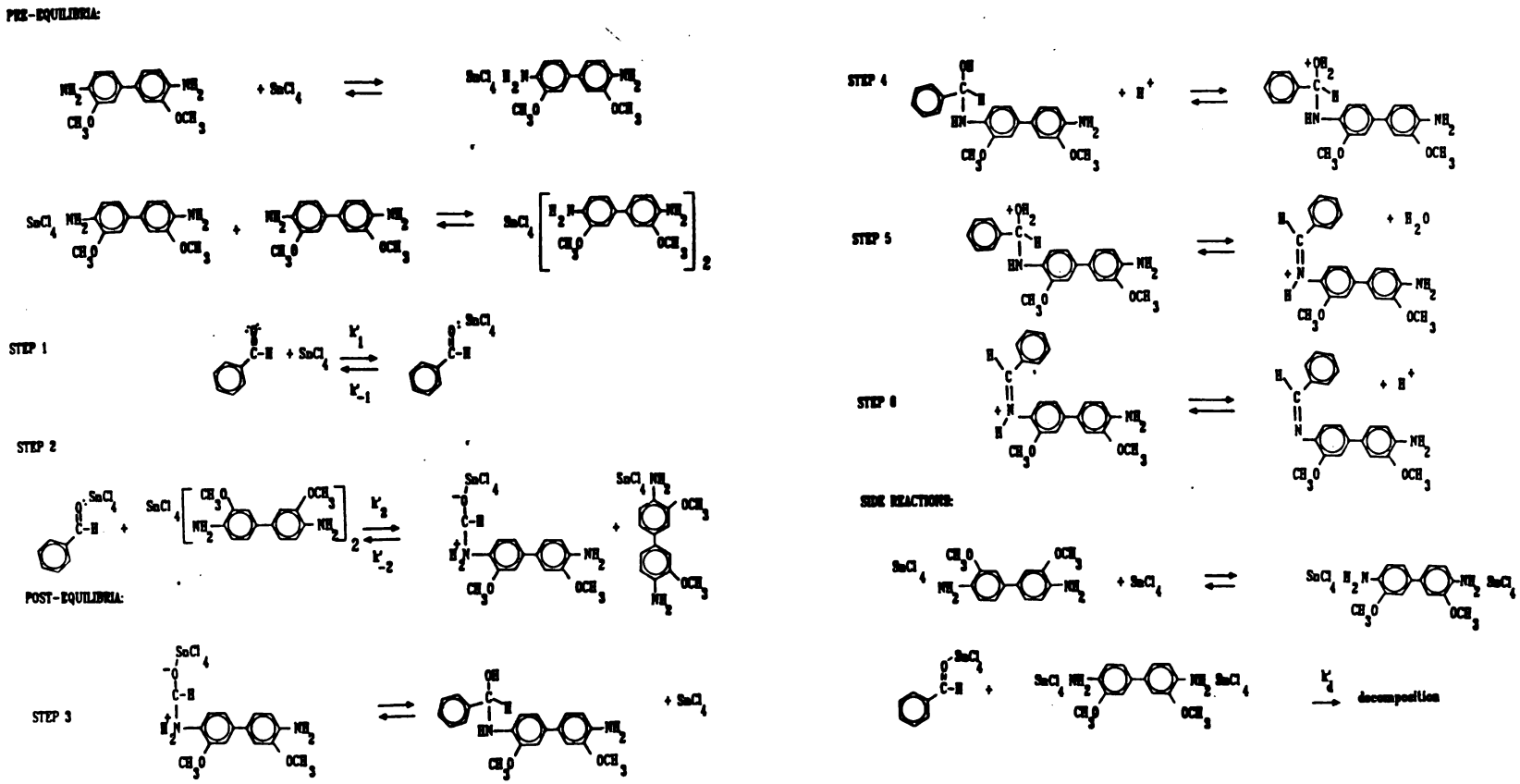

Figure 3-20. Proposed chemical mechanism for the stannic chloride catalysis of the reaction between aromatic aldehydes and o-dianisidine.

species over that of the S_2B species. As inferred from the stoichiometric equation, the minimum concentration of o-dianisidine should be set to not less than two times the concentration of the stannic chloride plus the concentration of the aldehyde present, $[B]_{min} = 2[S] + [A]$.

In the stannic chloride catalyzed path, hydrogen ions are needed for Step 4 to occur. In the absence of acetic acid and at short reaction times, the required hydrogen ions probably come from the solvolysis reaction of stannic chloride in ethanol[60,62], as shown in Equation 3.21.

$$SnCl_4 + 2\ CH_3CH_2HOH \longrightarrow SnCl_3OCH_2CH_3.HOCH_2CH_3 + HCl \qquad (3.21)$$

At long reaction times, Step 6 will provide the protons needed for Step 4 to occur. The presence of hydrogen ions in the absence of acetic acid suggests the possibility of the reaction proceeding simultaneously via a mechanism analogous to the one proposed for low acetic acid concentrations.

In the two paths catalyzed by acetic acid, the rapid steps following the rate-determining step can also be speculated to occur as shown in Figures 3-21 and 3-22. Both of the mechanisms proposed are consistent with the stoichiometric equation for Schiff base formation in water (Equation 3.1).

2. Proposed Theoretical Rate Law

Once reasonable mechanisms were proposed for the three paths by which o-dianisidine and 2,4-dichlorobenzaldehyde react to form products, the parameters in the experimental rate law were replaced by the corres-

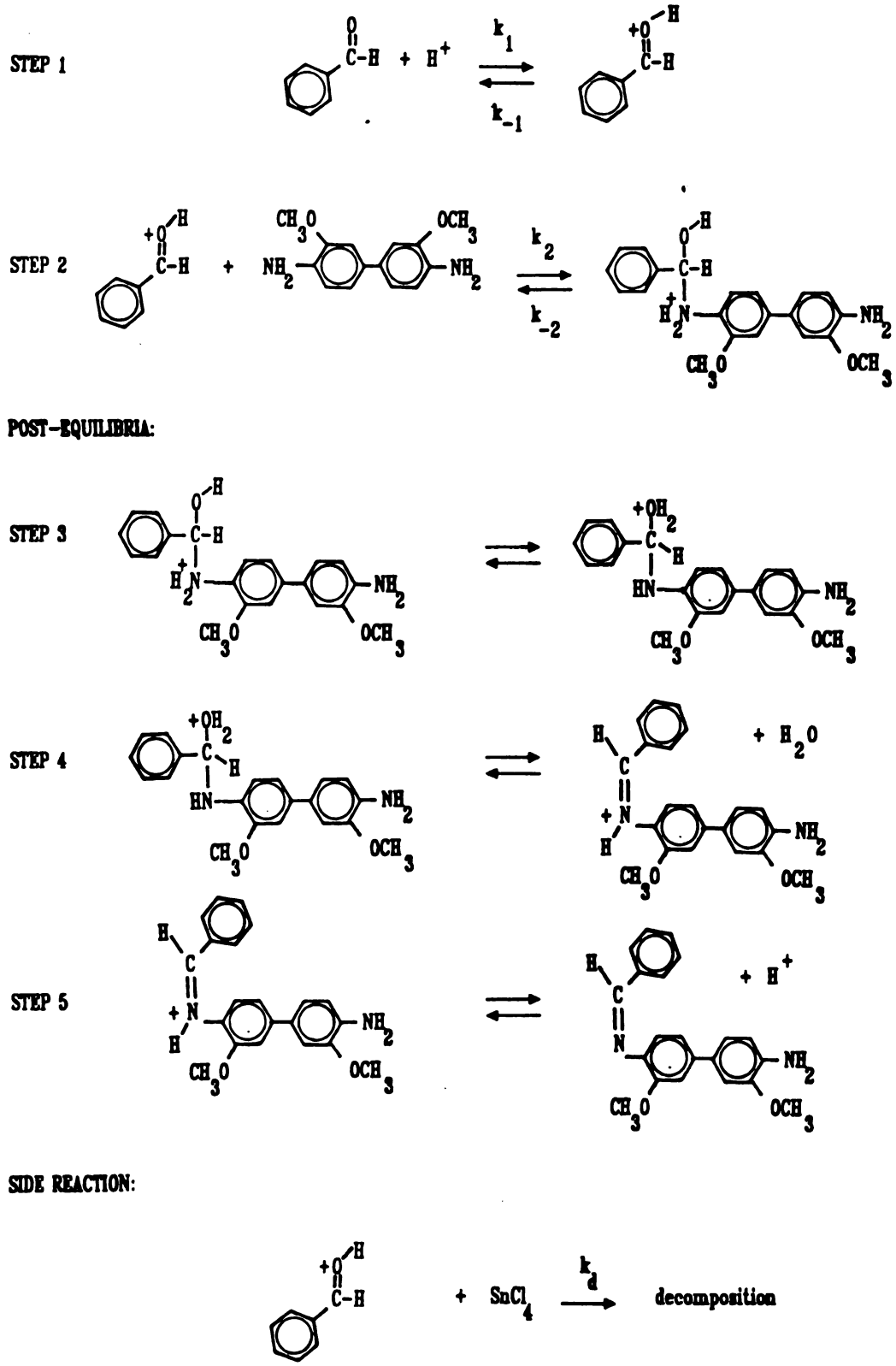

Figure 3-21. Proposed chemical mechanism for the reaction between aromatic aldehydes and o-dianisidine at low acetic acid concentrations.

PRE-EQUILIBRIA:

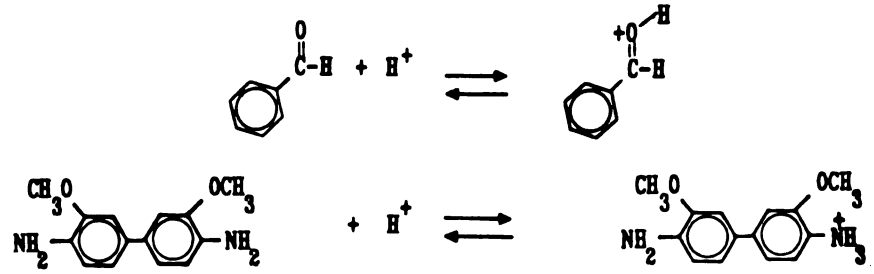

RATE DETERMINING STEP:

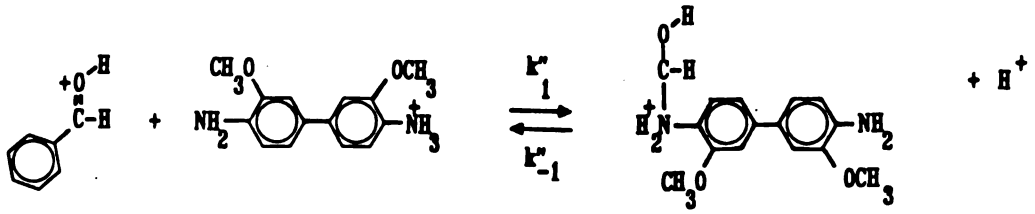

POST-EQUILIBRIA:

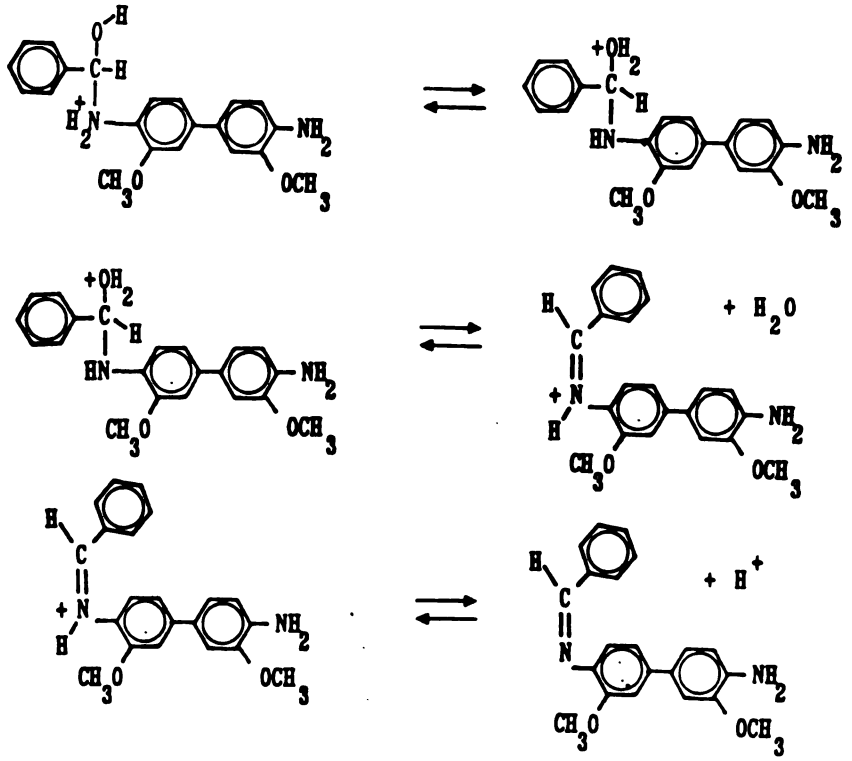

Figure 3-22. Proposed chemical mechanism for the reaction between aromatic aldehydes and o-dianisidine at high acetic acid concentrations.

ponding rate and equilibrium constants. The concentration terms were replaced by the formulas of the starting reagents according to their initial assignments: [A] = 2,4-dichlorobenzaldehyde = [$C_7H_4OCl_2$], [B] = o-dianisidine = [$C_{14}H_{16}N_2O_2$], [S] = stannic chloride = [$SnCl_4$], and [H^+] = $Ka^{1/2}$ [C_2H_4O]$^{1/2}$.

$$\text{Rate}=\frac{d[\text{product}]}{dt} = [C_7H_4OCl_2]\left[k''_1 K_{AH} K_{BH} K_a [C_2H_4O][C_{14}H_{16}N_2O_2] + \right.$$

$$+ \frac{k_1 k_2 K_a^{1/2} [C_2H_4O]^{1/2}[C_{14}H_{16}N_2O_2]}{k_{-1} + k_2[C_{14}H_{16}N_2O_2] + k_d[SnCl_4]}$$

$$\left. + \frac{k'_2 k'_1 K_{1SB} K_{2SB} [SnCl_4]^2 [C_{14}H_{16}N_2O_2]^2}{k'_{-1} + k'_d K_{1SB} K_{2SB} [SnCl_4]^2 [C_{14}H_{16}N_2O_2] + k'_2 K_{1SB} K_{2SB} [SnCl_4][C_{14}H_{16}N_2O_2]^2}\right] \quad (3.22)$$

Although the rate law seems to be quite complicated, the mechanisms for the three paths are very similar to one another and to the mechanism of Schiff base formation in water as is discussed in the next section.

3. Comparison with the Mechanism for Schiff Base Formation in Water

The mechanisms proposed for the acetic acid and stannic chloride catalyzed formation of Schiff bases in ethanol are very similar to that

for specific acid catalysis in water. Because only one of the two amino groups in o-dianisidine is protonated in ethanol, an increase in rate is still observed at considerably high acetic acid concentrations. In water, the carbinolamine formation is proposed to be hindered due to the protonation of the amine. These results are not contradictory. The small basicity of o-dianisidine, and the smaller dissociation constant of the ethanol relative to water are two reasons for the requirement of an initial protonation of the aldehyde prior to the amine attack.

In general, the proposed mechanisms for all three paths are very similar. The first step involves the reaction of the aldehyde with the catalyst, either H^+ or stannic chloride, followed by the formation of the protonated carbinolamine and a subsequent dehydration to form the product after loss of the final proton.

G. Analytical Implications

As was stated earlier, the purpose of performing kinetics studies on the o-dianisidine/aldehyde reaction was to gain some insight into the mechanism by which the reaction occurs. This should allow selection of the most appropiate conditions for the determination of aromatic aldehydes. The suggestions that follow are of value whether a kinetic-based procedure or, as in our case, an equilibrium-based method is used. First, the choice of reagent concentrations is discussed followed by a section on the choice of experimental conditions.

1. Reagent Concentrations

Of the two catalysts studied, stannic chloride is a better catalyst than acetic acid. With stannic chloride, the reaction attains

equilibrium in a shorter time, even though the stannic chloride concentration is three orders of magnitude less than that required with acetic acid.

The concentration of stannic chloride which results in fast reaction rates, but at which decomposition is not yet a problem, is in the range of 4.0×10^{-4} to 1.6×10^{-3} M at concentrations of o-dianisidine of about 6.3×10^{-3} M. To increase the rate further, a higher concentration of stannic chloride might be used, but an adjustment in the o-dianisidine concentration must be made to avoid the decomposition side reaction.

The o-dianisidine concentration should be as high as its solubility permits. A high o-dianisidine concentration not only increases the rate of the reaction, but also increases product formation. Hence, a larger amount of product formation is obtained for the same amount of aldehyde which increases the sensitivity of the method. A high o-dianisidine concentration is also helpful in decreasing the amount of decomposition observed at high concentrations of stannic chloride. As predicted by the stoichiometric equation, the o-dianisidine concentration should not be less than two times that of the stannic chloride plus that of the aldehyde to favor formation of the SB_2 complex in preference over the S_2B complex. The verification of this prediction is possible in Figures 3-8, 3-9, and 4-2, where the decomposition of product begins to be observed at concentration of stannic chloride higher than 2.50×10^{-3} M for a 6.31×10^{-3} M concentration of o-dianisidine. At the same time, the concentration of the o-dianisidine relative to that of the aldehyde should never be less

than 10:1, to favor the formation of the 1:1 aldehyde to o-dianisidine adduct in preference to the 2:1 adduct.

In the mechanism for the reaction path catalyzed by stannic chloride, pre-equilibria involving the formation of coordination complexes between o-dianisidine and stannic chloride were proposed. Mixing these two reagents in advance could, in principle, shorten the reaction time needed to attain equilibrium by a few seconds when using a continuous-flow analysis system.

2. Experimental Conditions

The first choice of experimental conditions is to decide which temperature to use. Although the effect of temperature was not rigorously studied in these kinetics experiments, it was observed that increasing the temperature increased the rate at which the reaction occurred. Therefore, temperatures above room temperature are recommended when implementing this reaction as an analytical procedure. Temperatures in the 30 to 50 °C range should be tested during optimization experiments.

A second concern deals with the possible interference of water in the method. All three proposed mechanisms form water as by-product. It has been documented in the literature, and observed during these kinetics studies, that the presence of water decreases product formation. Precautions that can be taken to remove the water interference include drying the ethanol, as in our case with molecular sieves, or using the standard addition method when analyzing samples containing water.

CHAPTER IV

THE ANALYTICAL METHOD

A. Chapter Overview

In this chapter, automation of an analytical method based on the reaction between o-dianisidine and aromatic aldehydes using only stannic chloride as catalyst is discussed. The method has been adapted to an air-segmented continuous-flow analysis system. First, the principles of continuous-flow analysis are presented, followed by a discussion of the effect of theory and hardware limitations on automation. Next, optimization of the experimental conditions for the reaction by the Modified Simplex method is described. To assess the usefulness of the method, the analytical figures of merit for thirteen aromatic aldehydes were determined; also, selectivity and interference studies were performed. Finally, the analytical method is applied to the determination of furfural in a practical sample.

B. Principles of ASCFA

Air-segmented continuous-flow analysis, ASCFA, was invented by Leonard Skeggs[68,69] in the early 1950's and was developed commercially in 1957 by the Technicon Corporation under the trade name AutoAnalyzer.

In ASCFA the sample and reagents are proportionally aspirated in an air-segmented flowing stream. Reaction takes place within the stream

and the product is detected sometime later as the segmented stream flows through the sample cell (bubble-through flowcell) of a recording photometer. A schematic diagram of an ASCFA system is presented in Figure 4-1.

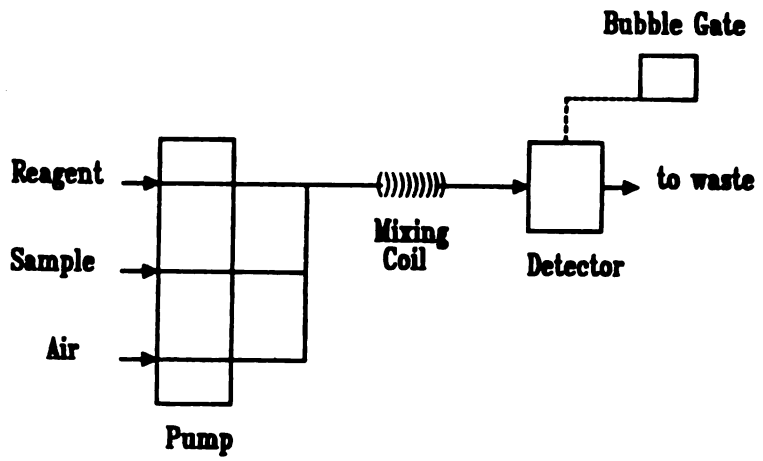

Figure 4-1. Diagram of an Air-Segmented Continuous-Flow Analysis System. Stream path is denoted by —— and the electrical signal by ---.

The removal of the air segments for the purpose of spectroscopic detection is done electronically by means of a "bubble gate". With a "bubble gate", the periodic fluctuations of the detector signal as air and liquid segments pass through the flowcell are used to synchronize data acquisition and storage. The flowcell volume is such that it can be totally filled with liquid between bubbles. The bubble gate electronics detects this condition and triggers data acquisition.

For many wet chemical analyses, an automated method is to be preferred to existing manual methods due to an increase in sample throughput, an improvement in precision, a decrease in the amount of

reagents consumed, and an increase in safety when handling toxic or dangerous materials. For example, o-dianisidine is suspected to be a carcinogen.

Due to the existence of a number of reviews on CFA[70-74], the discussion that follows focuses on the principles and hardware limitations that affect the automation of the analytical method based on the o-dianisidine reaction with aromatic aldehydes. The related technique, flow injection analysis (FIA) is not discussed here at all[75].

The desire to automate the analytical procedure placed several constraints on the actual development of the method. In air-segmented continuous-flow analysis, after the sample and reagents are mixed, they must remain in the reaction coil for a sufficient period of time for the reaction to proceed to an appreciable extent prior to detection. Dispersion can occur in the mixing devices during the addition of the reagents and in the reaction coil. In an analytical method dispersion decreases the the sensitivity of the method. Therefore, dispersion should be minimized in order to obtain lower detection limits. Dispersion effects in ASCFA systems are discussed in more detail in the next section.

C. Dispersion in ASCFA Systems

Dispersion in ASCFA arises from two distinct processes. The first is the longitudinal dispersion that occurs in unsegmented zones of the system (i.e., sampling tubes). The presence of air segments effectively reduces longitudinal dispersion in the manifold due to the break down of the parabolic flow profile characteristic of laminar flow. Also, the

air segments enhance mixing within each liquid segment due to the toroidal (bolus) flow that occurs in each of the liquid segments.

The second mode of dispersion is called axial dispersion and occurs in the air-segmented analytical stream. Axial dispersion is due to the stagnant liquid film that wets the walls of the manifold tubes allowing mass transfer between the liquid segments. In order to obtain hydraulic stability when using segmented streams, the manifold tubes must be fabricated from wettable materials. Therefore, axial dispersion cannot be eliminated. However, in principle it can be reduced to acceptable levels by proper system design.

In 1976, Snyder[76] derived an equation for dispersion as a function of those experimental variables of direct interest in the design of ASCFA systems (Equation 4.1). The basic assumptions of the model are: 1) air segment volumes are the minimun required to totally oclude a tube of a given diameter ($\approx 0.92\ d_t^3$); 2) the flow system is perfectly wetted; 3) the dispersion is completely determined by the reaction tubing (i.e., contributions to dispersion from other system components are ignored); 4) the reaction tubing is in the form of a coil; and 5) air-bubbles do not change in size after introduction into the system.

$$\sigma_t^2 = \left[\frac{538\, d_t^{2/3} (F + 0.92\, d_t^3\, n)^{5/3}\, \eta^{7/3}}{\gamma^{2/3} F D'_m} + \frac{1}{n} \right] \left[\frac{2.35 (F_t + 0.92\, d_t^3\, n)^{5/3}\, \eta^{2/3}\, t}{\gamma^{2/3} F d_t^{4/3}} \right] \quad (4.1)$$

In Equation 4.1, σ_t is the standard deviation of the peak expressed in seconds, d_t is the internal diameter of the manifold tube in cm, F is the liquid flow rate in ml s^{-1}, n is the air-segmentation

frequency in Hz, t is the residence time of the sample in the flow system in seconds, η is the viscosity of the liquid in poise, γ is the surface tension of the liquid in dyne cm^{-1}, and D'_m is an empirical diffusion coefficient (cm^2 s^{-1}) that pertains only to diffusion in coiled tubes. In this model, the cumulative individual Poisson dispersion of each sample segment is approximated to a Gaussian distribution; and dispersion is approximated to be equal to the square root of the displacement of the 50% maximum concentration point in the dispersed sample profile from the leading edge of the sample zone.

Snyder's dispersion model was used in the design of the ASCFA system for the reaction between o-dianisidine and aldehydes in order to minimize overall dispersion by optimizing the following key variables: manifold tube internal diameter (d_t), air-segmentation frequency (n), and flow rate (F). Previous models[77-80] by other authors do not relate axial dispersion to relevant experimental variables.

Before presenting how Snyder's model was used to design the ASCFA system, it is necessary to describe the different components that were used in implementing the modular ASCFA system.

D. Instrumentation

The four main components of the modular ASCFA system used in this research are: the pump, the light source, the detector, and the bubble gate. The detector and the bubble gate were constructed by Dr. C. J. Patton[73,81]. The pump was obtained from commercial sources, but modified to reduce pump pulsations. A brief description of each of the

system components is given, followed by a discussion of the limitations that each component imposed in the actual design of the ASCFA system.

1. The Pump

The Model IP-12 variable speed, 12 channel peristaltic pump (Brinkmann Instruments, Westbury, NY) used for all work reported here was modified by Patton[73]. He replaced the standard roller assembly (8 rollers) with one containing 16 rollers in order to reduce pump pulsations. To minimize pump pulsations further, air segments were added in phase with the pulsations as suggested by Habig et al[82]. This procedure reduces the air-segmentation frequency, n, to a narrow range of values that are determined by the pump speed and the number of pump rollers. The digital speed-control setting for this pump allows 00 to 99 linear control settings, which translates to an air-segmentation frequency range of 0.5 to 3.5 air bubbles per second. Consequently, in the design of the ASCFA system, the lower limit in the air-segmentation frequency, n_{min} = 0.5 bubbles s^{-1}, is imposed by the particular pump used while the upper limit, n_{max}, depends on the flowcell volume and the total flow rate of reagents through the manifold.

2. The Detector

As was stated before, the detector was designed by Dr. C.J. Patton as part of his doctoral research at MSU. For a full description of the operation and design of this detector, the reader is referred to Patton's thesis[73]. Components of this detector of direct relevance to the design of an ASCFA system for the o-dianisidine/aldehyde reaction are the interference filter and the flowcell used.

Wavelength selection (380 nm) was accomplished with 1.27 cm diameter, narrow bandwidth (≈ 8 nm), three-cavity, interference filter (# 15-10060, Ditric Optics, Hudson, MA).

A flowcell with sapphire windows, a 1.0 cm pathlength and an internal diameter of 0.05 cm was obtained commercially (PN 178-13724-02, Technicon Instruments, Tarrytown, NY). The use of this flowcell, with a volume of approximately 2 µl, further restricted the air segmentation frequency. At any flow rate, F, the upper limit for the segmentation frequency, n_{max}, can be calculated by dividing the flow rate by the liquid segment volume, V_s. The liquid segment was set at about 4 µl (twice the volume of the flowcell). Calculated values for n_{max} and n_{min} in conjunction with Snyder's dispersion model were used in the design of an ASCFAS manifold in which dispersion was reduced to the theoretical minimum.

3. The Light Source

Instead of the miniature tungsten-halogen lamp normally used with the modular ASCFAS, a conventional size tungsten lamp (12 V, auto bulb) housed in a Model EU-701-50 Heath Light Source was used. This was necessary to obtain enough radiant power at the 380 nm wavelength chosen for the analysis. With this light source, a 5.0 V signal was obtained for a 100% Transmittance reading.

4. The Bubble Gate

The signal from the detector is directed into a "bubble gate" circuit which serves to remove the effect of the air segments electronically. This method causes less longitudinal dispersion than physically debubbling the stream just before the flowcell. This "bubble

gate" was also constructed by Patton[73,81] as part of his doctoral research at MSU.

Besides the use of bubble-through flowcells, longitudinal dispersion can also be minimized with pecked sampling. Pecked sampling refers to the introduction of air segments between samples in the sampling tube. By reducing longitudinal dispersion in these two ways, the actual dispersion in the final ASCFA system can approach the theoretical limit predicted by Snyder's model.

E. Design of the ASCFAS Manifold

The design of the ASCFAS manifold was approached using Snyder's theoretical model of dispersion (Equation 4.1). In Snyder's model some of the variables (η, γ, D'_m, and t) were fixed by the particular chemistry and experimental requirements of the o-dianisidine/aldehyde reaction itself. The other variables (d_t, F, and n), are the ones actually optimized using Snyder's model. The theoretical optimization of these variables was done at two different temperatures, 20°C and 40°C.

Dispersion increases for more viscous reaction mixtures and for longer reaction times. For long reaction times (longer than one minute) elevated temperatures can be used in order to increase the reaction rate and to decrease the viscosity of the reaction mixture. Since high concentrations of acid result in viscous solutions the method to be developed should use low acid concentrations. Low acid concentrations also reduce the viscosity differences between the solutions that need to be mixed and thus improve mixing efficiency.

In air-segmented continuous-flow, it is not feasible to use temperatures significantly above room temperature because of the possible change in air bubble size once the bubble "pops" into the hot stream. Another problem in using elevated temperatures is the large vapor pressure of ethanol, especially at temperatures above 40°C. The increase in solvent vapor pressure with temperature can further increase the bubble size. An increase in bubble size leads to an increase in flow rate, which in turn causes a small increase in dispersion. In order to prevent these effects, an upper limit to the temperature was set at 50°C; for convenience the lower limit was set at room temperature (about 20°C).

In order to improve precision, the reaction should be at equilibrium before entering the flowcell. Figure 4-2 is a plot of the absorbance versus reaction time for the reaction between 2,4-dichlorobenzaldehyde (6.00×10^{-5} M) and o-dianisidine (6.31×10^{-3} M) at different concentrations of the stannic chloride catalyst. The reaction was essentially at equilibrium after 5.0 min of reaction time when using 1.59×10^{-3} M stannic chloride as the catalyst. Consequently, the sample residence time to be use in Snyder's model was chosen to be 5.0 min.

Tables 4-1 and 4-2 show the results obtained for the optimization of d_t, F, and n using Snyder's model at 20°C and 40°C respectively. In Table 4-1 (at 20°C), minimum axial dispersion ($\sigma_t \approx 2.48$ s) was predicted when d_t = 0.1 cm for a value of n = 1.0 and for F = 0.30 ml min^{-1}. At 40°C (Table 4-2), minimum dispersion ($\sigma_t \approx 1.91$ s) was predicted when d_t was again 0.1 cm, but for values of n in the range 1.0 to 2.0 s^{-1} and for F in the 0.30 to 0.60 ml min^{-1} range.

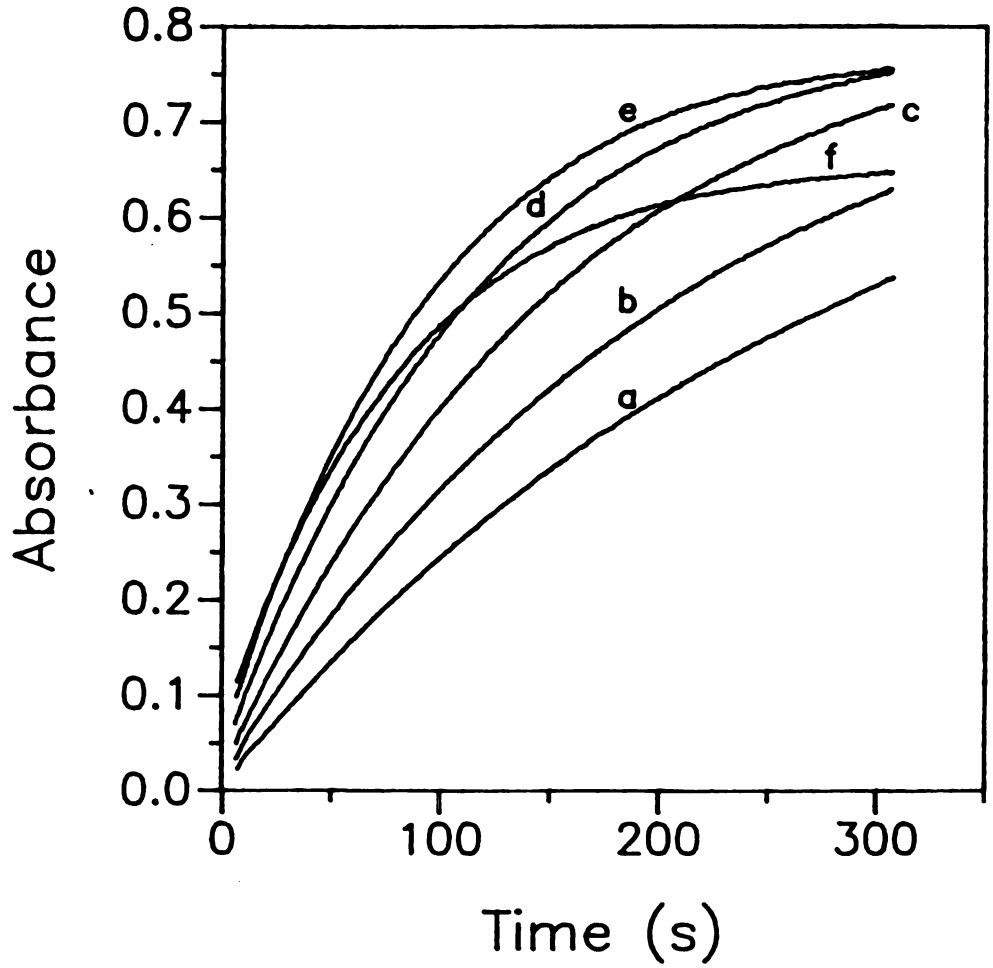

Figure 4-2. Effect of stannic chloride concentration on the reaction time. The 2,4-dichlorobenzaldehyde concentration was 6.00 X 10^{-5} M, while the o-dianisidine concentration was 6.31 X 10^{-3} M and those of stannic chloride were: a) 2.51 X 10^{-4} M, b) 3.98 X 10^{-4} M, c) 6.31 X 10^{-4} M, d) 1.00 X 10^{-3} M, e) 1.59 X 10^{-3} M, and f) 2.51 X 10^{-3} M.

Table 4-1. Calculated axial dispersion, σ_t, in seconds as a function of F, d_t and n at 20°C.

Tube ID	dt = 0.08 cm					dt = 0.10 cm					dt = 0.12 cm					
F (mL/min.) \ n (s^{-1})	0.5	1.0	1.5	2.0	2.5	0.5	1.0	1.5	2.0	2.5	0.5	1.0	1.5	2.0	2.5	n max.
1.00	5.07	4.17	3.87	3.74	3.68	4.54	3.87	3.68	3.63	3.65	4.22	3.70	3.62	3.71	3.85	4.2
0.60	4.11	3.33	3.07	2.97	2.94	3.70	3.13	3.00	3.00	3.04	3.47	3.07	3.07	3.20	3.41	2.5
0.50	3.85	3.10	2.86	2.76		3.46	2.92	2.80	2.81		3.24	2.90	2.93	3.09		2.1
0.40	3.53	2.85	2.62			3.20	2.71	2.61			3.01	2.74	2.80			1.7
0.30	3.18	2.56				2.89	2.48				2.77	2.56				1.3
0.20	2.78					2.57					2.52					0.8

Values for minor variables: γ = 23.0 dynes cm^{-1}, η = 0.01201 poise, and $D'_m = 3.0 \times 10^{-5}$ cm^2 s^{-1}.

Table 4-2. Calculated axial dispersion, σ_t, in seconds as a function of F, dt and n at 40°C.

Tube ID	dt = 0.08 cm					dt = 0.10 cm					dt = 0.12 cm					
F (mL/min.) \ n (s^{-1})	0.5	1.0	1.5	2.0	2.5	0.5	1.0	1.5	2.0	2.5	0.5	1.0	1.5	2.0	2.5	n max.
1.00	4.10	3.13	2.74	2.54	2.42	3.61	2.82	2.53	2.39	2.33	3.29	2.65	2.45	2.38	2.38	4.2
0.60	3.40	2.59	2.27	2.10	2.01	3.02	2.37	2.13	2.02	1.99	2.77	2.26	2.11	2.12	2.15	2.5
0.50	3.21	2.43	2.13	1.97		2.85	2.24	2.02	1.94		2.63	2.15	2.02	2.03		2.1
0.40	2.98	2.26	1.98			2.66	2.10	1.91			2.47	2.03	1.95			1.7
0.30	2.72	2.07				2.45	1.95				2.29	1.94				1.3
0.20	2.40					2.20					2.10					0.8

Values for minor variables: γ = 21.4 dynes cm^{-1}, η = 0.00834 poise, and $D'_m = 4.0 \times 10^{-5}$ cm^2 s^{-1}.

Overall, better results for the o-dianisidine/aldehyde reaction are expected at 40°C than at 20°C, because of the decrease in dispersion at 40°C and an increase in the rate of the reaction. Also, the viscosity and surface tension of the solutions are lower at the higher temperature. The reduction in the surface tension should increase the wettability of the manifold tubing, which in turn should aid in preserving the air-segmentation frequency pattern. The reduction of the viscosity is beneficial in the proper mixing of samples and reagents, which should enhance the response and reproducibility of the method.

At 40°C, it was found that there is a range of flow rates (0.30 to 0.60 ml min^{-1}) which could be used to design an ASCFA system in which dispersion is at its theoretical minimum for a five minute reaction time. Although the choice of the higher flow rate is advantageous due to the reduction of the dispersion caused by poor mixing, a flow rate of 0.40 ml min^{-1} was used to calculate the length of the reaction coil needed to ensure complete reaction. The reason for using this flow rate was to allow for possible flow rate changes when the experimental optimization of the ASCFAS variables was done using the Simplex method of optimization. At a 0.40 ml min^{-1} flow rate, and for a reaction time of five minutes, the calculated best dimensions for the reaction coil were found to be 0.10 cm ID X 2.55 m in length.

F. Simplex Optimization

Optimization is usually performed by adjusting one at a time the various factors that control the response to be optimized. If, however,

the parameters interact with one another, it has been shown that univariate optimization can fail to locate the true optimum[83].

Another approach to optimization, which was used in this research, is the Modified Simplex method[83-85]. In this method, all controlling factors are adjusted and the measured response is compared to previous responses at different values of each factor. The objective of the Simplex method is to identify, and to simultaneously follow the trends in the values for the different controlling factors that lead to an increase in the response of the system. In the Simplex terminology, a set of values for the controlling factors that give rise to a particular response is called a vertex. In an application with n controlling factors, n + 1 vertices are needed to create an n dimensional geometric figure called a simplex. The use of these geometric figures helps to visualize and guide the movement of the Simplex method towards the optimum. A simplex of two controlling factors is a triangle, of three factors is a tetrahedron, etc.

The movement of the simplex towards the region of optimum response is guided by a set of rules; only the basic rules are presented here. First, after the evaluation of the response at each vertex in the initial simplex, the vertex with the worst response is eliminated. Second, a new vertex is evaluated at a position that corresponds to the geometric opposite of the undesirable vertex. Third, if the new vertex gives the lowest response, then the second to lowest response in the old simplex is discarded, and a new vertex is selected opposite to the just discarded vertex. Fourth, expansions in the step size for locating the new vertex can be used as needed to allow rapid approach to the optimum.

Once near the optimum, contractions in the step size are useful in order to locate the exact optimum.

The Modified Simplex method makes use of a few other rules[85] that are not presented above. However, the four rules mentioned are enough for the reader to follow the four vertex simplex used in this work. The three factors optimized using the Simplex method are: the flow rate, the temperature and the stannic chloride concentration.

G. Experimental

1. Apparatus

A schematic of the modular ASCFA system employed in this work is shown in Figure 4-3. The main components of the ASCFA system are the peristaltic pump, the filter photometer (detector), and the electronic bubble gate. The description of each of these components was given before in pages 83 to 84.

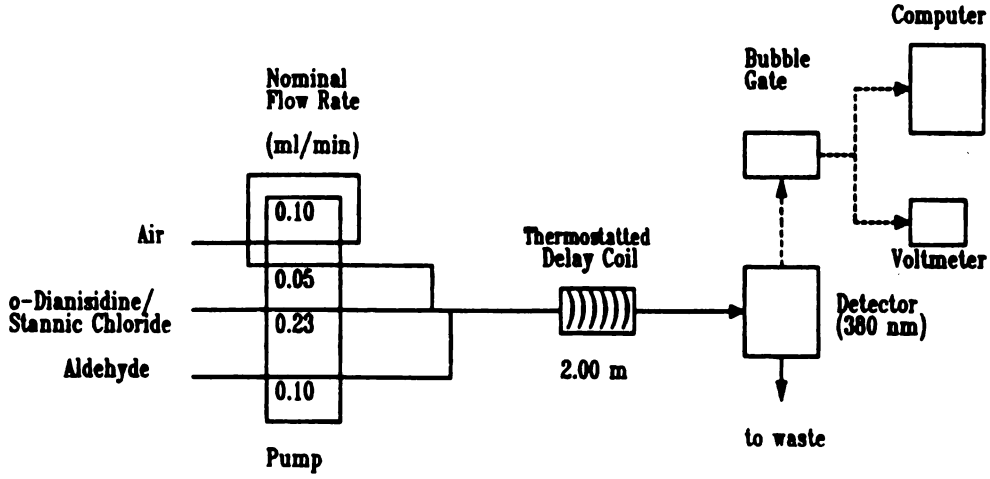

Figure 4-3. Modular Air Segmented Continuous-Flow System used in the determination of aromatic aldehydes. Stream flow path is denoted by —— and the electrical signal by ——.

All manifold coils were constructed using 0.10 cm ID X 0.17 cm OD Teflon tubing (#N-06417-41, Cole Parmer, Chicago, IL). The reaction coil was wrapped around a glass rod (0.5 in diameter) which was mounted in a water-tight Plexiglass jacket so that it could be thermostatted by means of circulating water from a water bath. The sample and reagents were added via 90° Plexiglass tees. Fisherbrand solvent flexible pump tubes (Fisher, Livonia, MI) were used instead of the standard polyethylene pump tubes because ethanol quickly hardens and renders useless the latter.

A Quick Basic program (Microsoft, Bellevue, WA) developed by Dr. Peter D. Wentzell, was modified to acquire, process and store data using an IBM data acquisition board (Mendelson Electronics Co. Inc., Dayton, OH) and an IBM-compatible personal computer (Bentley T, Round Rock, TX). The modified program was named 5VASCF. With this program the absorbance of four liquid segments were averaged as one data point every two seconds.

2. Procedure

All solutions were filtered using Millex 0.5 μm filters (No. SLSR 025 NS, Millipore Corp., Bedford, MA) prior to being aspirated into the manifold. This filtration prevents blockage of pump tubes and/or the flowcell due to particulate matter. Filtering also reduces detector noise. Three intersample air segments (IAS) were introduced at the start of each sample and wash interval by repetitive withdrawal and insertion of the sample tube in the particular solution (i.e., "pecking"). This provides a partial barrier to intersample mixing by longitudinal diffusion in the sampling tube. The sampling and wash

times were 90 s and 30 s, respectively. Air segmentation was carried out using the dual pump tube method described by Habig, et al[82].

The use of high temperatures for the reaction coil can, in principle, cause a problem concerning the possible change in air bubble size once it is introduced into the manifold. To diminish the change in air bubble size due to vaporization of solvent, the air was pre-equilibrated with ethanol at the selected temperature before aspiration into the manifold. This proved to be unnecessary since air bubble size change came mainly from expansion due to change in temperature rather than from change in solvent vapor pressure.

The filter photometer was operated in a single-beam mode because of relatively low light intensities at 380 nm. Therefore, the baseline was corrected, if needed, just prior to every sample reading to compensate for drift due to instability of the electronic circuits and of the light source. Baseline drift was about 1 to 2% per hour after a warming period of one hour.

3. Samples and Reagents

The stannic chloride and o-dianisidine solutions were prepared as described in Chapter III.

All aldehydes were of commercial origin. Solid aldehydes were recrystallized from ethanol and then vacuum dried. Melting points were determined in order to check identity and purity. Liquid aldehydes were distilled under nitrogen to prevent air oxidation.

All chemicals for the interference and selectivity studies (e.g., ketones, aliphatic aldehydes, and acetals) were also of commercial origin. These, too, were recrystallized or distilled prior to use.

Working standards were prepared by dilution of stock solutions using anhydrous ethanol as solvent.

4. Determination of Furfural in Creme de Menthe

Furfural was determined in Creme de Menthe by direct UV spectrophotometry at its wavelength of maximum absorbance (277 nm)[86]. These results were compared with those obtained by the ASCF o-dianisidine derivatization method. The liquor was first steam distilled to separate the furfural from other components present in the sample. Three sets of standards were prepared: one in which the standard addition technique was used prior to the steam distillation, a second set where standard additions were carried out after the steam distillation, and a third set where the standard additions were performed after an ether extraction of the steam-distilled sample.

a. Standard addition prior to the steam distillation

To 20.00 ml of Creme de Menthe in 25.0 ml volumetric flasks were added either 0.00, 1.00, 2.00 or 4.00 ml of 1.14 X 10^{-2} M solution of furfural and 0.600, 0.800 or 1.00 ml of 1.14 X 10^{-3} M solution of furfural. After diluting with ethanol, the samples were steam distilled separately. About 200 ml of the distillate were collected in 250.0 ml volumetric flasks which were cooled using ice baths. Once the distillates were at room temperature, the volume of liquid in the volumetric flasks was set to the mark with distilled water. Direct UV detection at 277 nm was used for analyzing these samples using water as the reference. The furfural content in Creme de Menthe was found to be 6.0 ± 0.5 mg/l.

b. Standard addition after the steam distillation

To test the effectiveness of the steam distillation, the sample to which no furfural was added prior to the steam distillation was subjected to standard addition afterwards. To 20.00 ml of this aqueous sample in 25.0 ml volumetric flasks were added either 0.00, 0.050, 0.100, 0.200, 0.500, 0.800 or 1.00 ml of 1.14 X 10^{-3} M furfural solution. After diluting with distilled water, the samples were analyzed using direct UV absorbance detection at 277 nm. The furfural content in Creme de Menthe was found to be 5.9 ± 0.3 mg/l.

c. Ether extraction after steam distillation

A 25.00 ml sample of Creme de Menthe was steam distilled. About 200 ml of distillate were collected. All the distillate was extracted with nine 20 ml portions of ethyl ether. The extractions were collected in a 200.0 ml volumetric flask and diluted with additional ether. After drying overnight with magnesium sulfate, the ethereal solution was filtered by gravity using a coarse-porosity fritted disc funnel. Exactly 175.0 ml of the ethereal solution was concentrated in a rotary evaporator. The residue left was quantitatively transferred to a 50.0 ml volumetric flask using anhydrous ethanol. Six samples were prepared by standard addition of 0.00, 0.300, 0.600, 1.00, 1.30, or 1.60 ml of a 1.14 X 10^{-3} M furfural solution to 8.00 ml of the above ethanolic solution in 10.0 ml volumetric flasks. After filtering the samples through 0.45 µm Millex HV filters, the samples were analyzed using the o-dianisidine ASCFA method. The amount of furfural in Creme de Menthe was found to be 2.0 ± 0.1 mg/l. After dilution of 4.00 ml of each of the above samples into 10.0 ml volumetric flasks with ethanol, they were

also analyzed by direct UV absorbance detection at 277 nm using ethanol as the reference. The amount of furfural was found to be 2.0 ± 0.5 mg/l.

H. Results

In this section the o-dianisidine reaction is adapted to an ASCFS. The analytical figures of merit for 13 aromatic aldehydes are determined. Also selectivity and interference studies are reported.

1. Optimization

The optimization of the colorimetric method to obtain maximum response for a representative aldehyde was carried out using the Simplex method. The parameters chosen for optimization were the photometric response (i.e., absorbance), flow system dispersion and the system signal noise. The three variables monitored were: temperature, flow rate, and the stannic chloride concentration.

The use of the Simplex method for this optimization is a necessity because the previously mentioned variables interact with one another. A univariate approach might have led to erroneous conclusions concerning the optimum values for these variables. Boundary limits to these variables and fixed values for other variables were established based on a general knowledge of the system. For instance, the o-dianisidine concentration was fixed at the maximum that could be dissolved at room temperature and which avoided precipitation in the tubing (0.100 g/20 ml ethanol = 0.0204 M). The upper limit of the stannic chloride concentration (1.00×10^{-2} M) was established by the decomposition observed at higher concentrations, while the lower limit (3.00×10^{-3} M), was the

minimum concentration of stannic chloride needed to observe an appreciable reaction. The temperature of the reaction coil was varied between 20 to 50°C to avoid problems of instability in the system due to excessive solvent vapor pressure at higher temperatures.

The pump speed control setting was varied over the range 28 to 70, which corresponds to flow rates of 0.25 to 0.63 ml min^{-1} (at room temperature). A regular bubble pattern was only attainable at pump speed settings of 50 and above. At these high pump speed settings, dispersion was a problem when using a 2.55 m long manifold tube. With a 2.00 m long manifold tube less dispersion was observed, but the response of the system was about 10% lower due to incomplete reaction. Dispersion in a 3.00 m long mani-fold tube was high at all speed settings, but the noise level was the lowest. To reduce dispersion and noise, the o-dianisidine was mixed in a 3:2 ratio (V/V) with the stannic chloride solution to be tested. This mixture was then dispensed using a single pump tube (0.23 ml/min nominal flow rate). This arrangement eliminated one addition tee from the ASCFAS manifold. Finally, the aldehyde chosen as the model compound for the ASCFAS optimization was 2,4-dichlorobenzaldehyde at a 2.00 X 10^{-4} M concentration.

The results of the Simplex optimization using a 2.00 m long mani-fold tube are summarized in Table 4-3. A scale from 0 to 3 (none to high) was used to describe the observed noise and dispersion in the system. The precision of the absorbance readings was ± 0.005 AU. The largest absorbance value of 0.62 was measured for vertex 12. Vertex 12 also showed low levels of noise and dispersion as did vertices 11 and 13. These last two vertices share variables in common with vertex 12. The optimum set of conditions for the ASCFA system were selected to be

Table 4-3. Optimization of the ASCF reaction between 2,4-dichlorobenzaldehyde and o-dianisidine using the Simplex method.

Vertex	Simplex Vertices	Time (s)	[$SnCl_4$] (mM)	Temperature (°C)	Speed Setting	Noise (0-3)	Dispersion (0-3)	Absorbance
1		146	6.0	30	50	0	3	0.41
2		143	7.0	30	50	0	2	0.43
3		143	8.0	35	50	1	3	0.50
4	1 2 3 4	134	8.0	35	55	1	3	0.48
5	2 3 4 5	139	9.0	35	45	2	2	0.50
6	3 4 5 6	145	9.0	40	40	3	2	0.56
7	3 5 6 7	130	10.0	45	45	2	3	0.59
8	5 6 7 8	115	10.0	50	50	1	2	0.59
9	6 7 8 9	118	9.0	50	50	1	2	0.61
10	7 8 9 10	111	8.0	50	50	1	2	0.60
11	7 9 10 11	120	7.0	50	50	1	1	0.60
12	9 10 11 12	130	7.0	45	50	1	1	0.62
13	9 11 12 13	128	8.0	45	50	1	1	0.61
14	9 12 13 14	132	6.0	45	50	1	2	0.60

those of vertex 12. These conditions were consider a safe choice because at 45°C a variation of 2-3°C in temperature will not cause decomposition at concentration of stannic chloride equal to 7.0×10^{-3} M.

The experimental flow rate for vertex 12 excluding air is 0.86 ml min^{-1}. The residence time of the sample from the point of aspiration to detection is about 135 seconds; and the air-segmentation frequency is 2.2 s^{-1}.

Once the sample and reagents are aspirated into the manifold, their concentration is diluted proportionally to the size of the pump tube used to aspirate them. The calculated net concentration for the sample and the two reagents during the optimization experiments for vertex 12 are: [aldehyde] = 5.97×10^{-5} M, [stannic chloride] = 1.67×10^{-3} M, and [o-dianisidine] = 7.32×10^{-3} M. The optimum concentration of stannic chloride was found to be roughly one fourth of that used for o-dianisidine.

Another parameter that was studied was the sampling time. Figure 4-4 shows the effect of sampling time on the response signal for a 1.37×10^{-4} M sample of furfural. The signal reaches a maximum value and shows a plateau for sampling times of 90 and 60 s. At smaller sampling times, the aldehyde begins to show a little less response and no flat portion of the signal is obtained due to dispersion. At a sampling time of 15 s, the signal looks like the ones obtained in a flow injection system and the response is reduced to 93% of the maximum obtained at sampling times of 60 or 90 s. At a feasible wash time of 15 s, sampling rates of 34, 48, 60, 80, and 120 samples per hour can be achieved with high reproducibility of the response signal at sampling times of 90, 60, 45, 30, and 15 s, respectively.

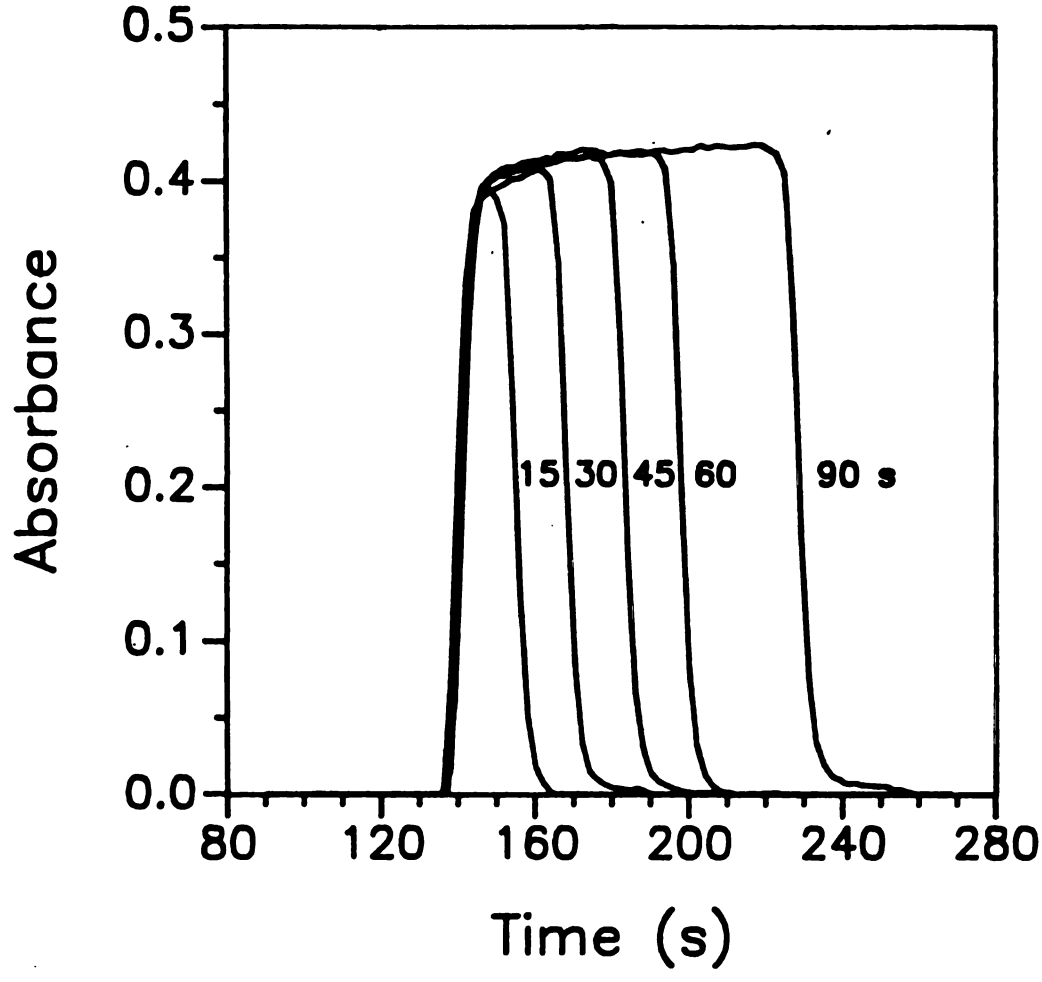

Figure 4-4. Effect of sampling time on the response signal during the determination of furfural using the o-dianisidine reagent. The furfural concentration was 1.37 X 10^{-4} M, while the stannic chloride concentration was 7.00 X 10^{-3} M and that of o-dianisidine was 0.0204 M.

In the analytical method, a sampling time of 90 s was used to prepare calibration curves in order to assess the true sensitivity of the method. During the selectivity and interference studies, a sampling time of 60 s was used instead. The wash time was 30 s in both cases. In a real world application of the o-dianisidine method, where sample throughput could be the major concern rather than lower detection limits, a sampling and wash time of 15 s are recommended.

2. The Analytical Method

Once the ASCFA system was optimized, calibration curves for 13 aromatic aldehydes were constructed to assess the usefulness of the o-dianisidine method. The figures of merit of o-dianisidine as a reagent for aromatic aldehyde detection are presented in Table 4-4. For each aldehyde, seven standards were prepared and four determinations were made for each standard as shown in Figure 4-5 for 2,4-dichlorobenzaldehyde. Next, weighted linear regression of the standard concentrations versus the absorbances obtained were performed using the KINFIT program. KINFIT calculated the slope, intercept and the errors of these two parameters for each calibration curve. As an example, Figure 4-6 shows the experimental points plus or minus one standard deviation and the weighted calibration curve (solid line) obtained for 2,4-dichlorobenzaldehyde.

The accuracy of the method for the determination of each aldehyde in an ideal sample (a standard of the particular aldehyde) was obtained by making eight absorbance measurements of a standard whose absorbance was around 0.50 AU. Column eight in Table 4-4 reports the relative standard deviation for the experimental absorbance measurements of the

Table 4-4. Figures of merit of the analytical method.

Aldehyde	Sensitivity ($l\ mol^{-1}\ cm^{-1}$)	Error of the slope ($l\ mol^{-1}\ cm^{-1}$)	Intercept (AU)	Detection Limit (M)	Linear Range (M)	RSD (%)	Accuracy (%)
p-Anisaldehyde	1362	14	0.009	6.3×10^{-6}	6.3×10^{-6}-6.0×10^{-4}	0.75	2.07
Benzaldehyde	2024	9	0.002	7.8×10^{-6}	7.8×10^{-6}-4.3×10^{-4}	0.71	0.14
5-Chlorosalicylaldehyde	5354	45	0.011	1.2×10^{-6}	1.2×10^{-6}-1.2×10^{-4}	0.45	0.88
Cinnamaldehyde	4490	22	0.010	1.7×10^{-6}	1.7×10^{-6}-2.0×10^{-4}	0.41	2.40
2,4-Dichlorobenzaldehyde	3085	7	0.005	4.1×10^{-6}	4.1×10^{-6}-3.0×10^{-4}	0.97	0.83
2,6-Dichlorobenzaldehyde	1630	15	-0.001	1.1×10^{-5}	1.1×10^{-5}-5.5×10^{-4}	0.56	0.57
2,5-Dimethoxybenzaldehyde	3740	15	-0.009	7.0×10^{-6}	7.0×10^{-6}-2.3×10^{-4}	0.72	5.6
3,5-Di-t-butyl-4-hydroxy-benzaldehyde	1359	13	-0.013	2.0×10^{-5}	2.0×10^{-5}-6.5×10^{-4}	0.79	0.09
Furfural	2820	10	0.002	5.7×10^{-6}	5.7×10^{-6}-3.2×10^{-4}	0.52	0.39
p-Hydroxybenzaldehyde	976	5	-0.001	1.9×10^{-5}	1.9×10^{-5}-8.0×10^{-4}	1.13	1.12
m-Nitrobenzaldehyde	2602	9	-0.005	8.7×10^{-6}	8.7×10^{-6}-3.5×10^{-4}	0.68	0.51
Salicylaldehyde	5916	22	0.006	1.9×10^{-6}	1.9×10^{-6}-1.4×10^{-4}	0.57	1.83
p-Tolualdehyde	1870	10	0.003	7.7×10^{-6}	7.7×10^{-6}-4.7×10^{-4}	0.94	1.44

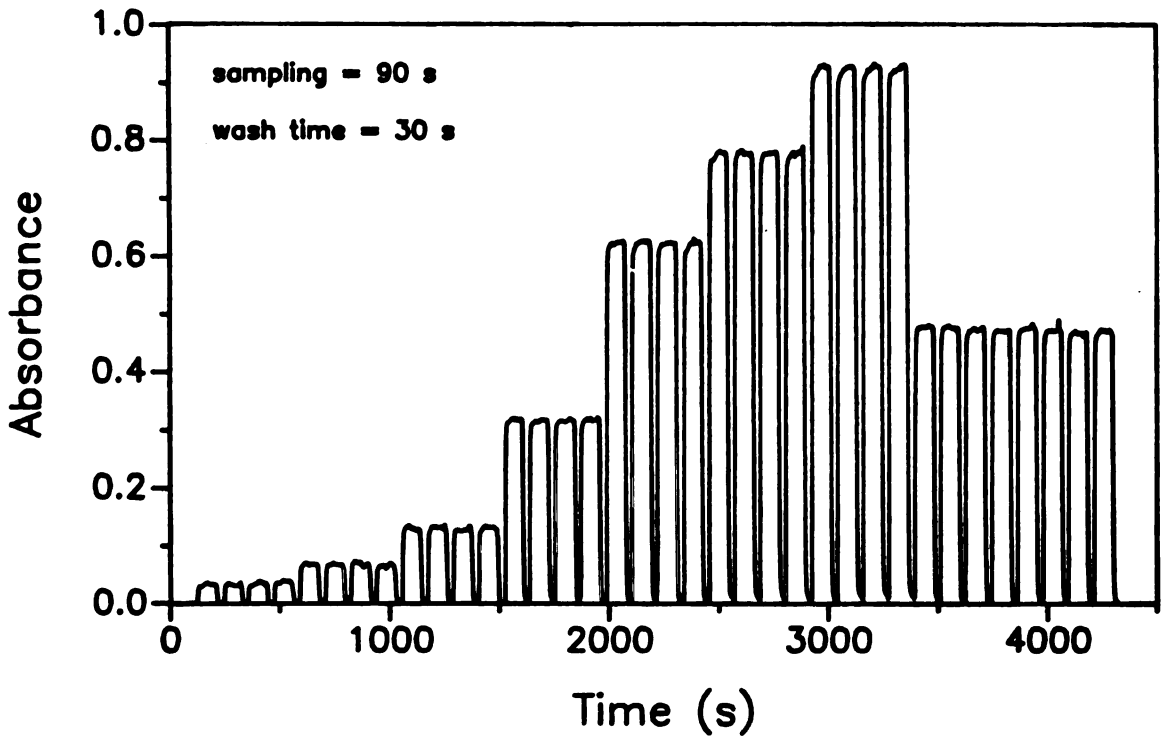

Figure 4-5. ASCFA of standards of 2,4-dichlorobenzaldehyde using the o-dianisidine reagent.

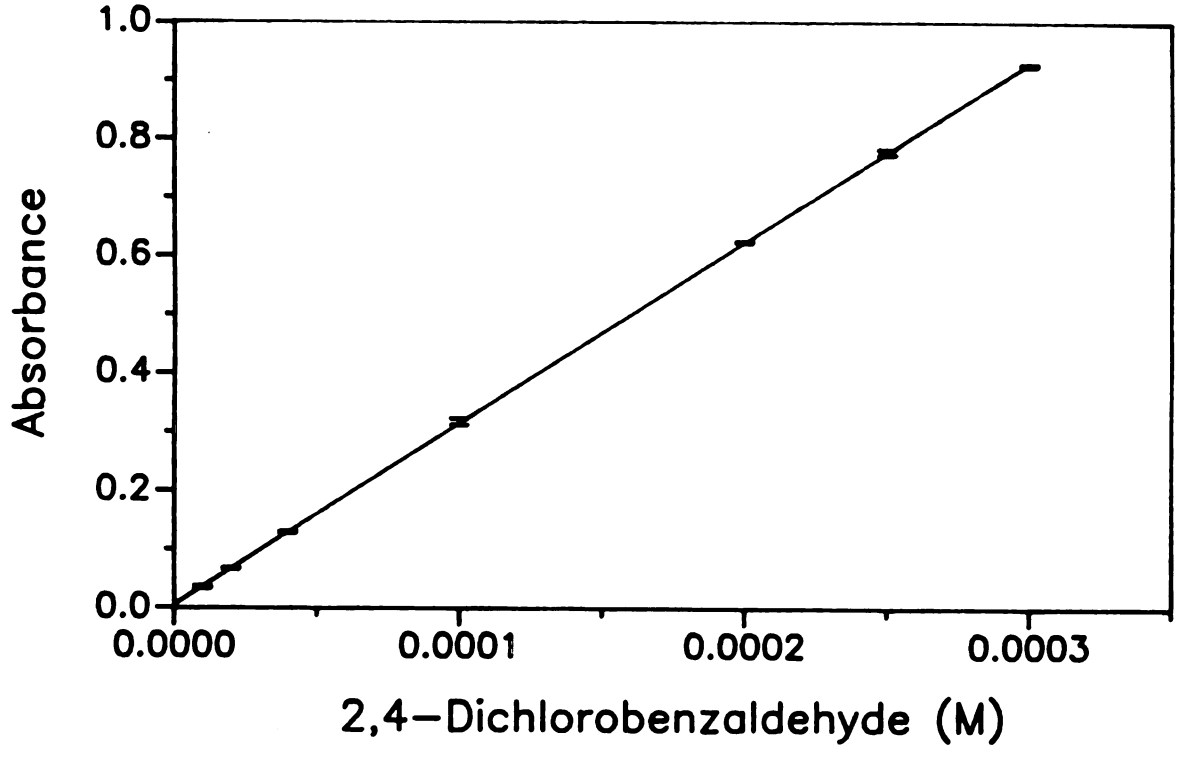

Figure 4-6. Weighted linear regression analysis for the determination of standards of 2,4-dichlorobenzaldehyde using the o-dianisidine reagent. The error bars represent the experimental points ± one standard deviation.

"ideal sample" and column nine reports the "ideal accuracy" of the method (i.e., error relative to the expected value according to the calibration curve).

The sensitivity of the o-dianisidine-aldehyde reaction was calculated for each aldehyde in units of 1 mol^{-1} cm^{-1}. The sensitivity was taken as the slope of the absorbance versus molar concentration plot. The reaction does not go to completion. Therefore, the sensitivity reported is not equal to the molar absorptivity of the particular adduct formed. The sensitivity calculated in this way is independent of the spectrophotometer used and can be used to compare this method with other spectrophotometric methods for aldehyde determination. The limits of detection and the linear dynamic range depend upon the particular instrument used, hence are poorer indexes for comparison between methods.

The limit of detection for each aldehyde was calculated as the concentration of the aldehyde that exhibited an absorbance equal to twice the standard deviation of the baseline noise. This is equivalent to using a reagent blank.

Due to constraints in the design of the bubble gate, absorbances higher than 1.0 cannot be measured in this system. At higher absorbances, the corresponding voltage is too low to trigger the gating electronics reliably. The upper limit of the linear dynamic range for most aldehydes was taken as either the highest concentration that exhibited linearity or the highest concentration tested that showed an absorbance of less than 1.0.

3. Selectivity Studies

The selectivity of the method was tested by reacting several ketones and aliphatic aldehydes under the same conditions used for the aromatic aldehyde determinations. The results obtained are presented in Table 4-5. In general, aliphatic and aromatic ketones showed the least response towards o-dianisidine. The average sensitivity for ketones was 7.1 l mol^{-1} cm^{-1}, about 400 times less than for aromatic aldehydes. Aliphatic aldehydes exhibit an average sensitivity of 15.6 l mol^{-1} cm^{-1}, about 184 times less than aromatic aldehydes. Only two α,β-unsaturated aldehydes (*trans* 2-butenal and tiglaldehyde) and one α,β-unsaturated ketone (*trans* chalcone) were studied, although their responses were quite different from one another, some generalizations can be made with regard to their sensitivity towards the o-dianisidine reagent. Apparently, α,β-unsaturated carbonyl compounds show an appreciable response with the o-dianisidine reagent and are possible spectral interferences in any intended application of this method.

Ketones as well as aliphatic aldehydes would be expected to react with o-dianisidine to the same extent as do aromatic aldehydes. The low response of these compounds with o-dianisidine arises from the position of the absorption band of their adducts, which is located in the ultraviolet region. Hence, these compounds react but do not show a spectral interference. However, a possible interference of ketones and aliphatic aldehydes arises because these compounds will consume some of the o-dianisidine which is required to react with the intended aromatic aldehyde. This will pose a problem if external standards are used, because the reaction equilibrium will favor more product formation in the standards than in the sample. This nonspectral interference can

Table 4.5 Selectivity studies of the o-dianisidine reaction

Compound	Sensitivity ($l\ mol^{-1}cm^{-1}$)
Acetone	8.77
2-Butanone	2.74
4-Methyl-2-pentanone	0.462
Cyclohexanone	32.7
Cycloheptanone	3.53
Acetophenone	0.71
p-Methylacetophenone	0.70
Benzophenone	7.07
trans Chalcone	92.6
Acetaldehyde	15.4
n-Butanal	10.4
2-Methylpentanal	22.6
2-Ethylhexanal	24.8
n-Heptanal	8.84
n-Decanal	11.9
trans 2-Butenal	753
Tiglaldehyde	38.0
Malonaldehyde *bis*-(dimethylacetal)	16.1

be corrected if the standard addition method of analysis is used. Blank interferences can also be eliminated in this way.

4. Interference Studies

To investigate further the usefulness of the o-dianisidine reagent for the determination of aromatic aldehydes, the effect of concomitants on the signal intensity was investigated, The aldehyde chosen for the interference studies was furfural in a 1.86×10^{-4} M concentration. The sampling and wash time were 60 and 30 s, respectively. All other experimental conditions were set to their optimum values as determined from the optimization experiments.

The first interferent studied was water. Since water is a product, it should show depressing effect on the analyte signal due to its displacement of the equilibrium towards reactants. Figure 4-7 shows the effect as the concentration of water is increased in the reaction medium. Indeed, a dramatic decrease in response is observed as the percent of water is increased. The maximum change in the equilibrium position occurs at concentrations of water below 5%. Above 8% the response ceases to decrease, but the signal becomes more and more erratic. These results indicate to the necessity of using the most anhydrous conditions possible for the determination. But far more important, they suggest the use of the standard addition method to correct for water interference in the analysis.

The presence of large amounts of water in strong acid medium probably were the reason that this reaction has not been used successfully before[4,5].

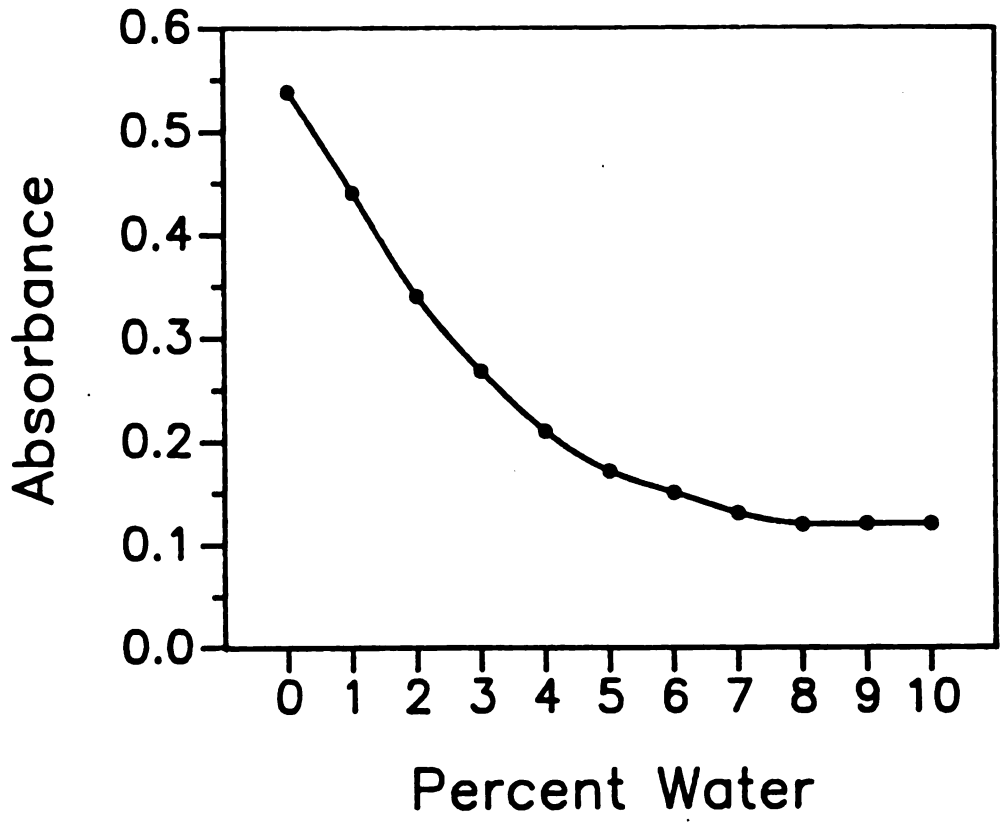

Figure 4-7. Water interference in the determination of furfural using the o-dianisidine reagent. The furfural concentration was 1.37 X 10^{-4} M The stannic chloride concentration was 7.00 X 10^{-3} M and that of o-dianisidine was 0.0204 M.

The interference of carboxylic acids was also studied. The catalytic effect of acetic acid was examined during the kinetics experiments. In the analytical method, little or no effect was expected to be observed if the reaction was already at equilibrium when the sample reached the detector. The two carboxylic acids used to test this interference were acetic acid and benzoic acid at concentrations of 608 and 589 mg/l, respectively. Acetic acid caused a 3.0% increase in the signal, while benzoic acid gave a 1.8% increase. These results indicate that the reaction is not at equilibrium when the sample reaches the detector. If carboxylic acids are suspected to be a concomitant in the matrix, their interference can be overcome by increasing the residence time of the sample in the reaction coil. A compromise between reaction coil length and dispersion must then be made. If this compromise is not possible, the reaction coil should be carefully thermostatted to improve precision. Another approach to this problem is the use of the standard addition method to effect the same increase of the signal in both sample and standards.

The possible implementation of the o-dianisidine method as an HPLC post-column detector reaction prompted the test of hexane interference in the o-dianisidine/aldehyde reaction. Five ethanolic samples of the aldehyde were prepared in which the hexane content was 0, 10, 20 and 40%. Upon analysis, no net effect of hexane on the signal was observed, but as the concentration of hexane was increased the baseline was observed to drift up somewhat. The cause of the drift could be either deposition of solid particulates on the cell windows or changes in the solution density. As the composition and density of the solution changes, it brings about a change in refractive index, which in turn

alters the absorbance. The lack of precipitation in the waste container and the flat top shape of the signals regardless of hexane concentration are indicative that the drift of the baseline is probably due to changes in the solution density rather than to precipitate formation.

An aldehyde sample containing 0.30% Brij 35 was also tested. Brij 35 is a surfactant used in aqueous ASCFA systems to improve the reproducibility of the bubble pattern. No improvement in the bubble pattern was observed in this system with ethanol as the solvent. In turn, a 3.2% decrease in the signal was observed.

The selection of furfural as the model aldehyde on which to do the interference studies was not without fore thought. Furfural was also selected as the target analyte when applying the o-dianisidine method to real samples.

5. Application to a Real Sample

The performance of the o-dianisidine ASCFA method for the determination of furfural in Creme de Menthe was compared with direct UV absorbance detection[86]. The liquor was steam distilled to separate the furfural from other components present in the sample. The standard addition technique was used to compensate for possible interferences. Three sets of standards were prepared as described on pages 95 to 96: one in which the standard addition technique was used prior to the steam distillation, a second set where the standard addition was carried out after the steam distillation, and a third one where the standard addition was performed after an ether extraction of the steam distilled sample.

In the direct spectrophotometric method the absorbances were measured at a wavelength of 277 nm on a Hitachi 200-Perkin-Elmer Spectrophotometer. A slit width of 1.00 nm and the fast response mode were used. In the ASCF analysis method the reaction coil was thermostatted at 45°C; sampling and wash time were 60 and 30 s, respectively. The o-dianisidine and $SnCl_4$ reagents were prepared as described previously and their concentrations were set to the optimum values as determined from the optimization experiments.

The results of the determination are summarized in Table 4-6. The lower furfural content in the ether extracted samples could be due to a low efficiency of the ether extraction or to a selective separation of furfural from any other components present that also may absorb at 277 nm.

Table 4-6. Determination of Furfural in Creme de Menthe

Standard Addition:	Detection Mode	mg Furfural/l
Before steam distillation	UV	6.0 ± 0.5
After steam distillation	UV	5.9 ± 0.3
After ether extraction of a steam distilled sample	UV	2.0 ± 0.5
After ether extraction of a steam distilled sample	o-dianisidine	2.0 ± 0.1

To test the percentage recovery of furfural during the ether extraction, a 20.00 ml sample of Creme de Menthe was spiked with furfural as to contain 11.0 mg/l of added furfural. The sample was then steam distilled and extracted with ether as described in the experimental section. The standard addition method was used to analyze

the sample via direct UV absorbance detection using ethanol as the reference. Upon analysis, the expected furfural content was 13.0 ± 0.5 mg/l (2.0 + 11.0 mg/l added). The amount of furfural found was 14.2 ± 0.8 mg/l. From this result the ether extraction efficiency is calculated to be ≈ 100%. Also, the absorption spectrum of an ether-extracted Creme de Menthe sample resembles more the spectrum of a pure furfural sample than does the spectrum of a steam-distilled Creme de Menthe sample. Therefore, the low furfural content in the ether extracted sample is probably due to a more selective separation of furfural from another component present that is absorbing also at 277 nm.

The o-dianisidine method has proved to be consistent with results from direct UV absorbance detection. Full advantage of the method would be realized when used in conjunction with a separation technique such as HPLC, where direct UV absorbance detection will not differentiate between aromatic aldehydes and ketones or aliphatic aldehydes.

I. Conclusions

Direct spectrophotometric determination of aromatic aldehydes in the ultraviolet region is about 5 to 10 times more sensitive method than derivatization with o-dianisidine. Other reported colorimetric methods for carbonyl groups are in general, also more sensitive than the o-dianisidine method. The o-dianisidine method, on the other hand, is automated, simple in instrumentation, and much more rapid than any of the colorimetric or fluorimetric methods reported in the literature. The most important argument, however, for using o-dianisidine for the

determination of aromatic aldehydes is the expected selectivity of the reaction. Selectivity becomes important in the analysis of complex matrices such as foods and waste waters, where trace amounts of substances like ketones and aliphatic aldehydes could interfere with direct spectrophotometric detection or with other colorimetric and fluorimetric methods.

In the o-dianisidine method developed here, a single set of experimental conditions for all aromatic aldehydes was selected. Therefore, it was necessary to compromise the sensitivity for some of the aldehydes in favor of a practical optimum for as many aromatic aldehydes as possible. For a particular application, better detection limits can probably be obtained if the reaction is optimized for the aldehyde of interest in terms of the choice of temperature, wavelength and concentration of the catalyst.

CHAPTER V

FUTURE PROSPECTS

A. Overview

Initially, it was thought that the method studied here could be used for colorimetric differential analysis of aldehydes since a wide range of colors for many aldehydes were reported by Wasicky and Frehden[2]. Indeed, several different colors were observed when using a 100% acetic acid medium; but at low acetic acid concentrations or when using stannic chloride as catalyst, this is not the case. Nevertheless, the reaction was found to be very selective, which brings about the possibility of using the o-dianisidine method in a post-column reaction detection system for HPLC. In this chapter, a brief introduction to post-column derivatization in connection with aldehyde determinations is followed by a presentation of the feasibility of using the o-dianisidine method for post-column aromatic aldehyde determination. Finally, a few other future applications and fundamental studies are suggested for the o-dianisidine-aldehyde reaction.

B. Derivatization in HPLC

High-performance liquid chromatography, HPLC, is used frequently in the separation of a wide range of compounds within the same class[87-89]. The most common detectors for HPLC are ultraviolet,

absorbance, visible absorbance, electrochemical, refractive index and fluorimetric detectors. To increase the sensitivity or specificity of photometric detectors in HPLC, pre-column or post-column derivatization can be applied[89-95]. In pre-column derivatization, the sample undergoes a chemical reaction prior to separation on the column. In post-column derivatization, the column effluent is combined with a particular reagent to effect a desired reaction prior to detection. In any case, the detectability of the desired compound is enhanced by forming derivatives which are more easily detected and/or possess different spectral characteristics. The advantages and disadvantages of both modes of operation have been summarized by Frei and Lawrence[89-91,95].

It is generally accepted that in post-column derivatization the reaction does not have to go to completion or to give well-defined derivatives. The most important aspect is the reproducibility of the system. A disadvantage of post-column derivatization in HPLC is that of possible non-compatibility between the optimal chromatographic eluent and the reaction requirements. Despite this disadvantage, numerous reports on post-column derivatization have been published, as evidenced by three books treating HPLC derivatization[89,93,94], and the many references therein.

Although numerous reagents have been reported for aldehyde pre-column derivatization, the reaction most widely used for this purpose is the formation of the 2,4-dinitrophenylhydrazones of carbonyl compounds. The HPLC separation of the 2,4-dinitrophenylhydrazones derivatives using reversed-phase columns gives better resolution than when using adsorption or normal-phase columns. Detection limits are obtained in the

nanogram range with UV absorbance detectors and in the picogram range with electrochemical detectors[96-98].

So far, only two post-column reactions for aldehydes have been reported. Gandelman and Birks[99] proposed the photoreduction-fluorescence detection for aliphatic aldehydes, alcohols and ethers using anthraquinone-2,6-disulfonate disodium salt. Krull, et al.[100], achieved the reduction of three aromatic aldehydes to the corresponding alcohol using a solid-phase borohydride resin reactor. This reactor can be configured either for pre- or post-column operations using both normal- and reversed-phase HPLC columns.

Of the two methods reported for post-column determination of aldehydes, the method by Gandelman and Birks is not specific enough to be of great value for aromatic aldehyde determinations. The method by Krull, et al. sometimes lacks chromatographic resolution between the initial aldehyde and the corresponding alcohol product. Therefore, the characterization of peaks in mixtures of aldehydes should be more difficult than by the proposed o-dianisidine reagent.

C. The Proposed Method

The three most important criteria that this reaction has to fulfill in order to be adapted as an HPLC post-column detection reaction are:

i) the reaction time has to be short (< 20 minutes)

ii) the reaction must be reproducible, and

iii) the solvent has to be compatible with the solvent used for HPLC elution.

The success obtained in automating the reaction of o-dianisidine with aromatic aldehydes should be considered as preliminary results showing the feasibility of the use of o-dianisidine as an HPLC post-column reagent. In the automated method, the reaction time has been decreased to 135 seconds by increasing the temperature to 45°C and using stannic chloride as the catalyst instead of acetic acid. The reproducibility of the reaction is good (average RSD = 0.71%) and the accuracy expected to be within the 1.0 or 2.0 % error range. The method is rapid and simple. Other advantages are that the reaction is run in ethanol which permits solution of most aldehydes, and that it requires lower acid concentration than most of the usual colorimetric or fluorimetric procedures used for aldehyde determination.

Since it was found that water must be absent from the reaction medium in order to obtain a good response for the majority of the aromatic aldehydes tested, bonded normal-phase liquid chromatography should be employed for the aldehyde separation. In bonded normal-phase chromatography, the commonly employed mobile phases are non-polar solvents (like hexane, heptane, and isoctane) plus small amounts of medium polarity solvents (like methylene chloride, tetrahydrofuran, chloroform, ethanol, methanol, or ethyl acetate). Ethanol, the solvent of choice for the o-dianisidine derivatization, is miscible with all the above mentioned solvents. Therefore, little difficulty with solvent incompatibility is expected. The possibility of using hexane was demonstrated during the interference studies. It is then possible that, by the combination of two different techniques, HPLC and ASCFA, an analytical system can be achieved in which aromatic aldehydes and some

α,ß-unsaturated carbonyl compounds can be quantitatively determined from complex mixtures.

An advantage of using the o-dianisidine post-column reaction is the possibility of using different detection modes simultaneously. For example, to detect with a UV absorbance detector immediately after the column and with the colorimetric detector after derivatization.

Finally, the expected improvement in selectivity using o-dianisidine as a post-column reaction should compensate for the decrease in detectability when compared to direct UV absorbance detection of aldehydes.

D. ASCF Kinetics Determinations

Aromatic aldehydes have different reactivities towards the o-dianisidine reagent. Therefore, kinetics-based determinations of aromatic aldehydes by reaction with o-dianisidine are possible via conventional methods[101] (initial rate, fixed time, two rate methods, etc.) using a variety of detection systems to monitor the progress of the reaction with time (spectrophotometers, stopped flow analyzers, etc.). It is also conceivable to perform kinetics determinations using air-segmented continuous-flow analyzers. In this approach, after sufficient time has elapsed for mixing, a segment of the analytical stream is stopped within the flowcell by turning off the pump. Because of the presence of bubbles the integrity of the analytical stream is preserved. Consequently, the progress of the o-dianisidine reaction can be monitored continuously over the desired time interval. This approach might seem to be somewhat cumbersome but there are some advantages to

it: small volume of samples and reagents will be required and multiple repetitions of experiments are possible with very little extra effort.

E. Other Studies

There is still room for improvements in the o-dianisidine method for aromatic aldehyde determination. For example, studies should be conducted to test the possibility of automating also the aldehyde extraction from aqueous matrices using the same continuous-flow system used to effect the derivatization. Studies in which air is replaced by nitrogen as the segmentation gas should be conducted to increase the sensitivity of the method by preventing the oxidation of aldehydes to carboxylic acids in the reaction coil. Finally, the search for a better catalyst should be continued.

LIST OF REFERENCES

LIST OF REFERENCES

1. Sawicki, E.; Sawicki, C. R. *Aldehydes Photometric Analysis*, Vol. 1-5, Academic Press, Inc., London, 1975-78.

2. Wasicky, R.; Frehden, O. *Mikrochim. Acta* 1937, *1*, 55.

3. Feigl, F. *Qualitative Analysis by Spot Test*, 3rd ed., Elsevier Publishing Company, New York, 1946; pp. 340-344.

4. Wearn, R. B.; Murray, W. M., Jr.; Ramsey, M. P.; Chandler, N. *Anal. Chem.* 1948, *20*, 922.

5. Cerda', V.; Mongay, C. *Analusis* 1976, *4(2)*, 94.

6. Attaway, J. A.; Wolford, R. W.; Dougherty, M. H.; Edwards, G. J. *J. Agr. Food Chem.* 1967, *15*, 688.

7. McKeag, R. G.; Hougen, F. W. *Anal. Chem.* 1977, *49*, 1078.

8. Cronin, D. A. *J. Chromatogr.* 1972, *64*, 25.

9. Kalo, P. *J. Chromatogr.* 1981, *205*, 39.

10. Bierl, B. A.; Beroza, M.; Ashton, W. T. *Microchim. Acta* 1969, *3*, 637.

11. Pang, T. B. *Yu Chi Hua Hsuch* 1981, *1*, 39; CA 95:72745f.

12. Pesez, M.; Poirier, P.; Bartos, J. *Practique de l'Analyse Organiche Colorimetrique*, Masson, Paris, 1966; pp. 140-141.

13. Sawicki, E.; Engel, C. R. *Anal. Chim. Acta* 1967, *38*, 315.

14. Zvilichovsky, G. *Tetrahedron Lett.* 1972, 2351.

15. Pesez, M.; Bartos, J. *Talanta* 1963, *10*, 69.

16. Heistand, R. N. *Anal. Chim. Acta* 1967, *39*, 258.

17. Qureshi, M.; Qureshi, S.; Singhal, S. C. *Anal. Chim. Acta* 1971, *53*, 361.

18. Qureshi, M.; Khan, I. A. *Fresenius Z. Anal. Chem.* 1978, *289*, 282.

19. Sawicki, E.; Stanley, T. W.; Hauser, T. R. *Chemist-Analyst* 1958, *47*, 31.

20. Rappoport, Z.; Sheradsky, T. *J. Chem. Soc. Part B* 1968, 277.

21. Grammaticakis, P. *Bull. Soc. Chim. France* 1954, 1372.

22. Hunig, S.; Utermann, J. *Chem. Ber.* 1955, *88*, 423.

23. Johnson, H.; Sawicki, E. *Talanta* 1966, *13*, 1361.

24. Yates, K.; Steward, R. *Can. J. Chem.* 1959, *37*, 664.

25. Keeney, M.; Basette, R. *J. Dairy Sci.* 1959, *42*, 945.

26. Feigl, F.; Libergott, E. *Anal. Chem.* 1964, *36*, 132.

27. Bartos, J.; Pesez, M. *Talanta* 1974, *21*, 1304.

28. Papadoyannis, I. N.; Kouimtzis, Th. A.; Vasilikiotis, G. S. *Microchem. J.* 1983, *28*, 344.

29. Nakamura, M.; Toda, M.; Saito, H.; Ohkura, Y. *Anal. Chim. Acta* 1982, *134*, 39.

30. Kaito, T.; Sagara, K.; Ikunaga, K. *Chem. Pharm. Bull.* 1979, *27*, 3167.

31. Zeitler, H. *Anal. Biochem.* 1978, *88*, 649.

32. Ohkura, Y.; Ohtsubo, K.; Zaitsu, K.; Kohashi, K. *Anal. Chim. Acta* 1978, *99*, 317.

33. Toyoto, U.; Taniguchi, H. *Bunseki Kagaku* 1972, *21(1)*, 76; CA 76:107699f.

34. Taniguchi, H.; Kazuo, M.; Keiko, T.; Saburo, N. *Yakugaku Zasshi* 1974, *94(6)*, 717; CA 82:7694f.

35. Ohkura, Y.; Zaitsu, K. *Talanta* 1974, *21*, 547.

36. Chayen, R.; Dvir, R.; Gould, S.; Harell, A. *Anal. Biochem.* 1971, *42*, 283.

37. Pietrzyk, D. J.; Chan E. P. *Anal. Chem.* 1970, *42*, 37.

38. Akira, S.; Makoto, O.; Shoji, T. *Anal. Sci.* 1987, *3(4)*, 359; CA 107:190109r.

39. Bekarek, V.; Klicnar, J.; Kristex, F.; Vecera, M. *Collection Czechoslov. Chem. Commun.* 1968, *33*, 994.

40. Srivastava, T. N.; Agarwal, M. *Indian J. Chem.* 1979, *17A*, 613.

41. Aggarwal, R. C.; Vara Prasada Rao, D. S. S. *Indian J. Chem.* 1982, *21A*, 735.

42. Kriza, A.; Negoiu, M. *Bul. Inst. Politech. Bucuresti, Ser. Chim.* 1986, *48*, 75; CA 107:108122h.

43. Yoe, J. H.; Jones, A. L. *Ind. Eng. Chem. Anal.* 1944, *16*, 111.

44. Meites, L. *An Introduction to Chemical Equilibrium and Kinetics*, 1st ed., Pergamon Press, New York, 1981.

45. Tabei, K.; Saitou, E. *Bull. Chem. Soc. Japan* 1969, *42*, 1440.

46. Jencks, W.P. in "Progress in Physical Organic Chemistry", Eds.: Cohen, S.G.; Streitwieser, A., Jr.; Taft, R.W. Vol. 2, Interscience-Wiley, New York, 1964.

47. Sayer, J. M.; Pinsky, B.; Schonbrunn, A.; Washtien, W. *J. Am. Chem. Soc.* 1974, *96*, 7998.

48. Rosenberg, S.; Silver, S. M.; Sayer, J. M.; Jencks, W. P. *J. Am. Chem. Soc.* 1974, *96*, 7986.

49. Sayer, J. M.; Edman, C. *J. Am. Chem. Soc.* 1979, *101*, 3010.

50. Lowry, T. H.; Richardson, K. S. *Mechanism and Theory in Organic Chemistry*, 2nd ed., Harper and Row, New York, 1981; pp. 635-642.

51. Rosin, J. Reagent Chemicals and Standards, 5th ed., D. Van Nostrand Co., Inc., London, 1967; pp 496-498.

52. Cordes, E. H.; Jencks, W. P. *J. Am. Chem. Soc.* 1962, *84*, 832.

53. Bates, R. G. *Determination of pH: Theory and Practice*, 2nd ed., John Wiley & Sons, New York, 1973; pp. 211-253.

54. Westcott, C. C. p*H Measurements*, Academic Press, New York, 1978; pp. 112-124.

55. Kilpatrick, M.; Eanes, D. R. *J. Am. Chem. Soc.* 1953, *75*, 586.

56. Dye, J. L.; Nicely, V. A. *J. Chem. Ed.* 1971, *48*, 443.

57. Motulsky, H. J.; Ransnas, L. A. *FASEB J.* 1987, *1*, 365.

58. Edwards, J. O.; Greene E. F.; Ross, J. *J. Chem. Educ.* 1968, *45*, 381.

59. Espenson, J. H. *Chemical Kinetics and Reaction Mechanisms*, Mc Graw Hill, New York, 1981.

60. Bradley, D. C.; Caldwell, E. V.; Wardlaw W. *Chem. Soc. J.* 1957, 3039.

61. Guenzet, J.; Camps, M.; Toumi, A. *C.R. Acad. Sc. Paris* 1972, *274*, 1211; CA 77:4688t.

62. Laubengayer, A. W.; Smith, Wm. C. *J. Am. Chem. Soc.* 1954, *76*, 5985.

63. Beattie, I. R. *Quart. Revs.* 1963, *17*, 382.

64. Keck, G. E.; Castellino, S.; Wiley, M. R. *J. Org. Chem.* 1986, *51*, 5478.

65. Jones, K.; Lappert, M. F. *Organometal. Chem. Rev.* 1966, *1*, 67.

66. Hine, J.; Craig, J. C., Jr.; Underwood, J. G.,II; Via F. A. *J. Am. Chem. Soc.* 1970, *92*, 5194.

67. Cordes, E. H.; Jencks, W. P. *J. Am. Chem. Soc.* 1963, *85*, 2843.

68. Skeggs, L. T., Jr. *Clin. Chem.* 1956, *2*, 241.

69. Skeggs, L. T., Jr. *Am. J. Clin. Pathol.* 1957, *28*, 311.

70. Snyder, L. R.; Levine, J.; Stoy, R.; Conetta A. *Anal. Chem.* 1976, *48*, 942 A.

71. Snyder, L. R. Anal. *Chim. Acta* 1980, *114*, 3.

72. Furman, W. B., Ed. *Continuous Flow Analysis: Theory and Practice*, Marcel Dekker, New York, 1976.

73. Patton, C. J. Ph. D. Thesis, Michigan State University, 1982.

74. Mottola, H. A. *Anal. Chem.* 1981, *53*, 1312 A.

75. Ruzicka, J.; Hansen, E. H. *Flow Injection Analysis*, 2nd ed., Interscience-Wiley, New York, 1988.

76. Snyder, L. R. *J. Chromatogr.* 1976, *125*, 287.

77. Hrdina, J. 6th Colloq. Amino Acid Analysis, Technicon Corp., Monograph No. 3, 1967.

78. Begg, R. D. *Anal. Chem.* 1972, *44*, 631.

79. Thiers, R. E.; Reed, A. H.; Delander, K. *Clin. Chem.* 1971, *17*, 42.

80. Walker, W. H. C.; Andrew, K. R. *Clin. Chim. Acta* 1974, *57*, 181.

81. Patton, C. J.; Rabb, M.; Crouch, S. R. *Anal. Chem.* 1982, *54*, 1113.

82. Habig, R. L.; Schlein, B. W.; Walters, L.; Thiers, R. E. *Clin. Chem.* 1969, *15*, 1045.

83. Spendley, W.; Hext, G. R.; Himsworth, F. R. *Technometrics*, 1962, *4*, 441.

84. Morgan, S. L.; Deming, S. N. *Anal. Chem.* 1974, *46*, 1170.

85. Burton, K. W. C.; Nickless, G. *Chemometrics and Intelligent Laboratory Systems*, 1987, *1*, 135.

86. Williams, S., Ed. *Official Methods of Analysis of the Association of Official Analytical Chemist*, 14th ed., 1984.

87. Johnson, E. L.; Stevenson, R. *Basic Liquid Chromatography*, Varian Associates, Inc., California, 1978.

88. Snyder, L. R.; Kirkland, J. J. *Introduction to Modern Liquid Chromatography*, 2nd ed., John Wiley & Sons, New York, 1979.

89. Lawrence, J. F. *Organic Trace Analysis by Liquid Chromatography*, Academic Press, Inc., New York, 1981.

90. Scholten, A. H. M. T.; Brickman, U. A. Th.; Frei, R. W. *J. Chromatogr.* 1981, *205*, 229.

91. Frei, R. W. *J. Chromatogr.* 1979, *165*, 75.

92. Scholten, A. H. M. T.; Brickman, U. A. Th.; Frei, R. W. *Anal. Chem.* 1982, *54*, 1932.

93. Lawrence, J. F.; Frei, R. W., Eds. *Chemical Derivatization in Analytical Chemistry*, Plenum Press, New York, Vol. 1, 1981.

94. Blau, K.; King, G. S., Eds. *Handbook of Derivaties for Chromatography*, Heyden and Son, London, 1978.

95. Frei, R. W. *Chromatographia*, 1982, *15(3)*, 161.

96. Jacobs, W. A.; Kissinger, P. T. *J. Liq. Chromatogr.* 1982, *5(4)*, 669.

97. Fung, K.; Grosjean, D. *Anal. Chem.* 1981, *53*, 168.

98. Reindl, B.; Stan, H. J. *J. Chromatogr.* 1982, *235*, 481.

99. Gandelman, M. S.; Birks, J. W. *Anal. Chem.* 1982, *54*, 2131.

100. Krull, I. S.; Xie, K. H.; Colgan, S.; Neue, U.; Izod, T.; King, R.; Bidlingmeyer, B. *J. Liq. Chromatogr.* 1983, *6(4)*, 605.

101. Perez-Bendito, D.; Silva, M. *Kinetics Methods in Analytical Chemistry*, John Wiley & Sons, New York, 1988.